

UNIVERSIDADE FEDERAL DE SANTA MARIA
CENTRO DE CIÊNCIAS NATURAIS E EXATAS
PROGRAMA DE PÓS-GRADUAÇÃO EM CIÊNCIAS BIOLÓGICAS:
BIOQUÍMICA TOXICOLÓGICA

Bruna Candia Piccoli

**PARÂMETROS MOLECULARES E BIOQUÍMICOS SOBRE A
EXPOSIÇÃO *per os* AGUDA E CRÔNICA A XENOBIÓTICOS
ELETROFÍLICOS EM INSETOS-MODELOS**

Santa Maria, RS
2020

Bruna Candia Piccoli

**PARÂMETROS MOLECULARES E BIOQUÍMICOS SOBRE A EXPOSIÇÃO *per os*
AGUDA E CRÔNICA A XENOBIÓTICOS ELETROFÍLICOS EM INSETOS-
MODELOS**

Tese apresentada ao Curso de Pós-Graduação em Ciências Biológicas: Bioquímica Toxicológica, da Universidade Federal de Santa Maria (UFSM, RS), como requisito parcial para obtenção do título de **Doutora em Ciências Biológicas: Bioquímica Toxicológica.**

Orientador: Prof. Dr. João Batista Teixeira da Rocha

Coorientador: Prof. Dr. Daniel Mendes Pereira Ardisson de Araújo

Coorientadora: Prof^ª. Dr^ª. Ana Lúcia Anversa Segatto

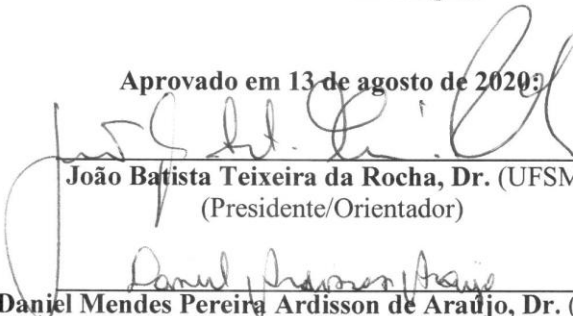
Santa Maria, RS
2020


Bruna Candia Piccoli

**PARÂMETROS MOLECULARES E BIOQUÍMICOS SOBRE A EXPOSIÇÃO *per os*
AGUDA E CRÔNICA A XENOBIÓTICOS ELETROFÍLICOS EM INSETOS-
MODELOS**

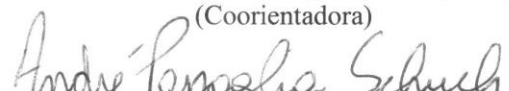
Tese apresentada ao Curso de Pós-Graduação
em Ciências Biológicas: Bioquímica
Toxicológica, da Universidade Federal de
Santa Maria (UFSM, RS), como requisito
parcial para obtenção do título de **Doutora em
Ciências Biológicas: Bioquímica
Toxicológica.**

Aprovado em 13 de agosto de 2020


João Batista Teixeira da Rocha, Dr. (UFSM)
(Presidente/Orientador)


Daniel Mendes Pereira Ardisson de Araújo, Dr. (UFSM)
(Coorientador)


Ana Lúcia Anversa Segatto, Dr^a. (IFRS)
(Coorientadora)


André Passaglia Schuch, Dr. (UFSM)


Bergmann Morais Ribeiro, Dr. (UnB)


Cristiane Lenz Dalla Corte, Dr^a. (UFSM)


Robson Luiz Puntel, Dr. (UNIPAMPA)

Santa Maria, RS
2020

DEDICATÓRIA

Dedico este trabalho a minha família e meus amigos que sempre me incentivaram e, de alguma forma, fizeram este sonho tornar-se realidade.

AGRADECIMENTOS

A concretização deste trabalho ocorreu, principalmente, pelo auxílio, dedicação e incentivo de várias pessoas. Agradeço a todos que, de alguma forma, contribuíram para a conclusão deste estudo e, de uma maneira especial, agradeço:

- a toda minha família, em especial, aos meus pais, Abrilino e Gislaine um muito obrigada. Grata por acreditarem no meu potencial, me incentivarem e tornar possível a realização deste e de tantos outros sonhos. A minha irmã Alice Candia Piccoli que também estava presente nestes momentos importantes, obrigada pela paciência. Ao meu namorado Rafael Santos da Silva que participou direta e indiretamente deste trabalho.

- ao meu orientador João Batista Teixeira da Rocha pela confiança em mim depositada e pela oportunidade concedida, grata pela orientação;

- aos meus coorientadores Ana Lúcia Anversa Segatto e Daniel Mendes Pereira Ardisson de Araújo que foram fundamentais na descoberta de uma nova área na pesquisa. Grata pela oportunidade de me coorientarem.

- a minha banca, André Passaglia Schuch, Bergmann Morais Ribeiro, Cristiane Lenz Dalla Corte e Robson Luiz Puntel pela disponibilidade em avaliar meu trabalho;

- a todos os colegas de laboratório, em especial, as coautoras e grandes amigos Fernanda D'Ávila da Silva, Cláudia Sirlene de Oliveira e Pablo Andrei Nogara que foram imprescindíveis na realização desta tese, não apenas pela ajuda nos experimentos e escrita, mas também pelo apoio e incentivo a mim concedido;

RESUMO

PARÂMETROS MOLECULARES E BIOQUÍMICOS SOBRE A EXPOSIÇÃO *per os* AGUDA E CRÔNICA A XENOBIÓTICOS ELETROFÍLICOS EM INSETOS-MODELOS

AUTORA: Bruna Candia Piccoli

ORIENTADOR: João Batista Teixeira da Rocha

COORIENTADOR: Daniel Mendes Pereira Ardisson de Araújo

COORIENTADORA: Ana Lúcia Anversa Segatto

A exposição contínua a pequenas doses de substâncias tóxicas causam alterações no perfil transcricional e na função de proteínas antes de causarem prejuízos físicos nos organismos. Os efeitos tóxicos podem surgir até mesmo após a interrupção da exposição. Conhecer o mecanismo de ação e identificar biomarcadores de toxicidade precoce para substâncias são interesses da comunidade científica. Como o ser humano está constantemente exposto a vários xenobióticos, torna-se necessário estudar os efeitos da exposição a dois ou mais agentes tóxicos concomitantemente. Para isso, é necessário estabelecer modelos experimentais para estudos translacionais. Dentre os xenobióticos destacam-se o metilmercúrio (MeHg^+) e o vinilciclohexeno (VCH), os quais ainda não possuem mecanismo de toxicidade completamente elucidados e apresentam propriedades eletrônicas semelhantes. Desta forma, este trabalho visa estudar os efeitos da exposição *per os* aguda, intermediária e crônica ao MeHg^+ e a possível reversão dos efeitos deste xenobiótico após a interrupção da exposição em parâmetros comportamentais e bioquímicos da barata *N. cinerea*, assim como, o efeito isolado e da interação do MeHg^+ e do VCH sobre o transcriptoma da mosca *D. melanogaster*, uma vez que estes compostos apresentam semelhanças nos seus mecanismos de toxicidade (afinidade por proteínas que contém $-\text{SH}$ e $-\text{SeH}$). As baratas foram expostas a dietas contendo 0 (controle), 2,5, 25 e 100 μg de MeHg^+ /g de dieta por 10, 30 e 90 dias. Grupos adicionais de baratas foram alimentados com as mesmas doses de MeHg^+ por 30 dias e depois foram submetidos a um período de desintoxicação por 60 dias. As ninfas expostas a 100 μg de MeHg^+ /g sucumbiram a uma alta taxa de mortalidade, juntamente com alterações bioquímicas (aumento da produção de espécies reativas de oxigênio e atividade da glutatona S-transferase, bem como diminuição da atividade da acetilcolinesterase) e alterações comportamentais. Observamos atraso na taxa de mortalidade e alterações comportamentais nas ninfas expostas a 100 μg de MeHg^+ /g por 30 dias e posteriormente submetidas a 60 dias de desintoxicação. Para avaliar o perfil transcricional da *D. melanogaster* foi realizado o sequenciamento de RNA de moscas expostas individual e concomitantemente a 1 mM de VCH e 200 μM de MeHg^+ por três dias. O VCH desregulou 38 genes (dos quais a maioria estava super-expresso), enquanto o MeHg^+ alterou 26 genes (14 genes sub-expressos). Já a coexposição do VCH + MeHg^+ alterou 72 genes com maior número de genes sub-expressos. Estes resultados sugerem que, embora os compostos pudessem ter alguns alvos proteicos semelhantes, o perfil transcricional após exposições individuais e coexposição foi diferente. O conjunto de proteínas que contém $-\text{SH}$ e $-\text{SeH}$ foi prospectado e identificamos a tioredoxina, glutaredoxina, glutatona S-transferase e glicose desidrogenase como alvos do VCH e/ou MeHg^+ . Em conjunto estes dados sugerem que o uso de insetos no estudo da toxicidade de compostos é relevante, sendo a *D. melanogaster* amplamente utilizada na pesquisa e a *N. cinerea* sendo validada como organismo experimental potencial para estudos translacionais. Indicamos também potenciais alvos do MeHg^+ e VCH que podem ser potenciais biomarcadores de toxicidade precoce a estes xenobióticos.

Palavras-chave: MeHg^+ ; VCH; modelo alternativo; toxicidade; transcriptoma.

ABSTRACT

MOLECULAR AND BIOCHEMICAL PARAMETERS ON ACUTE AND CHRONIC *per os* EXPOSURE TO ELECTROPHILIC XENOBIOTICS IN INSECT MODELS

AUTHOR: Bruna Candia Piccoli
SUPERVISOR: João Batista Teixeira da Rocha
CO-SUPERVISOR: Daniel Mendes Pereira Ardisson de Araújo
CO-SUPERVISOR: Ana Lúcia Anversa Segatto

Continuous exposure to small doses of toxic substances elicit changes in the transcriptional profile and function of proteins before causing physical damage to organisms. Toxic effects can appear even after exposure stops. Knowing the mechanism of action and identifying biomarkers of early substance toxicity are interests of the scientific community. As humans are continually exposed to several xenobiotics, it is necessary to study the effects of concomitant exposure to two or more toxic agents and establish experimental models for translational studies. Xenobiotics like methylmercury (MeHg⁺) and vinylcyclohexene (VCH) have similar electrophilic properties, albeit their combined toxicity profile has not been assessed. Thus, this work aims to study the effects of *per os* acute, intermediate and chronic exposure to MeHg⁺ and the possible reversal of the effects of this xenobiotic after the interruption of exposure in behavioral and biochemical parameters of the Lobster cockroach *N. cinerea*, as well as the individual and combined effect of MeHg⁺ and VCH on the transcriptional profile of the fly *D. melanogaster* since these compounds have similarities in their toxicity mechanisms (affinity for proteins containing –SH and –SeH). Cockroaches were exposed to diets containing 0 (control), 2.5, 25, and 100 µg of MeHg⁺/g of diet for 10, 30, and 90 days. Additional groups of cockroaches were fed the same doses of MeHg⁺ for 30 days and then underwent a detoxification period for 60 days. Nymphs exposed to 100 µg MeHg⁺/g succumbed to a high mortality rate, along with biochemical changes (increased production of reactive oxygen species and activity of glutathione S-transferase, as well as decreased acetylcholinesterase activity) and behavioral changes. We observed delayed mortality and behavioral changes in nymphs exposed to 100 µg MeHg⁺/g for 30 days with a subsequent 60 day detoxification period. To evaluate the transcriptional profile of *D. melanogaster*, RNA-sequencing of exposed flies was performed individually and concurrently at 1 mM VCH and 200 µM MeHg⁺ for three days. The VCH deregulated 38 genes (most of which were overexpressed), while MeHg⁺ altered 26 genes (14 down-regulated genes). The co-exposure of the VCH + MeHg⁺ altered 72 genes with a greater number of down-regulated genes. These results suggest that, although the compounds might have some similar protein targets, the transcriptional profile after individual exposures and co-exposure was different. The set of proteins that contains –SH and –SeH was explored and we identified thioredoxin, glutaredoxin, glutathione S-transferase, and glucose dehydrogenase as targets for VCH and/or MeHg⁺. Together, these data suggest that the use of insects in the study of compound toxicity is relevant, with *D. melanogaster* being widely used in research and *N. cinerea* being validated as a potential experimental organism for translational studies. We also indicate possible targets for MeHg⁺ and VCH that may be potential biomarkers of early toxicity to these xenobiotics.

Keywords: MeHg⁺; VCH; alternative model; toxicity; transcriptome

LISTA DE ILUSTRAÇÕES

APRESENTAÇÃO

| | | |
|------------|--|----|
| Figura 1 – | Ciclo do mercúrio no ambiente..... | 17 |
| Figura 2 – | Ingestão de peixe contaminado com MeHg ⁺ | 18 |
| Figure 3 – | Ataque nucleofílico realizado pelas proteínas ao MeHg ⁺ | 19 |
| Figura 4 – | Metabolização do vinilciclohexeno pelo citocromo P450 de humanos..... | 22 |
| Figura 5 – | Ataque nucleofílico realizado pelas proteínas ao VCD..... | 22 |
| Figura 6 – | Comparação dos órgãos humanos com órgãos funcionalmente análogos da <i>D. melanogaster</i> | 24 |
| Figura 7 – | Montagem dos transcritos baseado no genoma de referência..... | 28 |

ARTIGO 1

| | | |
|-------------|---|----|
| Figura 1 – | Experimental design..... | 33 |
| Figura 2 – | Kaplan-Meier survival curve of nymphs..... | 35 |
| Figura 3 – | Total food intake and MeHg ⁺ consumption by nymphs exposed to different doses of MeHg ⁺ | 35 |
| Figura 4 – | Time spent with the familiar object by nymphs exposed to MeHg ⁺ | 36 |
| Figura 5 – | Time spent with the unfamiliar object by nymphs exposed to MeHg ⁺ | 37 |
| Figura 6 – | Ratio of time spent with the familiar and unfamiliar object by the nymphs exposed to MeHg ⁺ | 38 |
| Figura 7 – | DCFHDA oxidation in the head and fat body of nymphs exposed to MeHg ⁺ | 39 |
| Figura 8 – | Glutathione S-transferase activity in the head and fat body of nymphs exposed to MeHg ⁺ | 40 |
| Figura 9 – | Acetylcholinesterase activity in the head of nymphs exposed to MeHg ⁺ | 41 |
| Figura 10 – | Molecular docking simulations of <i>N. cinerea</i> GST and MeHg ⁺ species..... | 41 |
| Figura 11 – | Molecular docking simulations between the cockroach AChE and MeHg ⁺ species..... | 42 |

ARTIGO 2

| | | |
|------------|--|----|
| Figura 1 – | Global mRNA expression of <i>D. melanogaster</i> chromosomes after acute feeding exposure and co-exposure to VCH and MeHg ⁺ | 48 |
| Figura 2 – | Venn diagram of significantly up- and down regulated genes in <i>D. melanogaster</i> after acute feeding exposure and co-exposure to VCH and MeHg ⁺ | 49 |
| Figura 3 – | Number of significantly deregulated genes in gene ontology in <i>D. melanogaster</i> after acute feeding exposure and co-exposure to VCH and MeHg ⁺ | 50 |
| Figura 4 – | Relative expression of selenoprotein-encoding genes of <i>D. melanogaster</i> after acute feeding exposure and co-exposure to VCH and MeHg ⁺ | 50 |
| Figura 5 – | Relative expression of thioredoxin genes of <i>D. melanogaster</i> after acute feeding exposure and co-exposure to VCH and MeHg ⁺ | 50 |
| Figura 6 – | Relative expression of glutathione S-transferase genes of <i>D. melanogaster</i> after acute feeding exposure and co-exposure to VCH and MeHg ⁺ | 50 |
| Figura 7 – | Relative expression of glutaredoxin genes of <i>D. melanogaster</i> after acute feeding exposure and co-exposure to VCH and MeHg ⁺ | 51 |

LISTA DE TABELAS

ARTIGO 1

| | |
|---|----|
| Tabela 1 – Predicted binding free energy (Kcal/mol) from docking between the GST and AChE enzymes with the MeHg ⁺ species..... | 42 |
|---|----|

LISTA DE ABREVIATURAS E SIGLAS

| | |
|-------------------|--|
| MeHg ⁺ | Metilmercúrio |
| VCH | Vinilciclohexeno |
| VCM1 | 4-vinilciclohexeno 1,2-epóxido |
| VCM2 | 4-vinilciclohexeno 7,8-epóxido |
| VCD | 4-vinilciclohexeno diepóxido |
| LAT | Transporte de aminoácidos neutros tipo L |
| OAT | Transportadores de ânions orgânicos |
| MRP | Resistência a múltiplas drogas |
| SNC | Sistema Nervoso Central |
| Cys | Cisteína/ Cysteine |
| Sec | Selenocisteína/ Selenocysteine |
| Val | Valina/ Valine |
| Phe | Fenilalanina/ Phenylalanine |
| Tyr | Tirosina/ Tyrosine |
| Trp | Triptofano/ Tryptophan |
| Ser | Serina/ Serine |
| Gly | Glicina/ Glycine |
| GSH | Glutathiona reduzida/ Reduced glutathione |
| GST | Glutathiona S-transferase/ Glutathione S-transferase |
| Trx | Tiorredoxina |
| TrxR | Tiorredoxina redutase |
| mEH | Hidrolase Microsomal Epóxido/ Microsomal epoxide hydrolase |
| SelG | Selenoproteína rica em glicina/ |
| Bthd | Selenoproteína Birthday/ Selenoprotein BthD |
| Sps2 | Selenofosfato sintetase 2/ |
| SELD | Seleneto, água diquinase |
| SelD | Selenide, water diquinase |
| Gld | Glicose desidrogenase/ Glucose dehydrogenase |
| Kel | Proteína kelch do canal do anel/ Ring canal kelch protein |
| mRNA | RNA mensageiro |
| rRNA | RNA ribossômico |
| tRNA | RNA transportador |
| miRNA | Micro RNA |
| RNA | Ácido ribonucleico/ Ribonucleic acid |
| RNA-seq | Sequenciamento de RNA/ RNA sequencing |
| DNA | Ácido Desoxirribonucleico/ Deoxyribonucleic acid |
| cDNA | DNA complementar/ complementary DNA |
| EDTA | Ethylenediaminetetraacetic acid |
| CDNB | 1-Chloro-2,4-dinitrobenzene |
| DTNB | 5,5'-Dithiobis(2-nitrobenzoic acid) |
| DCFH-DA | 2,7-Dichloro-dihydro-fluorescein diacetate |
| AChE | Acetilcolinesterase/ Acetylcholinesterase |
| ABP | Sítio de ligação acil/ Acyl binding pocket |
| PAS | Sítio aniônico periférico/ Peripheral anionic |
| OL | Omega Loop |
| OH | Buraco de oxiânion/ Oxyanion Hole |
| AS | Subsítio aniônico/ Anionic Subsite |

| | |
|--------------------------|--|
| PDB | Protein Data Bank |
| SEM | Standard error of mean |
| ANOVA | Análise de variância/ Analysis of variance |
| DEG | Gene diferencialmente expreso/ Differential expressed genes |
| FC | Fold change |
| GO | Gene ontology |
| CDS | Coding sequence |
| Rh1 | Rhodopsin |
| Dro | Drosocin / Drosocina |
| Im18 | Immune induced peptide |
| Cp16 | Chorion protein 16 / Proteína coriônica 16 |
| Cp18 | Chorion protein 18 / Proteína coriônica 18 |
| Hoip | NHP2-like protein / Proteína do tipo NHP2 |
| Fst | Frost / Congelamento |
| E(spl)mδ | Potenciador do gene mDelta do complexo Split |
| Kirre(duf) | <i>Dumbfounded</i> |
| Sns | Sticks and Stones |
| If | Integrin alpha-PS2 |
| Rols | Rolling pebbles |
| MyoG | Miogenina |
| ERO | Espécie reativa de oxigênio |
| tRNA ^{[Ser]Sec} | RNA transportador da selenocisteína |
| SerS | Seril-tRNA sintetase/ seryl-tRNA synthetase |
| PSTK | Fosfoseril-tRNA cinase/ Phosphoseryl-tRNA kinase |
| SEPSecS | Fosfoseril-tRNA selênio transferase/ phosphoseryl-tRNA selenium transferase enzyme |

LISTA DE SÍMBOLOS

| | |
|-----------------|----------------------------|
| Hg | Mercúrio |
| Hg ⁰ | Mercúrio elementar |
| HCl | Ácido clorídrico |
| MeHgCl | Methylmercury chloride |
| S | Enxofre/ Sulfur |
| Se | Selênio/ Selenium |
| -OH | Hidroxila |
| -SH | Tiol |
| -SeH | Selenol |
| ppm | Partes por milhão |
| mol | Molar |
| μM | Micromolar |
| mM | Milimolar |
| μg | Micrograma |
| mg | Miligrama |
| g | Gramma |
| kg | Quilograma |
| Å | Angstrom |
| nm | Nanômetro |
| cm | Centrômetro |
| μL | Microlitro |
| mL | Mililitro |
| % | Porcentagem |
| °C | Graus Celsius |
| s | Segundos |
| min | Minutes |
| h | Horas |
| Kcal | Quilocalorias |
| < | Menor |
| ± | Mais ou menos |
| RPKM | Reads Per Kilobase Million |

SUMÁRIO

| | | |
|----------|--|----|
| 1 | INTRODUÇÃO | 14 |
| 1.1 | XENOBIÓTICOS ELETROFÍLICOS..... | 15 |
| 1.1.1 | Metilmercúrio..... | 16 |
| 1.1.2 | Vinilciclohexeno..... | 21 |
| 1.2 | MODELOS EXPERIMENTAIS..... | 23 |
| 1.2.1 | <i>Nauphoeta cinerea</i> | 24 |
| 1.2.2 | <i>Drosophila melanogaster</i> | 25 |
| 1.3 | MODELAGEM MOLECULAR..... | 26 |
| 1.4 | TRANSCRIPTOMA..... | 26 |
| 1.4.1 | Sequenciamento de RNA e análise de expressão diferencial..... | 27 |
| 1.5 | JUSTIFICATIVA..... | 28 |
| 1.6 | OBJETIVO GERAL | 29 |
| 1.6.1 | Objetivos específicos..... | 29 |
| 2 | ARTIGO 1 – High level of methylmercury exposure causes persisted toxicity in <i>Nauphoeta cinerea</i> | 31 |
| 3 | ARTIGO 2 - Transcriptional analyses of acute <i>per os</i> exposure and co-exposure of 4-vinylcyclohexene and methylmercury-contaminated diet in adults of <i>Drosophila melanogaster</i> | 46 |
| 4 | DISCUSSÃO | 55 |
| 5 | CONCLUSÃO | 63 |
| 6 | PERSPECTIVAS | 63 |
| | REFERÊNCIAS BIBLIOGRÁFICAS | 63 |
| | APÊNDICE A – MATERIAL SUPLEMENTAR ARTIGO 1 | 76 |
| | APÊNDICE B – MATERIAL SUPLEMENTAR ARTIGO 2 | 80 |

APRESENTAÇÃO

Esta tese está descrita da seguinte forma: primeiramente é apresentada a introdução, com uma breve revisão sobre os temas abordados nesta tese, seguidos da justificativa e dos objetivos. A seguir, encontra-se o desenvolvimento na forma de dois artigos publicados em periódicos internacionais. As seções Introdução, Materiais e métodos, Resultados, Discussão, Conclusão e Referências bibliográficas encontram-se nos artigos e representam a íntegra deste estudo. No item discussão são apresentados interpretações e comentários gerais sobre os artigos. As referências bibliográficas apresentadas no final da dissertação referem-se às citações que aparecem no item introdução e discussão. Nos apêndices encontram-se os materiais suplementares dos artigos.

1 INTRODUÇÃO

A atividade antropogênica tem aumentado largamente a liberação de substâncias no meio ambiente, sendo estas conhecidamente tóxicas, bem como outras novas moléculas que possuem efeito desconhecido (TOUSOVA et al., 2017). Sendo assim, a população é constantemente exposta a uma ampla gama de xenobióticos (GRANDJEAN; LANDRIGAN, 2006). Sabe-se que a exposição contínua a pequenas doses de substâncias tóxicas retarda a ocorrência de efeitos físicos nos organismos, mas altera a expressão gênica e/ou a função de proteínas (WILSON et al., 2013; SCUMACI et al., 2018). A detecção de alterações na expressão gênica após exposição aguda a um determinado xenobiótico pode contribuir para o entendimento dos eventos moleculares iniciais e a sequência de eventos que causarão disfunção celular (HARTUNG et al., 2017), assim como, para a identificação de biomarcadores de toxicidade precoce (OLIVEIRA et al., 2020). Por sua vez, a exposição crônica possibilita a avaliação dos sinais e sintomas decorrentes do contato com o xenobiótico, assim como, a avaliação do(s) mecanismo(s) de toxicidade e, desta maneira, estratégias para revertê-los (ZAITSU et al., 2016; DANI; WALTER, 2018; MOHAMMADPOUR et al., 2019). Além disso, é sabido, que mesmo após a interrupção da exposição a uma substância tóxica, o indivíduo ainda pode apresentar sintomas relacionados a esta ou até mesmo o surgimento de sintomas de forma retardada (HARADA 1995; WEISS; CLARKSON; SIMON, 2002; EKINO et al., 2007).

Neste sentido, destacam-se xenobióticos como o vinilciclohexeno (VCH), um derivado do plástico, e o metilmercúrio (MeHg^+), composto orgânico de Hg considerado um dos mais tóxicos dentre esta classe. As formas quimicamente ativas destes compostos são consideradas eletrófilos, deste modo, possuem alta afinidade por grupamentos nucleofílicos, dentre os quais se destacam os grupos tiol (-SH) e selenol (-SeH) (OLIVEIRA et al., 2017). Estes grupamentos estão presentes na maioria das moléculas do sistema antioxidante (BISENHESH et al., 2014), portanto, acredita-se que o mecanismo de toxicidade do VCH e do MeHg^+ esteja relacionado com a inativação de peptídeos e proteínas (RIZZO et al., 2012; OLIVEIRA et al., 2017).

A utilização de modelos experimentais na pesquisa auxilia a descoberta da fisiologia, da etiopatogenia das doenças, da ação de medicamentos, dos efeitos das intervenções cirúrgicas e do mecanismo de toxicidade de xenobióticos (FERREIRA; HOCHMANN; BARBOSA, 2005). A substituição dos modelos experimentais mamíferos por modelos alternativos, como por exemplo, os insetos, é uma necessidade no meio científico, tendo em

vista a adesão dos 3Rs (substituição, redução e refinamento) no uso de animais de experimentação (CHELUVAPPA; SCOWEN; ERI, 2017; CLARK 2018; LANG et al., 2018). Os insetos têm ciclo de vida mais curto e sua manutenção é mais barata (redução de 100 vezes nos custos) do que os vertebrados, além de possuírem uma relação evolutiva com os mamíferos, o que permite estabelecer paralelos entre rotas metabólicas e de desenvolvimento (PETERSON et al., 2008; BERGER 2009).

1.1 XENOBIÓTICOS ELETROFÍLICOS

Xenobiótico se refere a qualquer produto químico (pesticidas, contaminantes ambientais, medicamentos, drogas de abuso, entre outros), extrínseco ao metabolismo, ao qual um organismo é exposto. Ao entrar no organismo, o xenobiótico pode ser eliminado, retido, sofrer alteração espontânea e/ou ser metabolizado. O metabolismo é dividido em três fases principais: fase I, fase II e transporte para excreção (CROOM, 2012). As reações da fase I são responsáveis por tornarem os xenobióticos mais hidrofílicos e fornecer sítios de ligação para reações de conjugação da fase II. As principais enzimas envolvidas na fase I de desintoxicação pertencem à superfamília de proteínas do citocromo P450 e são responsáveis por reações de oxirredução. Enzimas monooxigenases dependentes de flavina, epoxidases, hidroxilases, desidrogenases e amidases também fazem parte da fase I de desintoxicação (CROOM, 2012). Na fase II de desintoxicação ocorre a conjugação de xenobióticos (a maioria produtos das reações da fase I de desintoxicação) com moléculas como glutathiona, ácido glucurônico uridina difosfato ou 3'-fosfoadenosina-5'-fosfosulfato. O próximo passo é a eliminação destas moléculas que pode ocorrer através dos rins, trato gastrointestinal ou pulmões. Transportadores podem carrear os metabólitos conjugados para serem excretados pela urina ou bile, sendo a polaridade do xenobiótico e/ou de seus metabólitos o que definirá a via de eliminação. Neste sentido, moléculas hidrofílicas são excretadas pela urina, já moléculas lipofílicas são incorporadas à bile e eliminadas pelas fezes. Produtos voláteis e o CO₂, proveniente da metabolização do xenobiótico, são eliminados pelos pulmões. Outras rotas de eliminação menores incluem suor, lágrimas, cabelo e leite materno (CROOM, 2012).

Nos itens a seguir, comentaremos as formas de exposição, metabolização e excreção do MeHg⁺ e do VCH que se tem evidências até o momento. É importante ressaltar que embora nos referimos aos efeitos da exposição simultânea a estes xenobióticos, os humanos não necessariamente se expunham ao MeHg⁺ e do VCH ao mesmo tempo.

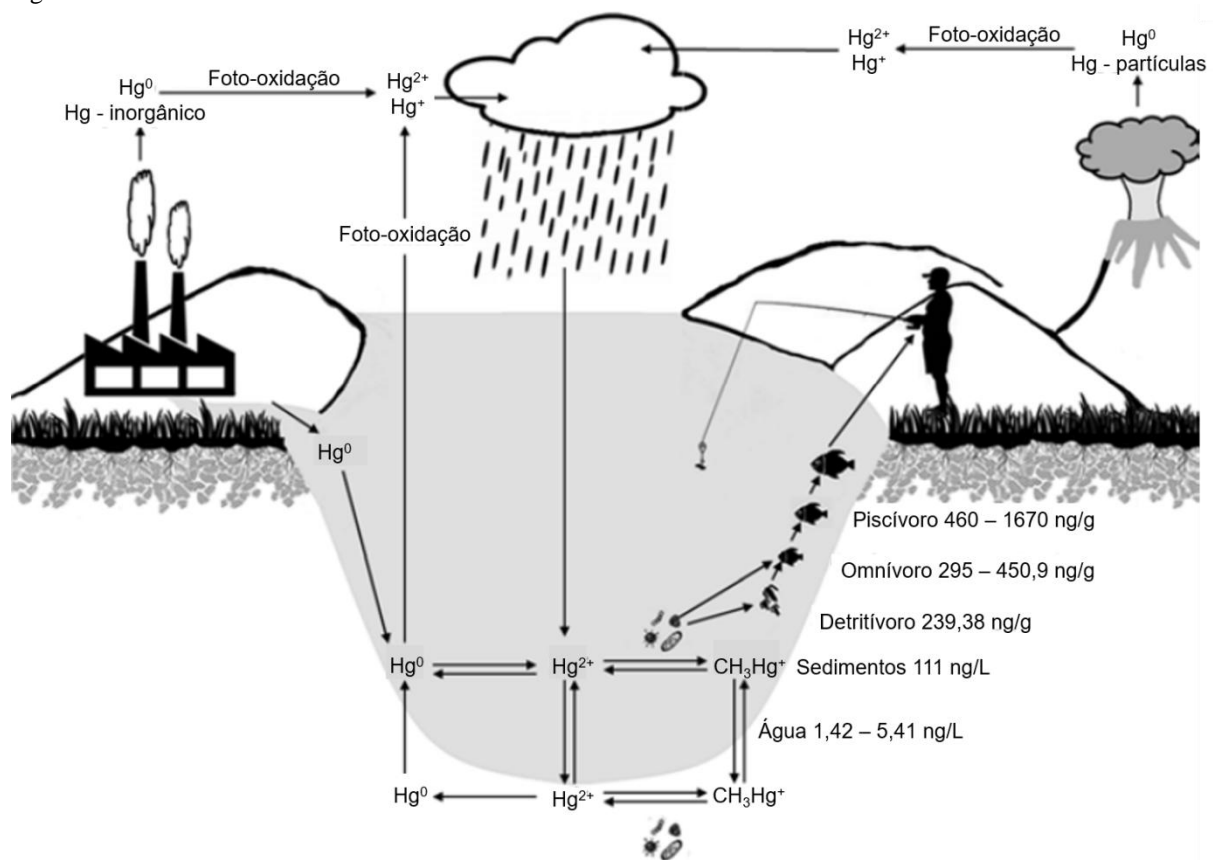
1.1.1 Metilmercúrio

O mercúrio (Hg) pode ser encontrado naturalmente no ambiente como produto do vulcanismo e da erosão e através da atividade antropogênica, como a mineração e resíduos de processos industriais (Figura 1) (MUNTEAN et al., 2014; OLIVEIRA et al., 2017). Este elemento pode ser encontrado na forma elementar (Hg^0), assim como, em diferentes estados de oxidação (Hg^+ e Hg^{2+}) ou mesmo presente em moléculas orgânicas. Quando o mercúrio inorgânico atinge o ambiente aquático, sofre metilação por micro-organismos (principalmente pelas bactérias dos gêneros *Pseudomonas*, *Stenotrophomonas*, *Desulfovibrio*, *Sphingobacterium*, *Comamonas*, *Pseudodesulfovibrio*, *Gemmobacter* e *Exiguobacterium*) formando o MeHg^+ (COMPEAU; BARTHA, 1985; LU et al., 2018; RANCHOU-PEYRUSE et al., 2018; XING et al., 2018). O MeHg^+ possui um alto potencial de biomagnificação na cadeia alimentar aquática, onde os níveis podem atingir a faixa de 1 mg MeHg^+ /kg em músculo em peixes predadores (OLIVEIRA et al., 2017). Além disso, o MeHg^+ também pode bioacumular nas plantas aquáticas e terrestres (BOENING 2000; CUI et al., 2017). Por isso, a ingestão é considerada a principal forma de contaminação por MeHg^+ e populações que consomem peixes habitualmente podem ser expostas a níveis elevados deste xenobiótico (CLARKSON; MAGOS; MYERS, 2003; HINTELMANN, 2010; MARTÍNEZ-SALCIDO et al., 2018). Como o Hg não possui nenhuma função bioquímica ou fisiológica conhecida nos seres vivos, à exposição a quaisquer formas deste metaloide (elementar, inorgânico e/ou orgânico) possui significado toxicológico (FARINA, ASCHNER; ROCHA, 2011; BRANDÃO et al., 2015).

No músculo dos peixes, o MeHg^+ encontra-se predominantemente ligado a cisteína (MeHg-S-Cys) da glutathiona (GSH) ou de proteínas (BRADLEY; BARST; BASU, 2017) (Figura 2). Após a ingestão de peixe contaminado, as proteínas que contém MeHg^+ são digeridas e liberam MeHg-S-Cys . O baixo pH e a alta concentração de Cl^- , faz com que o H^+ desloque o MeHg^+ formando $\text{Cys} + \text{MeHgCl}$. O MeHgCl pode ser aprisionado no muco estomacal e se ligar novamente a resíduos cisteinil de proteínas, como a mucina. Ambos MeHgCl (estômago) o MeHg-S-Cys (intestino) podem ser absorvidos (NOGARA et al., 2019a). O MeHgCl pode entrar nas células por difusão ou por processos ativos não específicos. O complexo MeHg-S-Cys ultrapassa a membrana celular dos enterócitos através do transportador de aminoácidos neutros tipo L (LAT) com gasto de energia (BRADLEY; BARST; BASU, 2017) ou pode envolver um ou mais membros da família dos transportadores de ânions orgânicos (OAT) (BRIDGES; ZALUPS, 2010). A absorção intestinal do MeHg^+

pelo trato gastrointestinal varia entre 12 % a 79 % em humanos (BRADLEY; BARST; BASU, 2017). Dentro dos enterócitos, podem ocorrer reações de troca de $-SH$ com a GSH e/ou outras proteínas que contêm $-SH$ e $-SeH$. Estes complexos podem acessar a corrente sanguínea através de proteínas associadas à resistência a múltiplas drogas (MRPs) e/ou LAT. Uma vez no sistema circulatório, o $MeHg^+$ se liga à hemoglobina e/ou proteínas que contêm $-SH$ como GSH e albumina e é transportado para os tecidos (NOGARA et al., 2019a).

Figura 1 – Ciclo do mercúrio no ambiente.

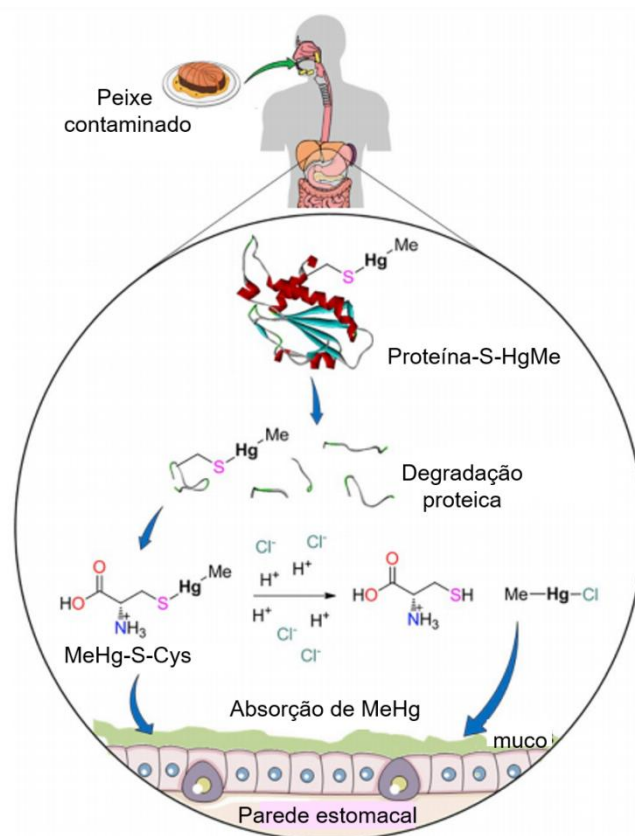


O mercúrio elementar (Hg^0) e inorgânico pode ser liberado no ambiente de forma antropogênica, como dejetos de fábricas e da atividade de mineração, como também de forma natural, através da atividade vulcânica e da erosão. O Hg^0 sofre oxidação gerando Hg^{2+} . Quando atinge o ambiente aquático, o Hg^{2+} sofre processo de metilação por micro-organismos, formando metilmercúrio ($MeHg^+$), o qual é biomagnificado na cadeia alimentar aquática. Populações que consomem peixes dos níveis mais altos da cadeia alimentar podem ser expostas a grandes quantidades de $MeHg^+$. Fonte: Oliveira et al. (2017).

A alta toxicidade do $MeHg^+$ deve-se ao fato desta molécula ser considerada um eletrófilo mole, possuindo elevada afinidade por nucleófilos moles, como os grupos $-SH$ e $-SeH$, o que ocorre também nos organismos vivos. Os grupos $-SH$ e $-SeH$ estão presentes nos aminoácidos cisteína e selenocisteína, respectivamente (FARINA, ASCHNER; ROCHA,

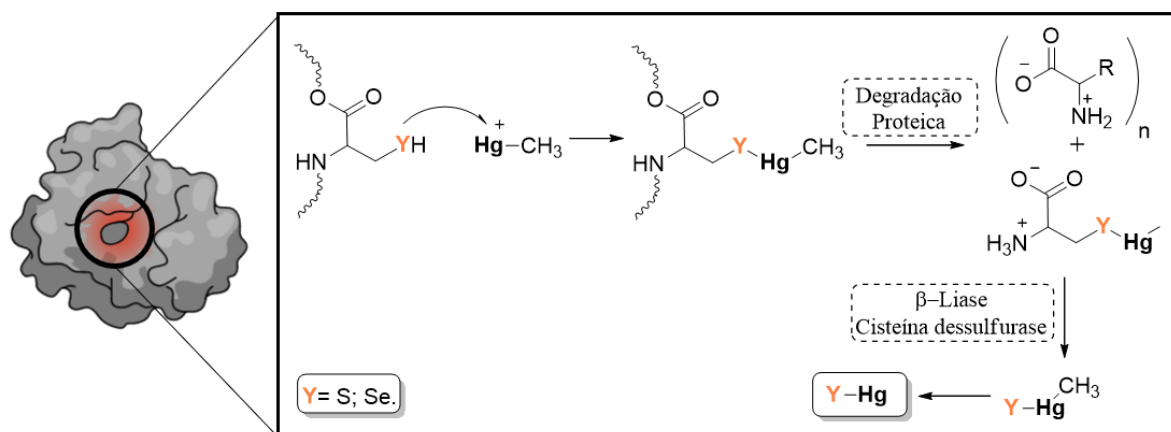
2011; ROCHA; PICCOLI; OLIVEIRA, 2017). A cisteína faz parte de compostos de baixa massa molecular, como a GSH, e de milhares de proteínas. Já a selenocisteína faz parte de um pequeno número de proteínas chamadas selenoproteínas, que correspondem a 25 selenoproteínas nos humanos, 24 nos camundongos e 37 nos peixes-zebra (ROCHA; PICCOLI; OLIVEIRA, 2017). Uma vez que o MeHg^+ se liga covalentemente a esses grupos, as proteínas que contém $-\text{SH}$ e as selenoproteínas perdem a função e são degradadas. As enzimas β -liase ou cisteína dessulfurase catalisam a reação que resulta na liberação do grupo sulfeto ou seleneto ligado ao átomo de Hg. O HgS e o HgSe são, provavelmente, biologicamente inertes (Figura 3) (OLIVEIRA et al., 2017).

Figura 2 – Ingestão de peixe contaminado com MeHg^+ .



Após a ingestão de peixe contaminado com MeHg^+ ocorre a digestão das proteínas ligadas a este xenobiótico no estômago, liberando MeHg-S-Cys . O baixo pH leva a protonação do átomo de S da Cys seguido por um ataque do átomo de Cl^- ao Hg, restituindo a Cys e liberando MeHgCl . Fonte: Nogara et al. (2019a)

Figura 3 - Ataque nucleofílico realizado pelas proteínas ao MeHg^+ .



Proteínas que contêm tiol e selenoproteínas, as quais contêm os grupamentos nucleofílicos $-\text{SH}$ e $-\text{SeH}$, respectivamente ($\text{Y} = \text{S}$ ou Se) podem atacar o Hg ligando-se covalentemente a este composto. Após a degradação da proteína, a enzima β -liase ou cisteína dessulfurase catalisa a liberação de grupo sulfeto ou seleneto ligado ao átomo de Hg (isto é, como HgS ou HgSe). FONTE: Adaptada de Oliveira et al. (2017).

Moléculas de baixa massa molecular (cisteína e GSH, por exemplo) e alta massa molecular, como as enzimas oxidoreduções, as quais contêm $-\text{SH}$, constituem o sistema antioxidante endógeno (BISEN-HERSH et al., 2014). Ainda não se tem conhecimento sobre a função de todas as selenoproteínas, mas muitas pertencem ao sistema antioxidante, como a glutatona peroxidase e a tioredoxina redutase em humanos (ROCHA; PICCOLI; OLIVEIRA, 2017). Acredita-se, que o principal alvo de toxicidade do MeHg^+ esteja relacionado a perda da função das proteínas que contêm $-\text{SH}$ e das selenoproteínas. Além disso, o MeHg^+ ligado à cisteína (MeHg-S-Cys) ultrapassa a barreira hematoencefálica através do LAT1 e LAT2 mimetizando a metionina em humanos (ASCHNER 1989; BRIDGES; ZALUPS, 2016) podendo causar danos ao Sistema Nervoso Central (SNC) (ZAREBA et al., 2002; OLIVEIRA et al., 2018). A acetilcolinesterase (AChE) é um dos alvos de MeHg^+ no SNC, esta enzima é um biomarcador da atividade colinérgica, a qual hidroliza o neurotransmissor acetilcolina em acetato e colina interrompendo a transmissão sináptica (MILATOVIC; DETTBARN, 1996; AHMED et al., 2006). Estudos já demonstraram que o MeHg^+ altera a atividade desta enzima o que pode causar alterações cognitivas e neuromusculares (ABOLAJI et al., 2014; 2015; MONTGOMERY et al., 2014; ADEDARA et al., 2015; 2016; PRINCE; RAND, 2018a; 2018b). O déficit de memória é uma das alterações cognitivas associadas à desregulação da AChE, embora também possa ter outras causas, o qual pode ser avaliado por testes comportamentais que incluem o teste de reconhecimento de objeto (LEGER et al., 2013).

Juntamente com os fatores citados acima, outro aspecto importante na toxicidade de MeHg^+ são os poucos mecanismos de desintoxicação conhecidos. Uma das estratégias bem documentadas envolve a enzima glutationa S-transferase (GST). Esta enzima conjuga xenobióticos eletrofílicos, como o MeHg^+ , com a GSH a fim de que este complexo seja eliminado do organismo (SHEEHAN et al., 2001). Devido a esse mecanismo, a GST é outra enzima que serve de marcador de toxicidade para MeHg^+ .

Dois grandes casos de envenenamento por MeHg^+ ficaram famosos na história. Um deles aconteceu na cidade de Minamata no Japão (1950–1975) onde indústrias que utilizavam Hg como catalisador na síntese de acetaldeído liberavam rejeitos contendo este metal nas águas da baía. O Hg^{2+} foi metilado pelas bactérias presentes no sedimento, sendo biomagnificado na cadeia alimentar aquática e os peixes atingiram níveis maiores de 50 ppm (EKINO et al., 2007). O consumo dos peixes contaminados pela população, ou seja, a exposição crônica ao MeHg^+ , gerou distúrbios neuropatológicos que variaram entre leve parestesia à ataxia, disartria, visão turva, deficiência auditiva, distúrbios olfativos e gustativos, retardo mental, paralisia cerebral e morte. Além disso, foram registrados novos casos de intoxicação por MeHg^+ 15 anos após o fim do surto caracterizando toxicidade tardia (WEISS; CLARKSON; SIMON, 2002). Resultados similares também foram encontrados em primatas (WEISS; CLARKSON; SIMON, 2002) e em roedores (RICE 1996). O segundo caso de envenenamento aconteceu entre os anos de 1971 e 1972 na área rural do Iraque onde a população ingeriu pão feito com farinha de trigo previamente tratada com MeHg^+ , o qual foi utilizado como fungicida (BAKIR et al., 1973). A população ingeriu trigo contaminado por poucas semanas, pois logo as autoridades alertaram sobre o perigo de intoxicação configurando, assim, uma exposição aguda ao MeHg^+ . Neste caso, o período médio de latência do aparecimento dos sintomas variou entre 16 – 38 dias, aproximadamente, e a gravidade dos sintomas foi proporcional ao nível de exposição (BAKIR et al., 1973; WEISS; CLARKSON; SIMON, 2002).

No Brasil, a bacia Amazônica destaca-se pela contaminação com metilmercúrio devido à mineração de ouro na região sendo a população ribeirinha, que se alimenta de peixe com frequência, muito afetada pelos efeitos do MeHg^+ (BASTOS et al., 2015; DÓREA; MARQUES, 2016). Além disso, recentemente os rompimentos das barragens com resíduo da mineração de ferro em Mariana (2015) e Brumadinho (2019), no estado de Minas Gerais, causaram aumento nos níveis de metais pesados nos rios Doce e Paraopeba, respectivamente. Em Mariana, os níveis de mercúrio, arsênio, cádmio, cobre, cromo e níquel aumentaram nas águas do rio Doce (FERNANDES et al., 2016) e as concentrações de As e Hg aumentaram

nos peixes afetados pela lama (FERREIRA et al., 2019). Em Brumadinho, o nível de Hg na água no primeiro trimestre após o rompimento da barragem ficou acima do limite permitido ($>0,2 \mu\text{g/L}$) e este valor normalizou a partir do segundo trimestre. Outros metais como Al, Pb, Fe e Mn permaneceram altos mesmo após um ano do rompimento da barragem (RAMOS et al., 2020). O monitoramento dos níveis de metais pesados nas regiões afetadas por estes desastres ambientais devem ser realizado a fim de que minimizem os efeitos à população.

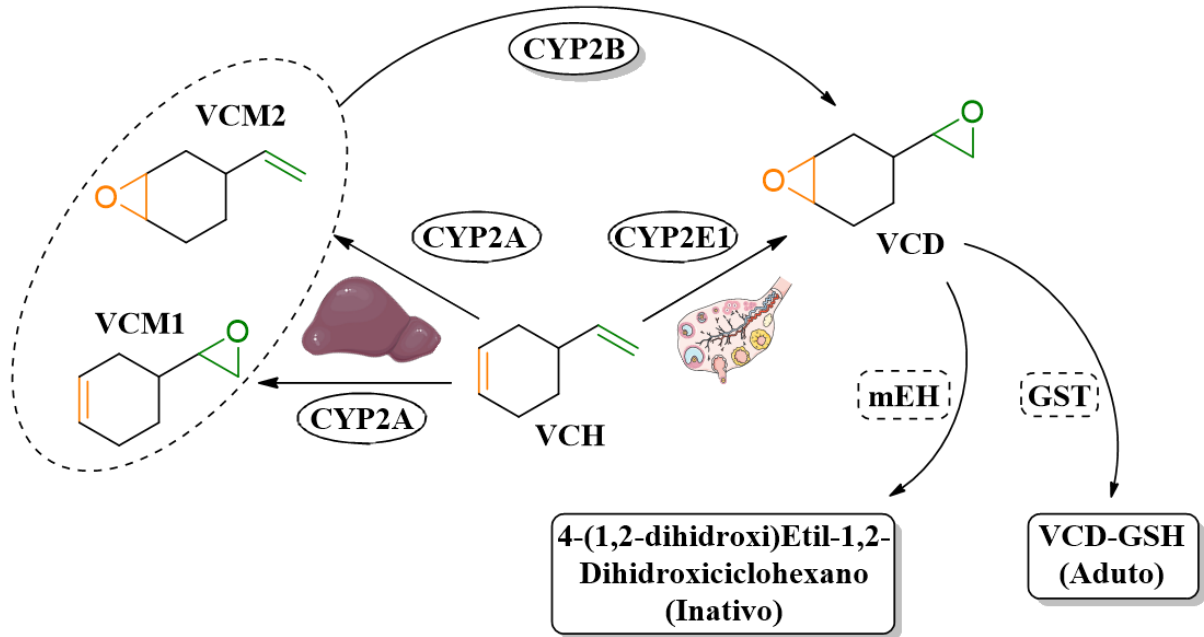
1.1.2 Vinilciclohexeno

O VCH está presente em plásticos, borrachas e pesticidas, desta forma, a exposição passiva a este composto pode acontecer através da ingestão, inalação e contato dérmico (BHATTACHARYA; KEATING, 2012). A exposição ao VCH pode ser considerada um problema de saúde pública por estar associada à toxicidade frente ao sistema reprodutor feminino (SPRINGER et al., 1996; MAYER et al., 2002; TRAN et al., 2018). Em sua estrutura há duas ligações duplas carbono-carbono. No organismo humano, citocromos localizados no fígado e nos ovários oxidam essas ligações (Figura 4). No fígado, o citocromo P450 2A oxida uma das ligações duplas formando dois possíveis metabólitos monoepóxidos (VCM1 - 4-vinilciclohexeno-1,2-epóxido e VCM2 - 4-vinilciclohexeno-7,8-epóxido). Posteriormente, o citocromo P450 2B oxida a ligação dupla restante formando o vinilciclohexeno diepóxido (VCD). Nos ovários, o citocromo P450 2E1 atua sobre o VCH formando VCD diretamente (KEATING et al., 2008). A inativação do VCD pode ocorrer pela enzima hidrolase microsossomal epóxido (mEH) levando a formação do 4-(1,2-dihidroxi)etil-1,2-dihidroxiciclohexano (CANNADY et al., 2002) ou envolvendo a GST a qual conjuga o VCD com a GSH a fim de que este complexo seja eliminado (RAJAPAKSA, 2007).

O metabolismo do VCH leva a formação de epóxidos, compostos contendo centros eletrofílicos os quais possuem afinidade por nucleófilos, com destaque para os grupamentos -SH e -SeH. Como dito anteriormente, estes grupamentos encontram-se, principalmente, em proteínas importantes para a homeostase redox da célula (ABOLAJI et al., 2015). Desta forma, os metabólitos do VCH poderiam causar estresse oxidativo por depleção destas proteínas (RIZZO et al., 2012). Além disso, o VCH e seus metabólitos estão fortemente relacionados à destruição dos folículos primários e primordiais causando menopausa precoce. Por sua vez, a menopausa precoce está associada ao maior risco de desenvolver doenças cardiovasculares, osteoporose, síndrome metabólica, câncer de ovário, doença de Alzheimer e

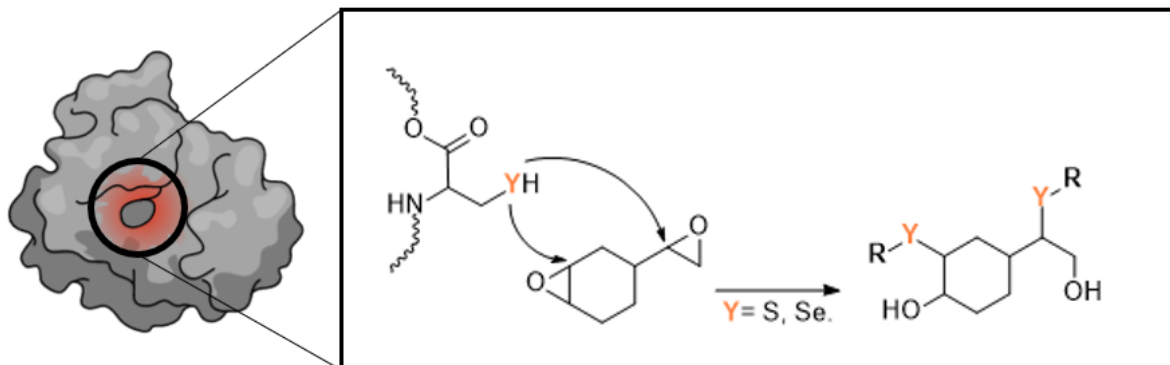
depressão (SOWERS; LAPIETRA, 1995; WARING et al., 1999; CARR, 2003; VANDERHYDEN, 2005; KAPPELER; HOYER, 2012).

Figura 4 – Metabolização do vinilciclohexeno pelo citocromo P450 de humanos.



O 4-vinilciclohexeno (VCH), quando metabolizado no fígado, sofre a primeira oxidação pelo citocromo P450 2A, sendo convertido em dois possíveis metabólitos monoepóxidos (VCM1 e VCM2). Posteriormente, ocorre uma nova oxidação pelo citocromo P450 2B transformando-o no seu metabólito diepóxido (VCD). Já nos ovários, o citocromo P450 2E1 transforma o VCH diretamente em VCD. As enzimas hidrolase microsomal epóxido (mEH) e glutathione S-transferase os transformam em metabólitos inativos. Fonte: Adaptada de Abolaji et al. (2014)

Figura 5 – Ataque nucleofílico realizado pelas proteínas ao vinilciclohexeno diepóxido.



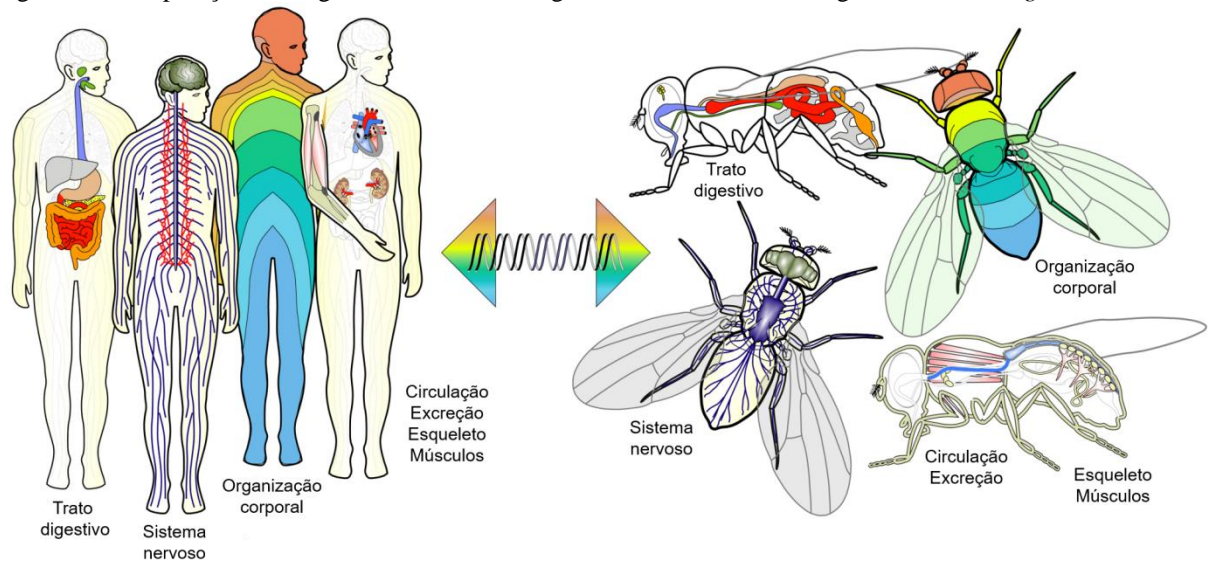
Proteínas que contêm tiol e selenoproteínas, as quais contêm os grupamentos nucleofílicos -SH e -SeH, respectivamente (Y = S ou Se) podem atacar os grupos époxido do vinilciclohexeno diepóxido (VCD) ficando ligados covalentemente a este composto. Desta forma, o VCD pode inativar a enzima. FONTE: Autor.

1.2 MODELOS EXPERIMENTAIS

A utilização de insetos (classe *Insecta*) no estudo de doenças humanas ocorre a mais de 100 anos com a mosca *D. melanogaster* e, mais recentemente, com a barata *N. cinerea*. Devido à conservação evolutiva, humanos e insetos possuem processos celulares e fisiológicos, assim como, muitos órgãos funcionalmente análogos (Figura 6) (ELPIDINA et al., 2001; UGUR; CHEN; BELLEN, 2016). O sistema digestório dos insetos é um tubo dorsal que se estende desde a boca até o ânus e apresenta órgãos funcionalmente análogos aos humanos. Os alimentos ingeridos sofrem processo de digestão no intestino médio, são absorvidos no intestino grosso e distribuídos para o organismo através da hemolinfa (SILVA; LEMOS; SILVA, 2012). Os insetos possuem órgãos acessórios do sistema digestivo como o corpo gorduroso, equivalente funcional ao fígado humano, o qual é responsável por funções metabólicas, que inclui desintoxicação de substâncias tóxicas (UGUR; CHEN; BELLEN, 2016). O sistema nervoso é composto por um cérebro localizado na cabeça, circundado por uma membrana seletiva, chamada de barreira hemolinfa-neural (SCHIRMEIER, S.; KLÄMBT, 2016). O cérebro é seguido de uma série de gânglios enfileirados em um cordão nervoso ventral, localizado sob o tubo digestivo.

Quanto à digestão, absorção e distribuição dos xenobióticos aos tecidos dos insetos, fizemos algumas predições de acordo com os dados encontrados na literatura até o momento. O intestino médio dos insetos, equivalente funcional ao estômago humano, possui pH de 6,0 – 7,2 na porção anterior e 8,8 – 9,3 na porção posterior e não possui HCl para auxiliar na digestão (ELPIDINA et al., 2001). O pH alto e a ausência de HCl impede a formação de MeHgCl, por isso hipotetizamos que o MeHg⁺ é absorvido no intestino grosso dos insetos somente ligado a uma molécula que contém tiol (MeHg-S-Cys, principalmente), diferentemente do que ocorre nos humanos (Figura 2). Com relação ao VCH, até o momento não há evidências que este xenobiótico participe de alguma reação química durante o processo de digestão e absorção intestinal. Após a absorção do MeHg-S-Cys e do VCH, estes xenobióticos atingem a hemolinfa que possui uma alta concentração de aminoácidos livres (SOWA; KEELEY, 1996). Os insetos não possuem GSH ou albumina circulante na hemolinfa, por isso, o MeHg⁺ é distribuído para os tecidos na forma de MeHg-S-Cys.

Figura 6 – Comparação dos órgãos humanos com órgãos funcionalmente análogos da *D. melanogaster*.



Embora humanos e moscas tenham fenótipos extremamente diferentes, muitos dos sistemas de órgãos são funcionalmente análogos aos vertebrados, incluindo os humanos. FONTE: Manchester Fly Facility (2015)

1.2.1 *Nauphoeta cinerea*

Novos modelos de invertebrados foram desenvolvidos para estudar os aspectos moleculares e os sinais evidentes de toxicidade (comportamento, crescimento, etc.) (LOVATO; ROCHA; DALLA CORTE, 2017; MRDAKOVIĆ et al., 2019; RAND; PRINCE; VOROJEIKINA, 2019). A barata *Nauphoeta cinerea*, entre outras, foi indicada como um modelo valioso para estudos toxicológicos (SHAMBAUGH 1969; RODRIGUES et al., 2013; MRDAKOVIĆ et al., 2019). Esta barata é ovovivípara, cujo embrião se desenvolve dentro de um ovo alojado na fêmea e eclode no oviducto materno (MOORE; GOWATY; MOORE, 2003). Também é hemimetábolo, ou seja, seu desenvolvimento envolve três fases distintas que são ovo, ninfa e estágio adulto sendo que a ninfa que eclode do ovo é similar ao indivíduo adulto. Durante o período de ninfa faz 7 – 8 mudas ou ecdises. Na última ecdise torna-se adulta sendo possível distinguir macho e fêmea. O ciclo de vida da *N. cinerea* é de aproximadamente um ano (SPRINGHETTI; CIOCI, 1961).

Estudos avaliando expressão gênica nesta barata tornaram-se viáveis recentemente após o sequenciamento do transcriptoma da cabeça e do corpo gorduroso (SEGATTO et al., 2018). Além disso, a exposição da *N. cinerea* ao Hg, e a derivados orgânicos como o MeHg⁺, reproduz algumas das alterações bioquímicas e comportamentais observadas em mamíferos (RODRIGUES et al., 2013; ADEDARA et al., 2015, 2016; AFOLABI et al., 2018).

Entretanto, um aspecto pouco explorado, mesmo em roedores, é a reversibilidade da toxicidade do MeHg^+ .

1.2.2 *Drosophila melanogaster*

A *Drosophila melanogaster*, também conhecida como mosca da fruta, é um modelo experimental alternativo amplamente utilizado na pesquisa a mais de 100 anos (UGUR; CHEN; BELLEN, 2016). A mosca da fruta é ovípara, ou seja, seu embrião se desenvolve dentro de um ovo em ambiente externo, fora do corpo da fêmea (NARASIMHA et al., 2019). É um inseto holometábolo, o que significa que faz metamorfose completa e seu ciclo de vida apresenta quatro estágios: ovo, larva, pupa e adulto. Do ovo eclode uma larva (bastante diferente do indivíduo adulto) que passa para o estágio de pupa, onde ocorre a metamorfose e se transforma em um indivíduo adulto (em aproximadamente 10 dias) sendo possível distinguir macho e fêmea. Como indivíduo adulto, esta mosca vive entre 60 e 100 dias dependendo das condições do meio (FERNÁNDEZ-MORENO et al., 2007).

Foi o primeiro organismo complexo a ter seu genoma sequenciado (ADAMS et al., 2000) sendo um dos mais bem anotados e funcionalmente caracterizados. Com isso, descobriu-se que aproximadamente 65 % dos genes que causam doenças humanas possuem homólogos nas moscas (CHIEN et al., 2002) e grande parte destes genes são expressos em tecidos equivalentes aos dos humanos (CHINTAPALLI; WANG; DOW, 2007). Desta forma, a *D. melanogaster* é um modelo experimental propício para estudos toxicogenômicos, sendo um modelo valioso na biologia translacional (REITER et al., 2001; UGUR; CHEN; BELLEN, 2016).

Quanto as prováveis proteínas alvos dos xenobióticos eletrofílicos, a mosca da fruta possui três selenoproteínas bem descritas, sendo elas: selenoproteínas Bthd (BTHD) (MARTIN-ROMERO et al., 2001), selenoproteína rica em glicina (SELG) (CASTELLANO et al., 2001) e seleneto, água diquinase (SELD) (HIROSAWA-TAKAMORI; JÄCKLE; VORBRÜGGEN, 2000), e duas putativas: glicose desidrogenase (GLD) (WHETTEN et al., 1988) e a proteína kelch do canal do anel (KEL) (ROBINSON; COOLEY, 1997). A *D. melanogaster* também possui milhares de peptídeos e proteínas que contém $-\text{SH}$, destacando-se aquelas contidas no sistema antioxidante (ORR; RADYUK; SOHAL, 2013). Estas moléculas podem ser alvo do VCH e do MeHg^+ nas moscas, devido a afinidade destes compostos por grupamentos $-\text{SH}$ e $-\text{SeH}$.

1.3 MODELAGEM MOLECULAR

Devido às semelhanças entre proteínas humanas e de insetos, análises *in vitro* e *in silico* da atividade de enzimas podem ser usadas para prever respostas humanas a xenobióticos. Neste contexto, a modelagem molecular se destaca por sua capacidade de analisar interações em nível atômico, entre xenobióticos e alvos de proteínas conhecidos, criando interações proteína-ligante (VESELINOVIĆ et al., 2015; BALACHANDRAN et al., 2015; LIU, S., et al., 2016; EVANGELISTA et al., 2016; DANTAS et al., 2018). Com isso, é possível visualizar os sítios de interação, identificar as interações químicas e os resíduos de amino ácidos envolvidos além de propriedades moleculares, tais como geometria, reatividade, e energias de reações. Desta forma, o uso da modelagem molecular é importante na toxicologia e farmacologia (FRIEDMAN; BOYE; FLATMARK, 2013; FERREIRA et al., 2014). Para complementar os dados obtidos nos testes *in silico*, é importante realizar outras abordagens, como os testes *in vitro*, *in vivo* e de biologia molecular.

1.4 TRANSCRIPTOMA

O genoma de um organismo fornece o mapa genético para que todas as proteínas sejam construídas. É relativamente estático ao decorrer da vida de um organismo, havendo apenas mudanças pontuais desencadeadas por mutações. Por sua vez, o transcriptoma, que se refere ao conjunto completo de genes ou espécies de RNA transcritas (mRNA, tRNA, rRNA, microRNA,...) em uma determinada célula, tecido ou organismo, é extremamente variável. Isto significa que o mesmo genoma pode gerar a diversidade de células necessárias para a construção de órgãos e sistemas. Além disso, o transcriptoma altera-se ao longo da vida celular e em resposta a sinais externos como doenças e exposição à xenobióticos (CHAMBERS et al., 2018).

Estudos sobre transcriptoma, em geral, tem como objetivo avaliar células, tecidos ou organismos sob uma condição específica (exposição à xenobióticos, por exemplo) ou patológica a fim de verificar mudanças na expressão gênica. A análise do transcriptoma é, portanto, uma ferramenta com potencial para a descoberta de novos diagnósticos ou alvos terapêuticos (ASSIS et al., 2014). Dentre as metodologias de transcriptoma, destacam-se o microarranjo e sequenciamento de RNA (RNA-seq) (OLIVEIRA et al., 2020). Estes métodos são capazes de avaliar/sequenciar milhares de genes presentes nas amostras. Devido a grande quantidade de dados gerados, uma das estratégias mais utilizadas é a análise de expressão

diferencial, onde a expressão dos genes de uma amostra é comparada com outra, em geral, um grupo controle (BRINKE; BUCHINGER, 2016). Além disso, existem análises de enriquecimento gênico, onde plataformas agrupam os genes com função similar ou que participam da mesma rota metabólica, auxiliando no entendimento dos dados. Dentre estas análises, destaca-se a ontologia dos genes que é a ferramenta mais abrangente disponível para pesquisar e organizar genes e seus produtos por função (ASHBURNER et al., 2000). Esta é usualmente dividida em três domínios: processo biológico, função molecular e componente celular. Cada um destes domínios é dividido em sub-domínios ou termos que especificam suas funções (ASHBURNER et al., 2000; CARBON et al., 2017).

Existem poucos estudos sobre o perfil transcricional de organismos multi-celulares após a exposição ao MeHg⁺ (PADHI et al., 2008; MAHAPATRA et al., 2010; SHIMADA et al., 2010; JENKO; KAROUNA-RENIER; HOFFMAN, 2012; HO et al., 2013; RADONJIC et al., 2013; YADETIE et al., 2013; CROES et al., 2014; LIU, Q., et al., 2016; HAUSEN et al., 2017) e nenhum após a exposição ao VCH.

1.4.1 Sequenciamento de RNA e análise de expressão diferencial

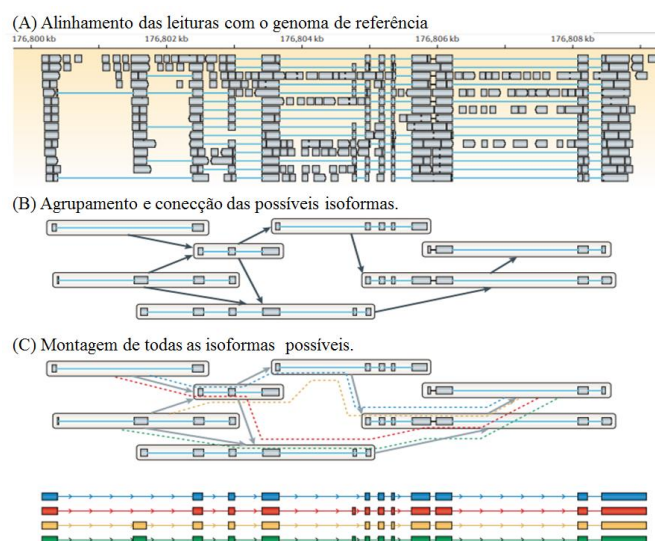
Dentre as metodologias para a obtenção de transcriptomas, destaca-se o RNA-seq. A maioria das técnicas de RNA-seq consiste no isolamento do RNA de interesse das amostras que se deseja sequenciar (cada grupo com suas réplicas biológicas), no caso deste estudo o mRNA. O mRNA é fragmentado e são acoplados adaptadores para reconhecimento e agrupamento das amostras. Para cada fita de RNA, é sintetizada uma fita de DNA complementar (cDNA), a qual é amplificada a fim de que se obtenham milhares de sequencias iguais. Cada fita de cDNA é sequenciada gerando uma leitura. Ao final do sequenciamento, o equipamento fornece milhões de leituras, que variam de 30 a 400 bases. A partir dessas leituras, os transcritos são montados e analisados utilizando-se ferramentas da bioinformática (MARTIN; WANG, 2011; OLIVEIRA et al., 2020). Ainda não há consenso sobre o número ideal de réplicas de cada grupo e o número mínimo de leituras que devem ser geradas em cada uma (LIU; ZHOU; WHITE, 2014; SCHURCH et al., 2016).

As leituras geradas no sequenciamento passam, primeiramente, por um processo de trimagem e filtragem. Esta etapa é composta, principalmente, pela remoção de leituras com score baixo na escala de qualidade de Phred (valor de Q) que está relacionada à probabilidade de erro de uma base em cada uma das posições em uma leitura, isto é, quanto maior a probabilidade de erro, menor será o score (EWING et al., 1998). Não há um valor

considerado ideal, mas em geral, os estudos utilizam valores de Q iguais a 20 e 30, que correspondem a 99 e 99,9% de precisão na determinação de cada base, respectivamente.

Após a trimagem é realizada a montagem dos transcritos através da montagem de novo, se o organismo não possui genoma conhecido (ROBERTSON et al., 2010), ou baseado no genoma ou transcriptoma de referência (MARTIN; WANG, 2011). A montagem de novo é realizada, basicamente, pela sobreposição das bases (ROBERTSON et al., 2010). Já a montagem baseada na referência envolve três etapas (Figura 7). A primeira é o alinhamento, propriamente dito, das leituras com a referência. Em seguida as leituras de cada locus são agrupadas e conectadas para que representem todas as possíveis isoformas e, por fim, todas as isoformas possíveis são montadas (MARTIN; WANG, 2011). Depois da montagem dos transcritos dos grupos que se deseja analisar, a expressão dos genes de uma amostra é comparada com outra e podem-se identificar os genes diferencialmente expressos (BRINKE; BUCHINGER, 2016).

Figura 7 – Montagem dos transcritos baseado no genoma de referência.



Primeiramente as leituras são alinhadas com o genoma (A). São agrupadas e conectadas para que representem todas as possíveis isoformas (B) e, posteriormente, todas as isoformas possíveis são montadas (C). Fonte: Martin; Wang (2011)

1.5 JUSTIFICATIVA

A população está constantemente exposta a substâncias tóxicas, de modo geral, em baixas concentrações. Destas substâncias, poucas possuem mecanismo de toxicidade

elucidado. Sabe-se que a exposição a pequenas doses de compostos tóxicos alteram a função/atividade das proteínas e a expressão gênica das células, mas demoram a causar efeitos visíveis na saúde dos organismos. Os metabólitos do VCH e o MeHg^+ são xenobióticos com propriedades eletrônicas semelhantes que se enquadram neste cenário, uma vez que estão presentes principalmente nos plásticos e nos peixes, respectivamente. Essas são moléculas estudadas há algum tempo, mas os alvos moleculares iniciais e biomarcadores de toxicidade precoce ainda não foram identificados. Além disso, pouco se sabe sobre a reversibilidade dos efeitos causados por estes xenobióticos, com destaque para o MeHg^+ . Desta forma, torna-se importante avaliar o perfil transcricional após a exposição aguda ao VCH e ao MeHg^+ , de forma individual, e também o efeito da interação entre eles, já que possuem afinidade pelos mesmos grupamentos em sistemas biológicos e, também se a interrupção da exposição ao MeHg^+ pode reverter os efeitos causados por este xenobióticos em marcadores eletrofílicos e no sistema colinérgico. Aliado a isso, o estabelecimento de modelos experimentais invertebrados permite uma avaliação mais rápida e barata de toxicidade. Essa metodologia vai ao encontro dos 3Rs no uso de animais de experimentação.

1.6 OBJETIVO GERAL

Avaliar os efeitos isolados e da interação do VCH e do MeHg^+ sobre o perfil comportamental, bioquímico e transcricional de insetos a fim de identificar possíveis alvos e mecanismos de toxicidade destes compostos.

1.5.1 Objetivos Específicos

- Avaliar possíveis alterações enzimáticas de *N. cinerea* após a exposição aguda, intermediária e crônica a MeHg^+ .
- Avaliar a possível reversão dos efeitos causados pelo MeHg^+ após a interrupção da exposição em *N. cinerea*.
- Propor a possível interação entre MeHg^+ e enzimas alvo.
- Avaliar possíveis alterações comportamentais de *N. cinerea* após a exposição aguda, intermediária e crônica ao MeHg^+ .
- Avaliar possíveis alterações no perfil transcricional de *D. melanogaster* após a exposição aguda a VCH e MeHg^+ individual e concomitantemente.

- Identificar genes que codificam proteínas contendo grupamentos nucleofílicos de *D. melanogaster*.

- Propor genes alvos de toxicidade para VCH e MeHg^+ em *D. melanogaster*.

2 ARTIGO 1 - High level of methylmercury exposure causes persisted toxicity in *Nauphoeta cinerea*

Environmental Science and Pollution Research
<https://doi.org/10.1007/s11356-019-06989-9>

RESEARCH ARTICLE



High level of methylmercury exposure causes persisted toxicity in *Nauphoeta cinerea*

Bruna C. Piccoli¹ · Jéssica C. Alvim¹ · Fernanda D. da Silva¹ · Pablo A. Nogara¹ · Olawande C. Olagoke¹ · Michael Aschner² · Cláudia S. Oliveira^{1,3,4} · João B. T. Rocha¹

Received: 11 July 2019 / Accepted: 6 November 2019
 © Springer-Verlag GmbH Germany, part of Springer Nature 2019

Abstract

Methylmercury (MeHg⁺) is a neurotoxicant abundantly present in the environment. The long-term effects of MeHg⁺ have been investigated in rodents, yet data on the long-term or persisted toxicity of MeHg⁺ in invertebrates is scanty. Here, we examined the acute, intermediate, and chronic effects upon dietary administration of MeHg⁺ in nymphs of *Nauphoeta cinerea*. Besides, the potential reversibility of the toxic effects of MeHg⁺ after a detoxification period was evaluated. Nymphs were exposed to diets containing 0 (control), 2.5, 25, and 100 µg MeHg⁺/g of diet for 10, 30, and 90 days. Additional groups of nymphs were fed with the same dose of MeHg⁺ for 30 days and then were subjected to a detoxification period for 60 days. The nymphs exposed to 100 µg MeHg⁺/g succumbed to a high mortality rate, along with multiple biochemical (increase of reactive oxygen species production and glutathione S-transferase activity, as well as decrease in the acetylcholinesterase activity) and behavioral alterations. We observed delayed mortality rate and behavioral alterations in nymphs exposed to 100 µg MeHg⁺/g for 30 days and subsequently subjected to 60 days of detoxification. However, the biochemical alterations did not persist throughout the detoxification period. In conclusion, our results established the persistent toxic effect of MeHg⁺ even after a prolonged detoxification period and evidenced the use of *N. cinerea* as an alternative model to study the toxicity of MeHg⁺.

Keywords Methylmercury · Cockroach · Neuro-locomotor dysfunction · Heavy metal · Docking · Toxicology

Responsible editor: Philippe Garrigues

Electronic supplementary material The online version of this article (<https://doi.org/10.1007/s11356-019-06989-9>) contains supplementary material, which is available to authorized users.

✉ Cláudia S. Oliveira
claudia.bioquimica@yahoo.com.br

✉ João B. T. Rocha
jbtrocha@yahoo.com.br

¹ Departamento de Bioquímica e Biologia Molecular, Centro de Ciências Naturais e Exatas, Universidade Federal de Santa Maria, Santa Maria, RS, Brazil

² Department of Molecular Pharmacology, Albert Einstein College of Medicine, Bronx, NY, USA

³ Instituto de Pesquisa Pelé Pequeno Príncipe, Curitiba, PR, Brazil

⁴ Faculdades Pequeno Príncipe, Curitiba, PR, Brazil

Introduction

Mercury (Hg) is an environmental contaminant naturally distributed in the earth's crust (Clarkson 1993). However, the use of Hg in industrial activities, as pharmaceutical preservative, and as a component of medical devices contributes to the ever-increasing environmental Hg levels along with deforestation and coal burning (Oliveira et al. 2017a, 2018, 2019; Nogara et al. 2019a, 2019b). Streets et al. (2017) estimated that approximately 1540 gigagrams of Hg had already been released into the atmosphere by anthropogenic activities from 1850 until 2010. Though the levels of anthropogenic Hg release have been decreasing, the long-term persistence of Hg in the environment is of great health concern (Zhang et al. 2016; Rudd et al. 2018).

Interest in the toxic effects of methylmercury (MeHg⁺) started after the Minamata outbreak (Japan, ~1950–1975). Briefly, industrial effluents containing Hg²⁺ and MeHg⁺ were released into Minamata Bay. Marine fauna showed levels of Hg varying from 5 (oysters) to 40 ppm (crabs and fish) (Harada 1995). The consumption of contaminated seafood

by the local population culminated in a wide range of neuropathological phenotypes, which depended on the exposure levels, and varied from slight paresthesia to ataxia, dysarthria, blurred vision, hearing impairment, olfactory and gustatory disturbances, mental retardation, cerebral palsy, and death (Weiss et al. 2002; Ekino et al. 2007). Of particular concern, several cases of delayed neurotoxicity were reported in adults exposed to relatively high levels of mercury both in the Minamata and Iraq outbreaks (Weiss et al. 2002; Newland 2010). The delayed toxicity of MeHg⁺ has also been demonstrated in rodents (Rice 1996).

MeHg⁺ is a soft electrophile, which in accordance with Pearson's theory has a high affinity for soft nucleophilic centers, particularly, the thiol (–SH) and selenol (–SeH) groups, which are present in the amino acids cysteine and selenocysteine, respectively. The formation of MeHg⁺ complexes with –SH or –SeH-containing proteins usually cause the loss of function of targeted proteins (Oliveira et al. 2017a, 2019; Nogara et al. 2019a).

Toxicological studies with MeHg⁺ have commonly used mammals as the primary experimental models (Bisen-Hersh et al. 2014; Oliveira et al. 2017b). However, the MeHg⁺-induced toxicity in vertebrates can vary even in closely related species (for instance, mice and rats) (Magos 1976; Naganuma and Imura 1984; Stein et al. 1988; Doi 1991). Thus, in view of the necessity of adherence to the 3Rs (replacement, reduction, and refinement) (Cheluvappa et al. 2017; Clark 2018; Lang et al. 2018), new invertebrate models have been developed to study both the molecular aspects and the overt signs of toxicity (behavior, growth, etc.) (Lovato et al. 2017; Mrdaković et al. 2019; Rand et al. 2019). Indeed, one aspect that has been little explored, even in rodents, is the reversibility of MeHg⁺ toxicity. The mammals' replacement with alternative animal models, for instance, insects, which are faster (~ 10 times) and cheaper to maintain (~ 100-fold reduction in costs) than vertebrates, and usually have an evolutionary relationship with mammals, could afford invaluable alternative and complementary models (Peterson et al. 2008; Berger 2009).

The cockroach *Nauphoeta cinerea* and other cockroaches have been indicated as valuable models for toxicological studies (Shambaugh 1969; Rodrigues et al. 2013; Mrdaković et al. 2019). Of particular importance, the exposure of *N. cinerea* to Hg has been reported to reproduce some of the biochemical and behavioral alterations observed in mammals (Rodrigues et al. 2013; Adedara et al. 2015, 2016a; Afolabi et al. 2018). However, to our knowledge, no previous studies have been performed detailing the effects of chronic exposure, as well as the potential reversibility of MeHg⁺ toxicity after a detoxification period. Here, we used *N. cinerea* to examine the short-, intermediate-, and long-term toxicity of different doses of MeHg⁺. As indicated above, only a few studies have investigated the reversibility of MeHg⁺ toxicity. Thus, here, we examined the possible reversibility of MeHg⁺ effects after

cessation of exposure in cockroaches, using behavior, electrophilic toxicity markers (i.e., reactive species production, glutathione S-transferase (GST) activity), and acetylcholinesterase (AChE) activity.

Material and methods

Chemicals

All chemicals were of analytical grade. Methylmercury chloride (MeHgCl), glutathione (GSH), ethylenediaminetetraacetic acid (EDTA), 1-chloro-2,4-dinitrobenzene (CDNB), acetylthiocholine iodide, 5,5'-dithiobis(2-nitrobenzoic acid) (DTNB), and 2,7-dichloro-dihydro-fluorescein diacetate (DCFHDA) were purchased from Sigma-Aldrich (St. Louis, MO, USA).

Cockroach husbandry

N. cinerea was provided by the Departamento de Bioquímica e Biologia Molecular at Universidade Federal de Santa Maria, RS, Brazil. Cockroaches were maintained in plastic boxes (25.8 × 17.8 × 8.5 cm) with fairly constant temperature 23.9 ± 2.6 °C (min - max: 21.8–26.0 °C), under 12 h dark/light cycle conditions. The cockroaches had *ad libitum* access to water and food.

Diet preparation

The diet was prepared as described by Adedara et al. (2015). Briefly, the basal (control) diet was composed of commel (50%), wheat flour (35%), sucrose (10%), casein (2.5%), skimmed milk powder (2%), and salt (0.5%). MeHgCl was dissolved in ethanol, mixed in the diet (1 mL ethanol:1 g diet), and left to dry. The control diet was mixed with the equivalent volume of ethanol.

Methylmercury exposure

Nymphs of *N. cinerea* (~ 2 cm) were fed with different doses of MeHgCl (0, 2.5, 25, and 100 µg MeHgCl per gram of diet) in two different experimental protocols, according to Fig. 1. In protocol 1, 50 nymphs per group were fed with MeHgCl for 10, 30, or 90 days. After the exposure periods, behavioral and biochemical tests were performed. Protocol 2 was based on the study of Adedara et al. (2015). Therefore, we performed a 30-days exposure to MeHgCl (50 nymphs per group), and we consider twice the exposure time (60 days) as a detoxification period consuming control diet. Subsequently, behavioral and biochemical tests were conducted. The food intake and the number of dead nymphs were recorded daily. Each experimental procedure consisted of three to five independent replicates.

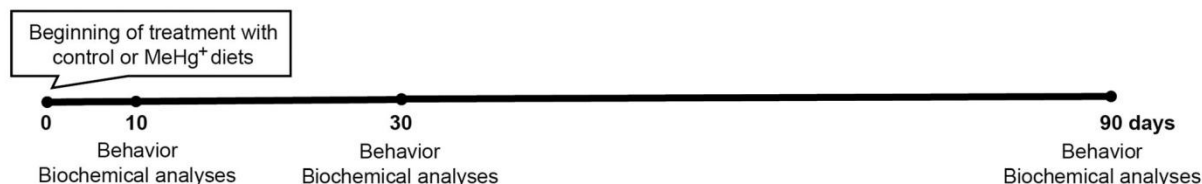
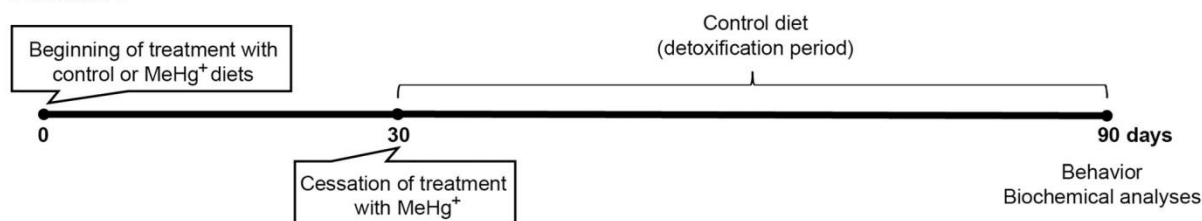
Protocol 1:**Protocol 2:**

Fig. 1 Experimental design

The doses of MeHg⁺ tested in this study are following the levels of MeHg⁺ found in fish of the Amazon region. It is estimated that the riverine communities consume ~170 g of fish/day according to their hair Hg concentration (Dórea and Marques 2016). According to fish consumption (Dórea and Marques 2016) and MeHg⁺ levels in fish at the Amazon region (Bastos et al. 2015), it was possible to assess that the riverine population consumes approximately 1.5 to 46.7 µg MeHg⁺/day of detritivorous and herbivorous fish, 4.4 to 84.0 µg MeHg⁺/day of omnivorous and planktivorous fish, and 8.7 to 211.1 µg MeHg⁺/day of carnivorous and piscivorous fish.

Behavioral task

Nymphs were subjected to a new object recognition test. Each nymph was placed in a plastic box (25.8 × 17.8 × 8.5 cm) with a familiar object (resembling its husbandry apparatus) and an unfamiliar object, as shown in Fig. S1. Recordings were made during a 10 min period using a Canon EOS 1100D camera, and behavioral parameters were manually analyzed. These included time spent exploring the familiar object and exploring the unfamiliar object. Twenty randomly selected nymphs were recorded in each treatment group.

Biochemical analyses**Sample preparation**

After the behavioral task, nymphs were cryoanesthetized, and head and fat body were excised for biochemical analyses (DCFHDA oxidation and GST and AChE activities). A pool of three excised heads and fat bodies were homogenized with

0.1 M phosphate buffer, pH 7.4 (heads: 900 µL of buffer; fat body: 600 µL of buffer), and centrifuged at 10,000g for 10 min at 4 °C to obtain the supernatant. For biochemical analyses, nine to twelve sample pools of each group were used.

DCFHDA oxidation

DCFHDA assay was determined as described by Pérez-Severiano et al. (2004). The reaction system consisted of potassium phosphate buffer pH 7.4 (75 mM), DCFHDA (5 µM), and 5 µL of sample. The fluorescence was monitored with a spectrophotometer Spectra Max plate reader, at 488-nm excitation and 525-nm emission for 20 min with an interval of 30 s. Results were expressed as the mean of fluorescence intensity delta per minute per milligram of tissue.

GST activity

GST activity was determined according to Habig and Jakoby (1981). The system consisted of potassium phosphate buffer pH 7.4 (70 mM), EDTA (1 mM), GSH (3.20 mM), CDNB (0.8 mM), and 12 µL of sample. The reaction was monitored with a spectrophotometer Spectra Max plate reader at 340 nm for 20 min with an interval of 30 s. Results were expressed as the mean absorbance delta of GSH-CDNB conjugate per minute per milligram of tissue.

AChE activity

AChE activity was determined as described by Ellman et al. (1961). The system consisted of potassium phosphate buffer pH 7.4 (10 mM), DTNB (1 mM), acetylthiocholine (0.8 mM), and 30 µL of sample. The activity was monitored with a

spectrophotometer Spectra Max plate reader at 412 nm for 20 min with an interval of 30 s. Results were expressed as the mean absorbance delta of thiocholine per minute per milligram of tissue.

Docking simulations

AutoDock Vina 1.1.1 (Trott and Olson 2009) was used in the molecular docking simulations with exhaustiveness of 100. The ligands, methylmercury chloride (Cl-HgMe), and its putative metabolites Cys-HgMe and GSH-HgMe were created using the software Avogadro 1.1.1 (Hanwell et al. 2012), and the program MOPAC2012 (<http://openmopac.net/MOPAC2012>), following the semi-empirical PM6 (Stewart 2007) geometry optimization (taking into account the dielectric constant of water – EPS = 74). The structures of the ligands and enzymes in the *pdbqt* format were generated by AutoDockTools, where the ligands were considered flexible (with PM6 charges), and the enzymes rigid (with Gasteiger charges) (Morris et al. 2009). As the AutoDock Vina program did not present parameters for the Hg atom, it was replaced by Zn in the *pdbqt* file (both atoms are in the same family in the periodic table and share similar properties). The results from docking were analyzed with the Accelrys Discovery Studio 3.5 software (<http://www.3dsbiovia.com>).

Cockroach GST docking

The structure of cockroach GST, as a dimer, was obtained from protein homology modeling, using the Swiss-Model server (<https://swissmodel.expasy.org>) (Arnold et al. 2006). The primary sequence of cockroach GST was obtained from UniProt (<http://www.uniprot.org>), with the code A0A2P8Z129, and the template was gotten from the Protein Data Bank (<https://www.rcsb.org/pdb>) (PDB ID 4Q5R) (Mueller et al. 2014). The protein structure was analyzed by PROCHECK, Verify 3D (available in the SAVES v5.0 - <http://servicesn.mbi.ucla.edu/SAVES>), and by the Protein Structure Analysis - ProSA server (Wiederstein and Sippl 2007). The validation of the GST models showed that the structures presented conformation similar to the native proteins (Fig. S2). To study if GST could catalyze the reaction between MeHg⁺ molecules and GSH, the molecular docking was carried out with the grid box centered in the active site from chain A (because is the GSH binding site), on the coordinates $x = 38.5$, $y = 47.0$, and $z = -53.0$, with the size 15^3 Å. The binding pose of GSH (substrate) in the GST enzyme was obtained from the homology modeling.

Cockroach AChE docking

For the simulation between AChE from cockroach and the MeHg⁺ species, the structure of AChE type 1 was

obtained following the protocol described by Silva et al. (2018). First, to verify the MeHg⁺ binding sites, a blind docking was performed ($x = -40.83$; $y = 12.37$; $z = -40.28$, $78 \times 66 \times 66$ Å). As some ligands could access the AChE active site, the molecular docking with the grid box on AChE active site was performed aiming to improve the interaction between ligand and receptor. The grid box was centered in the coordinates $x = -38.48$; $y = 2.77$; $z = -37.92$, with the size 25^3 Å. After that, to study if the MeHg⁺ ligands could interact with the cysteine residue, a molecular docking with the Ile396, Cys397, and Tyr444 lateral chains flexible was done (because these residues present a hindrance effect with the Cys) using the previous docking configuration.

Statistical analyses

Results were expressed as mean \pm SEM. Data on survival percentage was plotted in the Kaplan-Meier curve and analyzed by Log-rank test for trend. The presence of outliers was assessed according to ROUT in the data derived from behavioral and biochemical analyses. The data distribution was tested for normality according to D'Agostino-Pearson test, and one or two-way ANOVA was carried out when appropriate, followed by Dunnett's post hoc test (normal data) or Kruskal-Wallis followed by Dunn's post hoc test (non-normal data). The results were considered significant when $p \leq 0.05$.

Results

Percentage of survival

Log-rank test indicated no significant difference in survival of cockroach nymphs exposed to 2.5 and 25 $\mu\text{g MeHg}^+/\text{g}$ of diet for 30 days, followed by a 60-day detoxification period, compared with control (Fig. 2a). Conversely, the group fed with 100 $\mu\text{g MeHg}^+/\text{g}$ for 30 days, followed by 60-days detoxification period [chi-square (1) = 205.8, $p < 0.0001$], as well as those fed with 2.5, 25, and 100 $\mu\text{g MeHg}^+/\text{g}$ for 90 days [chi-square (1) = 4636, $p = 0.0313$; chi-square (1) = 24, $p < 0.0001$; chi-square (1) = 201, $p < 0.0001$, respectively], showed significant reduction in survival compared with the control group. Interestingly, some of the nymphs exposed to 100 $\mu\text{g MeHg}^+/\text{g}$ died during molting as illustrated in Fig. 2b and c.

Food and MeHg⁺ intake

Total food and MeHg⁺ intake by the nymphs are shown in Fig. 3. Two-way ANOVA revealed a significant interaction between treatment and time on the total food intake of nymphs exposed to MeHg⁺ for 90 days

Fig. 2 Kaplan-Meier survival curve of nymphs exposed to different doses of MeHg⁺ (0, 2.5, 25, and 100 µg MeHg⁺/g of food) for 30 or 90 days (a). Percentage of nymphs that died during molting relating to the total number of insects present in each group (b) and examples of death during molting (c). The survival curve was analyzed by the Log-rank test and was considered significantly different from the control group when $p \leq 0.05$. The percentage of nymphs that died during molting was analyzed by one-way ANOVA, followed by Dunnett's post hoc test

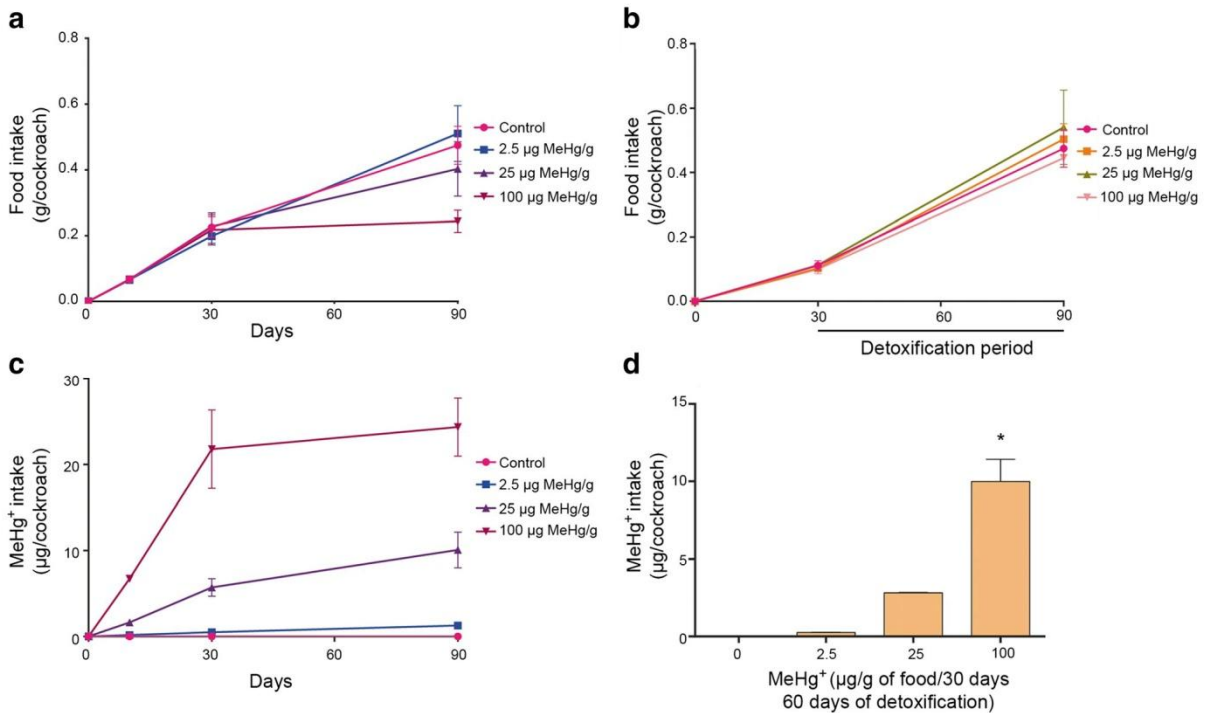
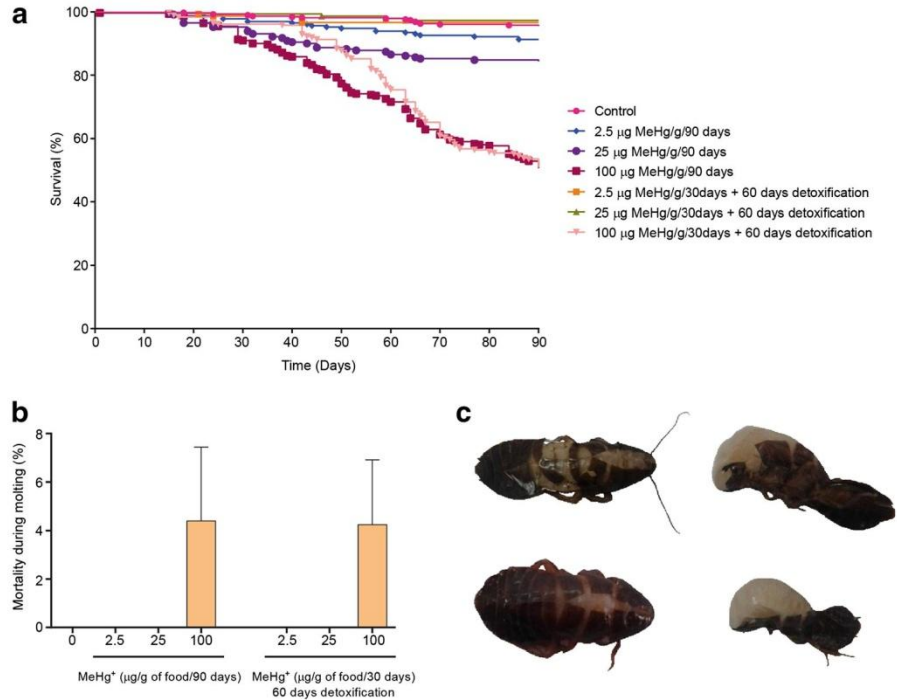


Fig. 3 Total food intake (a and b) and MeHg⁺ consumption (c and d) by nymphs exposed to different doses of MeHg⁺ for 90 days (a and c) or 30 days followed a detoxification period (b and d). Data were expressed as mean \pm SEM ($N = 3-5$ replicates with 50 nymphs each) and analyzed

by two-way ANOVA followed by Tukey post hoc test (a-c) or one-way ANOVA followed by Dunnett's post hoc test (d). *Significantly different from the control group ($p \leq 0.05$)

[$F(9,52)=2.436$; $p=0.0215$] (Fig. 3a) due to the increase of the food consumption time-dependent for all groups with the exception of the group exposed to 100 $\mu\text{g MeHg}^+$ /g of food, which had similar food intake between the days 30 and 90 of exposure. The nymphs exposed to MeHg^+ for 30 days followed by 60 days of detoxification period (Fig. 3b) presented a significant main effect of the time [$F(2,30)=134.5$; $p<0.0001$] on total food intake due to increased consumption time-dependent for all groups.

The quantity of MeHg^+ consumed by the nymphs was estimated based on the nymphs' diet intake (Fig. 3c and d). Two-way ANOVA indicated a significant interaction between treatment and time on MeHg^+ intake by nymphs exposed to MeHg^+ for 90 days [$F(9,56)=14.59$; $p<0.0001$] (Fig. 3c). In fact, the control group and nymphs exposed to 2.5 $\mu\text{g MeHg}^+$ /g of food showed no increase in MeHg^+ intake along the time. Nymphs exposed to 25 and 100 $\mu\text{g MeHg}^+$ /g of food increased MeHg^+ consumption up to 30 days of exposure, and subsequently it was similar (between 30 and 90 days). Regarding MeHg^+ intake of nymphs exposed to MeHg^+ for 30 days followed by 60 days of detoxification period, one-way ANOVA indicated that the nymphs exposed to 100 $\mu\text{g MeHg}^+$ /g of food have a significant increase in MeHg^+ intake when compared to control group [$F(3,8)=41.91$; $p<0.0001$] (Fig. 3d).

Behavioral analyses

Time spent with the familiar object

The percentage of time that the nymphs spent with the familiar object is shown in Fig. 4. Statistical analysis did not indicate a significant difference of nymphs treated with MeHg^+ for 10 and 30 days (Fig. 4a and b, respectively). Kruskal-Wallis analysis revealed effect of the treatment on nymphs exposed to MeHg^+ for 90 days [$H=18.71$; $p=0.0003$] (Fig. 4c) and on nymphs exposed to MeHg^+ for 30 days followed by 60 days of detoxification [$H=16.63$; $p=0.0008$] (Fig. 4d). In both exposure protocols, nymphs exposed to the highest dose of MeHg^+ showed a decrease in the time spent with the familiar object when compared with the control group.

Time spent with the unfamiliar object

The percentage of time that the nymphs spent with the unfamiliar object is shown in Fig. 5. Kruskal-Wallis analysis revealed effect of the treatment in nymphs exposed to MeHg^+ for 30 days [$H=22.68$; $p<0.0001$] (Fig. 5b), 90 days [$H=21.10$; $p<0.0001$] (Fig. 5c), and in nymphs exposed to MeHg^+ for 30 days followed by 60 days of detoxification [$H=9.344$; $p=0.025$] (Fig. 5d). In fact, the nymphs exposed to the highest dose of MeHg^+ for 30 days showed a decrease

Fig. 4 Time spent with the familiar object by nymphs exposed to MeHg^+ for 10 days (a), 30 days (b), 90 days (c), and 30 days followed by 60 days of detoxification (d). Data were expressed as mean \pm SEM ($N=20$) and analyzed by one-way ANOVA followed by Dunnett's post hoc test (a and b) or Kruskal-Wallis followed by Dunn's post hoc test (c and d). *Significantly different from the control group ($p\leq 0.05$)

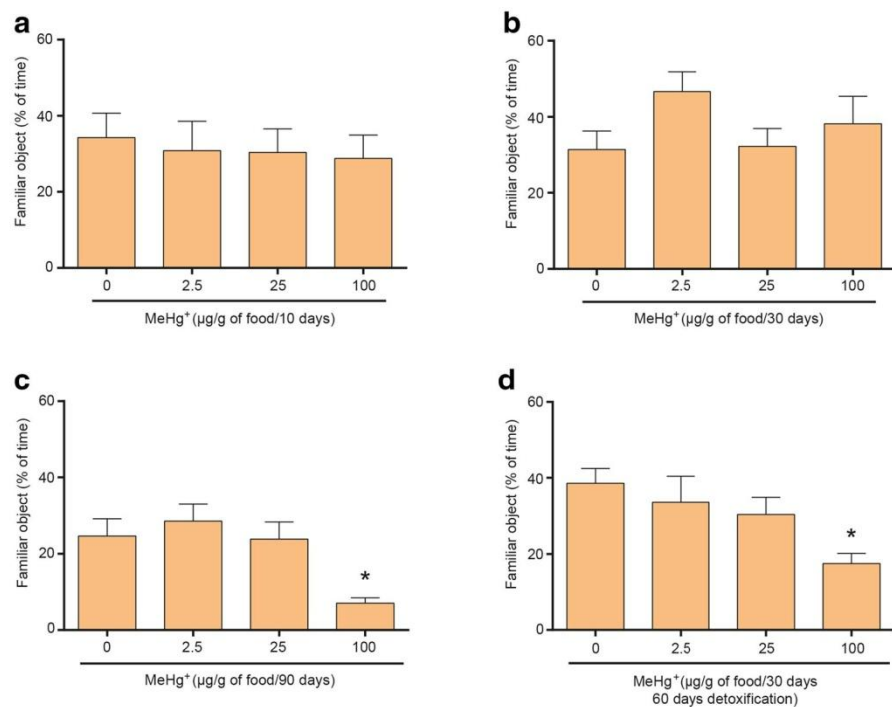
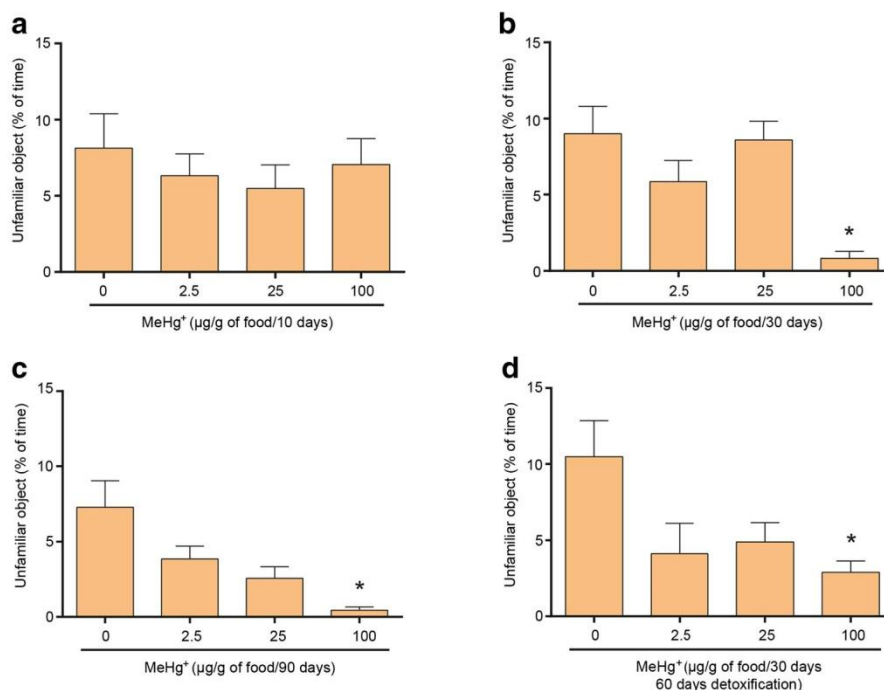


Fig. 5 Time spent with the unfamiliar object by nymphs exposed to MeHg⁺ for 10 days (a), 30 days (b), 90 days (c), and 30 days followed by 60 days of detoxification (d). Data were expressed as mean \pm SEM ($N = 20$) and analyzed by Kruskal-Wallis followed by Dunn's post hoc test. *Significantly different from the control group ($p \leq 0.05$)



in the time spent with the unfamiliar object, which was not reversed after the cessation of exposure. In addition, nymphs exposed to 100 µg MeHg⁺/g of food for 90 days also showed the same pattern.

Ratio of time spent with the familiar object and with the unfamiliar object

Results of the ratio of time spent with the familiar to time spent with the unfamiliar object are shown in Fig. 6. One-way ANOVA revealed effect of treatment only on nymphs treated with MeHg⁺ for 30 days [$F(3,61) = 9.945$; $p < 0.0001$]. Nymphs exposed to the highest dose of MeHg⁺ for 30 days showed a higher ratio due to the less time spent exploring the unfamiliar object (Fig. 5b). The nymphs exposed to the toxicant for 90 days or for 30 days followed by 60 days of detoxification had a similar ratio because they explored both objects (familiar and unfamiliar) for a short period (Fig. 6c and d).

Biochemical analyses

DCFHDA oxidation

DCFHDA oxidation is shown in Fig. 7. One-way ANOVA revealed no effect of the treatment in the nymphs' heads (Fig. 7a–d). In contrast, one-way ANOVA revealed effect of the treatment in the fat body of the nymphs exposed to MeHg⁺ for 10 [$F(3,32) = 4.315$; $p = 0.0115$] (Fig. 7e) and 90 days [$F(3,40) = 4.738$; $p = 0.0064$] (Fig. 7h). Specifically, the

exposure to the highest dose of MeHg⁺ for 10 and 90 days caused an increase in reactive oxygen species levels in the fat body of nymphs when compared to the control group.

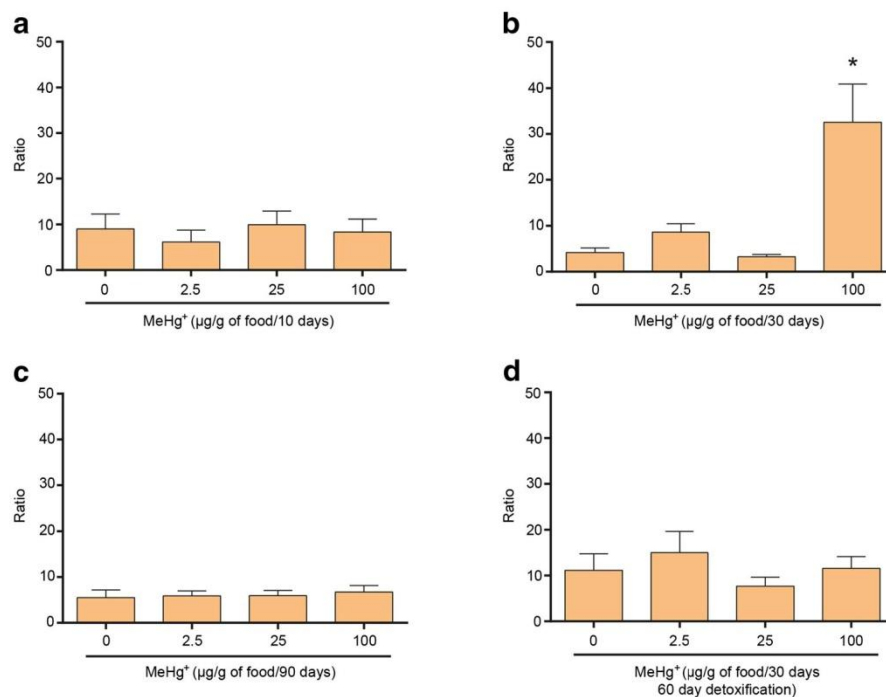
GST activity

GST activity is shown in Fig. 8. In the nymphs head, one-way ANOVA indicated effect of MeHg⁺ only after 90 days of exposure to the highest dose (Fig. 8c) [$F(3,44) = 20.72$; $p < 0.0001$]. One-way ANOVA also revealed effect of treatment in the fat body after 10 (Fig. 8e) [$F(3,32) = 4.118$; $p = 0.0141$], 30 (Fig. 8f) [$F(3,31) = 4.819$; $p = 0.0072$], and 90 (Fig. 8g) [$F(3,44) = 11.02$; $p < 0.0001$] days of MeHg⁺ exposure. MeHg⁺ induced an increase in GST activity after exposure to the highest dose in the acute (fat body), intermediate (fat body), and chronic (head and fat body) exposure paradigms. Detoxification reversed the effects caused by MeHg⁺ on the fat body of nymphs, with GST activity returning to basal levels (Fig. 8h).

AChE activity

Figure 9 shows the AChE activity in the head of MeHg⁺-exposed nymphs. One-way ANOVA indicated effect of treatment on AChE activity after 10 [$F(3,31) = 3.923$; $p = 0.0175$] (Fig. 9a) and 90 [$F(3,44) = 5.870$; $p = 0.0018$] (Fig. 9c) days of MeHg⁺ exposure. Nymphs exposed to 2.5 and 100 µg MeHg⁺/g diet for 10 days and to the highest dose of MeHg⁺ for 90 days showed a decrease in AChE activity when compared to the control group (Fig. 9a and c). Nymphs fed with

Fig. 6 Ratio of time spent with the familiar and unfamiliar object by the nymphs exposed to MeHg⁺ for 10 days (a), 30 days (b), 90 days (c), and 30 days followed by 60 days of detoxification (d). Data were expressed as mean \pm SEM ($N=20$) and analyzed by Kruskal-Wallis followed by Dunn's post hoc test (a and d), or by one-way ANOVA followed by Dunnett's post hoc test (b and c). *Significantly different from the control group ($p \leq 0.05$)



MeHg⁺ for 30 days followed by a detoxification period showed no significant difference in AChE activity (Fig. 9d).

Docking simulations

GST and MeHg⁺ species

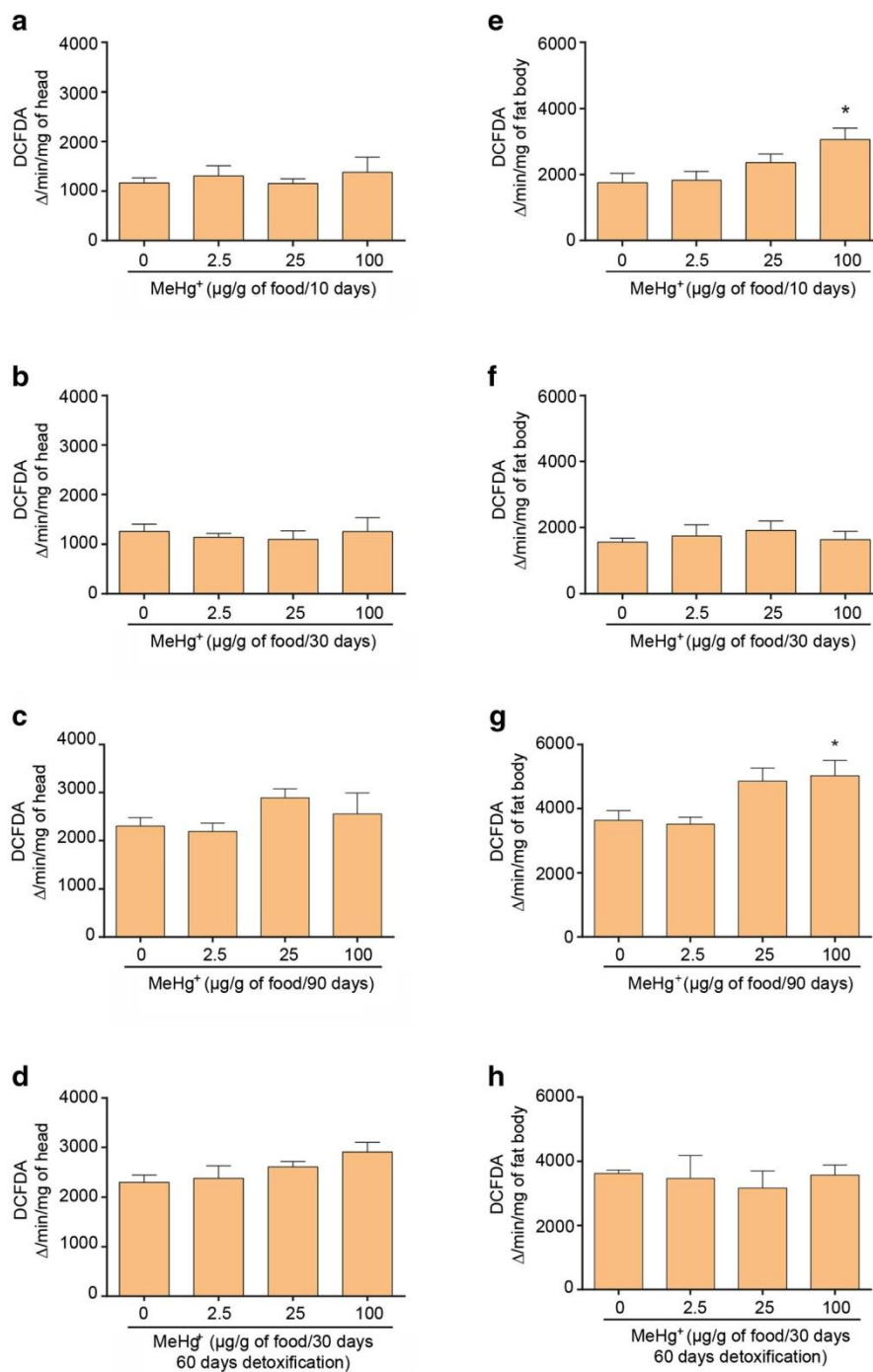
To better understand the results of the biochemical tests, we performed the binding simulations between the GST enzyme and MeHg⁺ species (Cl-HgMe and Cys-HgMe) (Fig. 10). Cl-HgMe and Cys-HgMe interact with the sulfur atom from the GSH, in the active site of GST (distances between S and Hg 3.3 to 4.5 Å). Cl-HgMe is stabilized in the active site of GST mainly by hydrophobic interactions between its methyl moiety, the isopropyl group of Val12, and the phenyl ring of Phe110 and Tyr163 residues. The Cys-HgMe molecule interacted (by the carboxylic moiety) with the benzene ring of Phe110 (by electrostatic π -anion interactions), and with the hydroxyl group of Tyr108 (by H-bond). According to the binding free energy (ΔG), Cys-HgMe bound more favorably with GST than Cl-HgMe (Table 1).

AChE and MeHg⁺ species

In a first step, the blind docking demonstrated that the MeHg⁺ species (Cl-HgMe, Cys-HgMe, and GSH-HgMe) could interact with the AChE in several binding sites (superficial and internal) besides of the active site,

mainly by electrostatic interactions with glutamate and/or aspartic residues (Fig. S3). Docking simulations in the active site of the enzyme were performed to improve the interactions. The Cl-HgMe molecule is stabilized by electrostatic π -cation interactions between the indol ring from Trp343 and the phenyl ring from the Phe440 residues, as well as an H-bond between the Cl atom and the hydroxyl moiety from Ser310 (Fig. 11a). The Cys-HgMe showed H-bonds with the Gly229 and Tyr232 residues, through its carboxylic and ammonium moieties, respectively, as well as Hg interactions with the hydroxyl groups from Tyr439 and Tyr443 residues (Fig. 11b). The GSH-HgMe molecule showed H-bonds with Gly228/229/230 and Tyr439 residues, in addition to an intramolecular H-bond, electrostatic π -cation and π -anion interactions with the Tyr443 and Trp195, respectively, Hg interactions with the hydroxyl group of Tyr232, and electrostatic interactions with the phenyl group of Tyr443 and with the carboxylic moiety from Asp183 (Fig. 11c). Furthermore, the ΔG (Table 1) indicates that all molecules could interact favorably with the AChE. However, the binding of GSH-HgMe is preferential to those of Cys-HgMe and Cl-HgMe. In addition, to verify if the MeHg⁺ molecules could interact with the reduced cysteine residue (Cys397), and improve the interactions, we performed docking simulations with the lateral chains from Ile396, Cys397, and Tyr444 flexible. According to simulations, the Cl-HgMe and GSH-HgMe

Fig. 7 DCFHDA oxidation in the head (**a–d**) and fat body (**e–h**) of nymphs exposed to MeHg⁺ for 10 (**a** and **e**), 30 (**b** and **f**), and 90 days (**c** and **g**), as well as 30 days followed by 60 days of detoxification (**d** and **h**). Data were expressed as mean \pm SEM ($N=9-18$) and analyzed by one-way ANOVA followed by Dunnett's post hoc test (**a**, **c**, **e**, **f**, **g**, and **h**) or Kruskal-Wallis followed by Dunn's post hoc test (**b** and **d**). *Significantly different from the control group ($p \leq 0.05$)

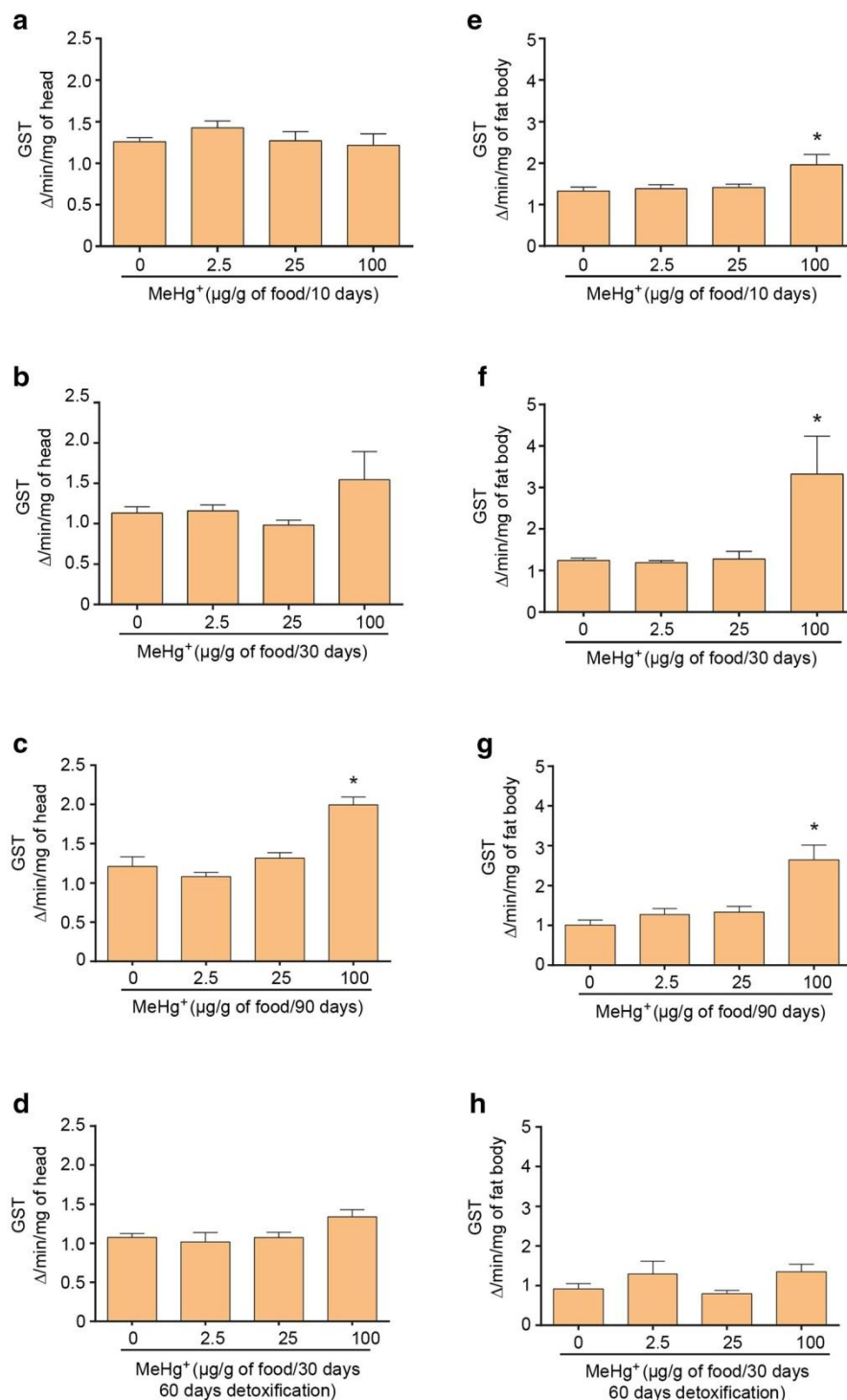


showed the shortest S^{III}Hg distance (3.2 and 5.6 Å, respectively), indicating a possible reaction between them, while the Cys-HgMe demonstrated 8.6 Å of distance (Fig. S4).

Discussion

In this study, we evaluated the effects of short-, intermediate-, and long-term exposure to MeHg⁺ on nymphs of

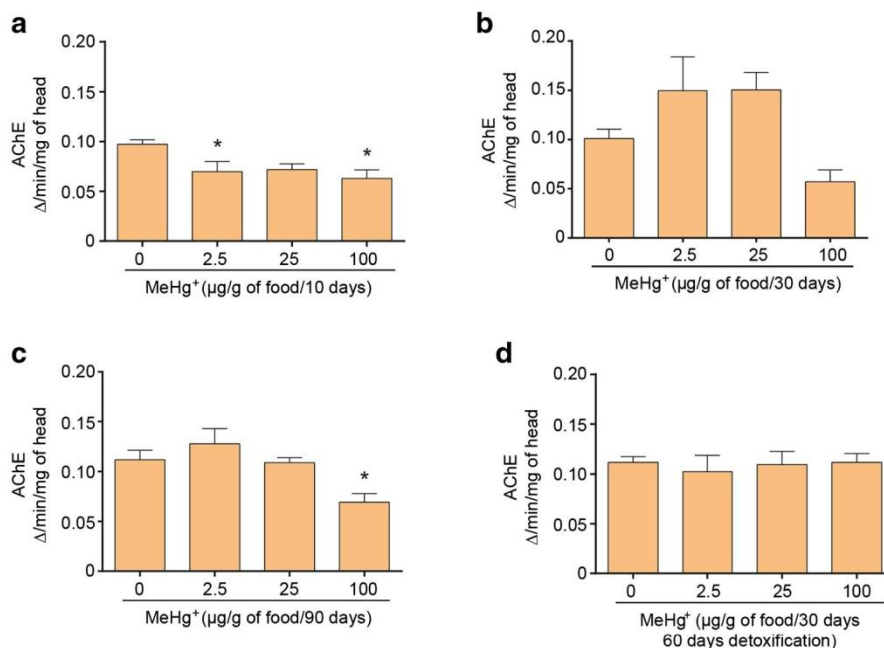
Fig. 8 Glutathione S-transferase activity in the head (a–d) and fat body (e–h) of nymphs exposed to MeHg⁺ for 10 (a and e), 30 (b and f), and 90 days (c and g), as well as 30 days followed by 60 days of detoxification (d and h). Data were expressed as mean \pm SEM ($N=9-18$) and analyzed by one-way ANOVA followed by Dunnett's post hoc test (e, e, f, and g) or Kruskal-Wallis followed by Dunn's post hoc test (a, b, d, and h). *Significantly different from the control group ($p \leq 0.05$)



N. cinerea, as well as the possible reversal of MeHg⁺-induced toxic impairments after discontinuation of exposure. MeHg⁺ led to behavioral and biochemical alterations,

characterized by changes in DFCHDA oxidation, as well as GST and AChE activities. The detoxification period reversed some of the biochemical alterations caused by

Fig. 9 Acetylcholinesterase activity in the head after 10 (a), 30 (b), and 90 days (c), as well as 30 days followed by 60 days of detoxification (d). Data were expressed as mean \pm SEM ($N = 9-18$) and analyzed by one-way ANOVA followed by Dunnett's post hoc test (a-c) or Kruskal-Wallis test followed by Dunn's post hoc test (d). *Significantly different from the control group ($p \leq 0.05$)



MeHg⁺; however, it failed to reverse the survival rate and only partially reversed the behavioral parameters. Of particular toxicological significance, the exposure to diets containing the highest level of MeHg⁺ (100 μg MeHg⁺/g of diet) for 30 days led to delayed mortality (observed between 30 and 90 days, detoxification period), which

reached the same levels as in cockroaches maintained on 100 μg MeHg⁺/g diet for 90 days.

Prolonged exposure to MeHg⁺ (i.e., for 90 days) reduced the survival at all the tested doses. As discussed above, the highest dose of MeHg⁺ exposure reduced the percentage of nymphs' survival, even after the detoxification period (Fig. 2).

Fig. 10 Molecular docking simulations of *N. cinerea* GST and MeHg⁺ species [Cl-HgMe (a) and Cys-HgMe (b)]. The active site from chain A of GST is highlighted in the square. The MeHg⁺ species and the GSH are represented in ball and stick, and the main residues involved in the interactions are in stick models. The H-bonds, electrostatic, hydrophobic, and mercury interactions are shown in green, orange, pink, and blue dotted lines, respectively

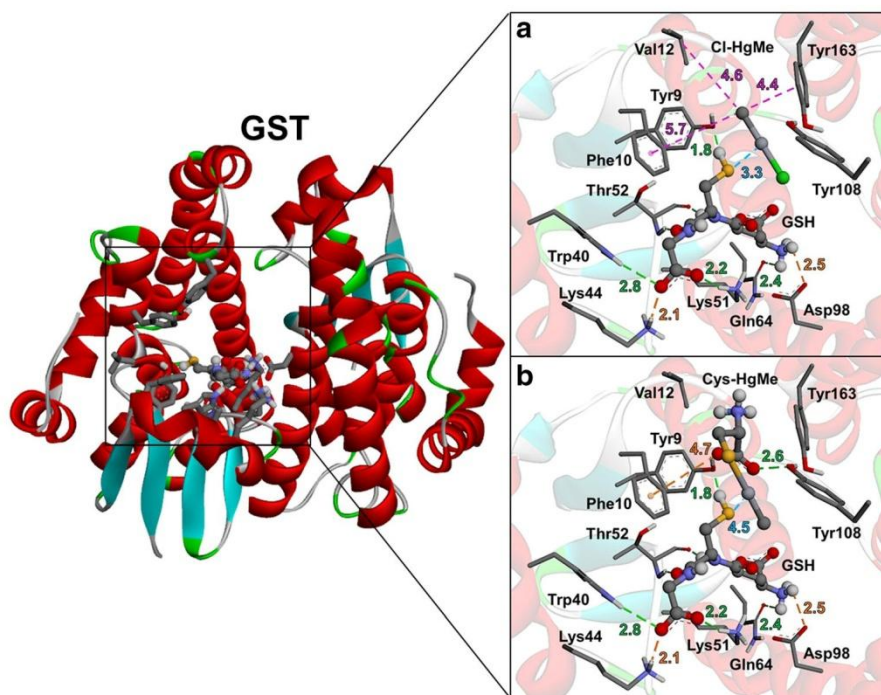


Table 1 Predicted binding free energy (Kcal/mol) from docking between the GST and AChE enzymes with the MeHg⁺ species. n.d. = not determined

| ΔG (Kcal/mol) | Cl-HgMe | Cys-HgMe | GSH-HgMe |
|-----------------------|---------|----------|----------|
| GST | -1.6 | -3.4 | n.d. |
| AChE | -2.2 | -4.7 | -6.8 |

The molting-related deaths indicated possible dysfunction in the neuromotor physiology of the insects, which hampered their capacity to leave the exoskeleton. Similarly, Rand et al. (2019) observed that fruit flies exposed to MeHg⁺ in the larval stage 3 had a decrease in the eclosion rate; still, some of the insects presented morphological alterations. In our study, motor dysfunction was also observed in the behavioral tasks characterized by lesser mobility and reduced time of exploration of the familiar and unfamiliar objects in MeHg⁺-exposed nymphs (Figs. 4, 5, and 6). These observations corroborate earlier findings on altered behavioral parameters in insects exposed to several toxic agents (Abolaji et al. 2014, 2015; Adedara et al. 2015, 2016a, 2016b; Afolabi et al. 2018). The reduction in the percent of exploration time of a familiar object, as well as in the percent survival observed in the group

treated with the highest MeHg⁺ dose for 30 days followed by the detoxification period, is presumed to reflect persistent toxicity, corroborating reports in both humans and rodents (Rice 1996; Weiss et al. 2002; Newland 2010). To the best of our knowledge, the data presented here are the first to describe this type of delayed toxicity in insects.

MeHg⁺ possesses high affinity for -SH and -SeH groups ubiquitously found in living organisms as part of the amino acids cysteine and selenocysteine, respectively. MeHg⁺ is not found freely in the organisms but is bound to cysteine and GSH, or other -SH and -SeH-containing proteins (Nogara et al. 2019a; Oliveira et al. 2019). These functional groups are frequently present in the active site of oxidoreductase enzymes due to their high chemical reactivity (Hatfield et al. 2014; Oliveira et al. 2018). The enzymatic antioxidant system of living cells contains some important oxidoreductases (Salami et al. 2016). Therefore, the inhibition of oxidoreductases containing either -SH or -SeH by MeHg⁺ can induce oxidative stress (Adedara et al. 2015). Here, we observed that MeHg⁺ caused oxidative stress in the fat bodies of nymphs after 10 and 90 days of exposure (Fig. 7). These results corroborate previous observations in *Drosophila melanogaster* (Chauhan and Chauhan 2016) and *Naphoeta cinerea* exposed to MeHg⁺ (Afolabi et al. 2018).

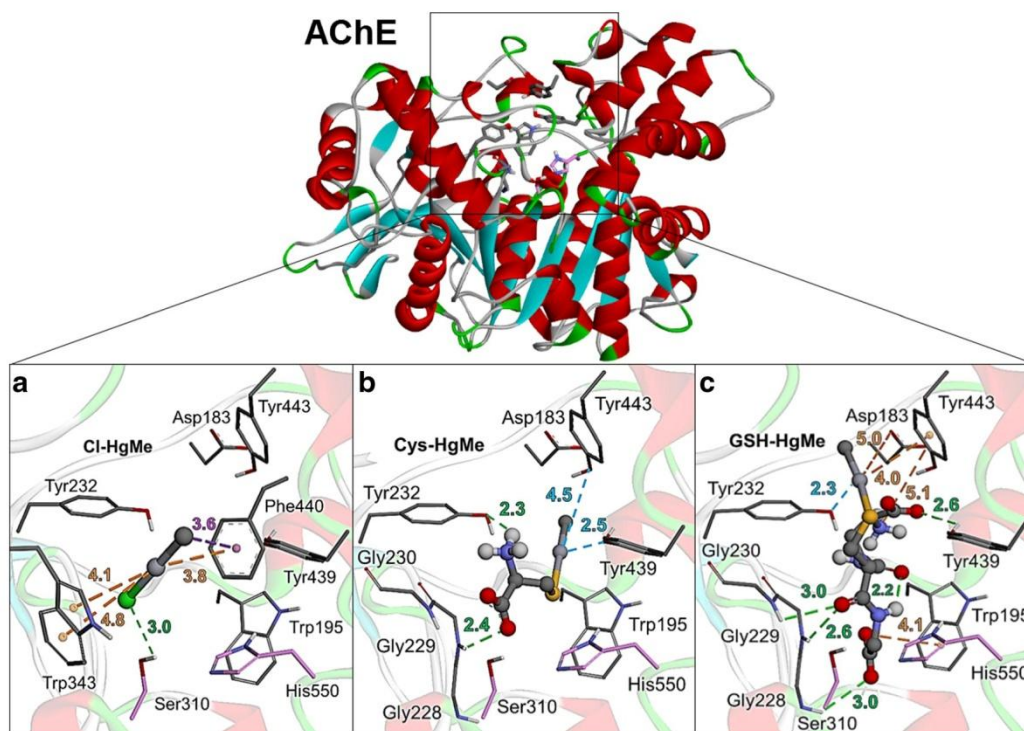


Fig. 11 Molecular docking simulations between the cockroach AChE and MeHg⁺ species (Cl-HgMe (a), Cys-HgMe (b), and GSH-HgMe (c)). The AChE active site is highlighted. The MeHg⁺ species are represented in ball and stick, and the main residues involved in the interactions

are in stick models. The H-bonds, electrostatic, hydrophobic, and mercury interactions are shown in green, orange, pink, and blue dot lines, respectively

GST, a phase II detoxification enzyme that catalyzes the reaction of GSH with electrophiles (Sheehan et al. 2001), can be used as a biomarker of environmental contamination (Liu et al. 2015; Carvalho-Neta and Abreu-Silva 2013). To investigate if GST could catalyze the conjugation of MeHg⁺ with GSH, molecular docking simulations were carried out between *N. cinerea* GST and the Cl-HgMe and Cys-HgMe molecules. The simulations showed that the MeHg⁺ species bound to the GST active site, with intermolecular interactions between the sulfur atom from GSH and the Hg atom from MeHg⁺ (Cl-HgMe and Cys-HgMe) (Fig. 10). These data indicate that nymphs' GST could catalyze the formation of GSH-HgMe (detoxification reaction), corroborating *in vivo* analyses in which we previously found increased activity in the head and fat body of nymphs after MeHg⁺ exposure (Fig. 8). Vorobjekina et al. (2017) corroborated our study, indicating that GST is an important enzyme in the metabolism of MeHg⁺ in flies. This indicates that the GST may be involved in the process of the insect-xenobiotics detoxification process. There is a small number of studies about cockroach metabolism and detoxification of xenobiotics; at the same time, the studies have been showing that this enzyme activity is increased in cockroaches challenged with a given toxicant (Habes et al. 2006; Mrdaković et al. 2019; Waczuk et al. 2019).

Previous studies have established the susceptibility of AChE to MeHg⁺ in cockroaches (Adedara et al. 2016a; Afolabi et al. 2018), flies (Abnoos et al. 2013), and rodents (Li et al. 2018). AChE catalyzes the degradation of acetylcholine into acetate and choline in the synaptic cleft, and it has been indicated as a potential biomarker of toxicity of distinct xenobiotics (Assis et al. 2018; Rodrigues et al. 2018). Herein, AChE activity in the nymphs' head decreased upon both acute and chronic exposure to the highest dose of MeHg⁺ (Fig. 9). To better characterize how MeHg⁺ might inhibit AChE, mainly because AChE does not possess free -SH groups involved in the catalysis, an *in silico* molecular docking simulation was performed. The interaction between Cl-MeHg and its putative metabolites, Cys-HgMe and GSH-HgMe, with the AChE from nymphs was determined. Both MeHg⁺ species could interact with the AChE in superficial and internal binding sites, besides of the active site (Fig. S3). In the active site, both molecules interact in the region of the acyl binding pocket (ABP) and the peripheral anionic subsite (PAS) (Fig. 11). Donepezil and huprine derivatives (classical AChE inhibitors) have been previously shown to interact at these sites (Kryger et al. 1999; Ronco et al. 2011; Silva et al. 2018). Accordingly, the binding of the MeHg⁺ species to the AChE active site seems to avoid enzyme and substrate (acetylcholine) interaction. Also, a possible interaction between Cl-HgMe and GSH-HgMe with the Cys397 residue was verified (Fig. S4), indicating a possible adduct formation and consequently denaturing the enzyme active site.

Conclusion

Taken together, our data demonstrated that environmentally relevant doses of MeHg⁺ caused biochemical (increase in the GST activity and ROS production and inhibition of AChE activity) and behavior (decrease in the exploration) alterations. Interestingly, some of the results persisted even after the end of the exposure. These results corroborate previous results observed in rodents and humans, indicating that *N. cinerea* is a candidate for translational research before testing with vertebrates.

Funding information B.C.P. was supported by CAPES/PROEX (88882.182155/2018-01). F.D.S. was supported by CAPES/PROEX (88882.182125/2018-01). P.A.N. was supported by CAPES/PROEX (88882.182123/2018-01). O.C.O is a recipient of the 2017 CNPq-TWAS (FR no. 3240299312) Postgraduate Fellowship. MA was supported by grants from the National Institute of Environmental Health Sciences, NIEHS R01ES07331, NIEHS R01ES10563, and NIEHS R01ES020852. The authors were financially supported by the Brazilians' development agencies: CNPq, FAPERGS/CNPq, 12/2014-PRONEX: n° 16/2551-0000, CAPES/PROEX (23038.004173/2019-93; n° 0493/2019), CAPES - Finance Code 001, and INCT-EN: For Cerebral Diseases, Excitotoxicity and Neuroprotection.

References

- Abnoos H, Fereidoni M, Mahdavi-Shahri N, Haddad F, Jalal R (2013) Developmental study of mercury effects on the fruit fly (*Drosophila melanogaster*). *Interdiscip Toxicol* 6:34–40. <https://doi.org/10.2478/intox-2013-0007>
- Abolaji AO, Kamdem JP, Lugokenski TH, Nascimento TK, Waczuk EP, Farombi EO, Loreto ÉLS, Rocha JBT (2014) Involvement of oxidative stress in 4-vinylcyclohexene-induced toxicity in *Drosophila melanogaster*. *Free Radic Biol Med* 71:99–108. <https://doi.org/10.1016/j.freeradbiomed.2014.03.014>
- Abolaji AO, Kamdem JP, Lugokenski TH, Nascimento TK, Waczuk EP, Farombi EO, Loreto ÉLS, Rocha JBT (2015) Ovotoxicants 4-vinylcyclohexene 1,2-monoepoxide and 4-vinylcyclohexene diepoxide disrupt redox status and modify different electrophile sensitive target enzymes and genes in *Drosophila melanogaster*. *Redox Biol* 5:328–339. <https://doi.org/10.1016/j.redox.2015.06.001>
- Adedara IA, Rosemberg DB, Souza DO, Kamdem JP, Farombi EO, Aschner M, Rocha JBT (2015) Biochemical and behavioral deficits in the lobster cockroach *Nauphoeta cinerea* model of methylmercury exposure. *Toxicol Res* 4:442–451. <https://doi.org/10.1039/C4TX00231H>
- Adedara IA, Rosemberg DB, Souza DO, Farombi EO, Aschner M, Rocha JBT (2016a) Neuroprotection of luteolin against methylmercury-induced toxicity in lobster cockroach *Nauphoeta cinerea*. *Environ Toxicol Pharmacol* 42:243–251. <https://doi.org/10.1016/j.etap.2016.02.001>
- Adedara IA, Rosemberg DB, de Souza D, Farombi EO, Aschner M, Souza DO, Rocha JBT (2016b) Neurobehavioral and biochemical changes in *Nauphoeta cinerea* following dietary exposure to chlorpyrifos. *Pestic Biochem Physiol* 130:22–30. <https://doi.org/10.1016/j.pestbp.2015.12.004>

- Afolabi BA, Adedara IA, Souza DO, Rocha JBT (2018) Dietary co-exposure to methylmercury and monosodium glutamate disrupts cellular and behavioral responses in the lobster cockroach, *Nauphoeta cinerea* model. *Environ Toxicol Pharmacol* 64:70–77. <https://doi.org/10.1016/j.etap.2018.09.003>
- Arnold K, Bordoli L, Kopp J, Schwede T (2006) The SWISS-MODEL workspace: a web-based environment for protein structure homology modelling. *Bioinformatics* 22:195–201. <https://doi.org/10.1093/bioinformatics/bti770>
- Assis CRD, Linhares AG, Cabrera MP, Oliveira VM, Silva KCC, Marcuschi M, Maciel Carvalho EVM, Bezerra RS, Carvalho LB Jr (2018) Erythrocyte acetylcholinesterase as biomarker of pesticide exposure: new and forgotten insights. *Environ Sci Pollut Res* 25:18364–18376. <https://doi.org/10.1007/s11356-018-2303-9>
- Bastos WR, Dórea JG, Bernardi JV, Lauthartte LC, Mussu MH, Lacerda LD, Malm O (2015) Mercury in fish of the Madeira river (temporal and spatial assessment), Brazilian Amazon. *Environ Res* 140:191–197. <https://doi.org/10.1016/j.envres.2015.03.029>
- Berger J (2009) Preclinical testing on insects predicts human haematotoxic potentials. *Lab Anim* 43:328–332. <https://doi.org/10.1258/la.2008.007162>
- Bisen-Hersh ER, Farina M, Barbosa F Jr, Rocha JBT, Aschner M (2014) Behavioral effects of developmental methylmercury drinking water exposure in rodents. *J Trace Elem Med Biol* 28:117–124. <https://doi.org/10.1016/j.jtemb.2013.09.008>
- Carvalho-Neta RNF, Abreu-Silva AL (2013) Glutathione S-transferase as biomarker in *Sciades herzegii* (Siluriformes: Ariidae) for environmental monitoring: the case study of São Marcos Bay, Maranhão, Brazil. *Lat Am J Aquat Res* 41:217–225. <https://doi.org/10.3856/vol41-issue2-fulltext-2>
- Chauhan V, Chauhan A (2016) Effects of methylmercury and alcohol exposure in *Drosophila melanogaster*: potential risks in neurodevelopmental disorders. *Int J Dev Neurosci* 51:36–41. <https://doi.org/10.1016/j.ijdevneu.2016.04.010>
- Cheluvappa R, Scowen P, Eri R (2017) Ethics of animal research in human disease remediation, its institutional teaching; and alternatives to animal experimentation. *Pharmacol Res Perspect* 5:1–14. <https://doi.org/10.1002/prp2.332>
- Clark JM (2018) The 3Rs in research: a contemporary approach to replacement, reduction and refinement. *Br J Nutr* 120:1–7. <https://doi.org/10.1017/S0007114517002227>
- Clarkson TW (1993) Mercury: major issues in environmental health. *Environ Health Perspect* 100:31–38. <https://doi.org/10.1289/ehp.9310031>
- Doi R (1991) Individual difference of methylmercury metabolism in animals and its significance in methylmercury toxicity. In: Suzuki T, Imura N, Clarkson TW (eds) *Advances in mercury toxicology*. Rochester Series on Environmental Toxicity. Springer, Boston. https://doi.org/10.1007/978-1-4757-9071-9_4
- Dórea JG, Marques RC (2016) Mercury levels and human health in the Amazon Basin. *Ann Hum Biol* 43:349–359. <https://doi.org/10.1080/03014460.2016.1192682>
- Ekino S, Susa M, Ninomiya T, Imamura K, Kitamura T (2007) Minamata disease revisited: an update on the acute and chronic manifestations of methyl mercury poisoning. *J Neurol Sci* 262:131–144. <https://doi.org/10.1016/j.jns.2007.06.036>
- Ellman GL, Courtney KD, Andress JRV, Featherstone RM (1961) A new and rapid colorimetric determination of acetylcholinesterase activity. *Biochem Pharmacol* 7:88–95. [https://doi.org/10.1016/0006-2952\(61\)90145-9](https://doi.org/10.1016/0006-2952(61)90145-9)
- Habes D, Morakchi S, Aribi N, Farine J-P, Soltani N (2006) Boric acid toxicity to the German cockroach, *Blattella germanica*: alterations in midgut structure, and acetylcholinesterase and glutathione S-transferase activity. *Pestic Biochem Physiol* 84:17–24. <https://doi.org/10.1016/j.pestbp.2005.05.002>
- Habig WH, Jakoby WB (1981) Assays for differentiation of glutathione S-transferases. *Methods Enzymol* 77:398–405. [https://doi.org/10.1016/S0076-6879\(81\)77053-8](https://doi.org/10.1016/S0076-6879(81)77053-8)
- Hanwell MD, Curtis DE, Lonie DC, Vandermeersch T, Zurek E, Hutchison GR (2012) Avogadro: an advanced semantic chemical editor, visualization, and analysis platform. *Aust J Chem* 4:17. <https://doi.org/10.1186/1758-2946-4-17>
- Harada M (1995) Minamata disease: methylmercury poisoning in Japan caused by environmental pollution. *Crit Rev Toxicol* 25:1–24. <https://doi.org/10.3109/10408449509089885>
- Hatfield DL, Tsuji PA, Carlson BA, Gladyshev VN (2014) Selenium and selenocysteine: roles in cancer, health, and development. *Trends Biochem Sci* 39:112–120. <https://doi.org/10.1016/j.tibs.2013.12.007>
- Kryger G, Silman I, Sussman JL (1999) Structure of acetylcholinesterase complexed with E2020 (Aricept®): implications for the design of new anti-Alzheimer drugs. *Structure* 7:297–307. [https://doi.org/10.1016/S0969-2126\(99\)80040-9](https://doi.org/10.1016/S0969-2126(99)80040-9)
- Lang C, Kolaj-Robin O, Cirefice G, Taconet L, Pel E, Jouette S, Buda M, Milne C, Charton E (2018) Replacement, reduction, refinement - animal welfare progress in european pharmacopoeia monographs: activities of the European pharmacopoeia commission from 2007 to 2017. *Pharmeur Bio Sci Notes* 2018:12–36
- Li P, Du B, Chan HM, Feng X, Li B (2018) Mercury bioaccumulation and its toxic effects in rats fed with methylmercury polluted rice. *Sci Total Environ* 633:93–99. <https://doi.org/10.1016/j.scitotenv.2018.03.185>
- Liu H, He J, Zhao R, Chi C, Bao Y (2015) A novel biomarker for marine environmental pollution of pi-class glutathione S-transferase from *Mytilus coruscus*. *Ecotoxicol Environ Saf* 118:47–54. <https://doi.org/10.1016/j.ecoenv.2015.04.012>
- Lovato FL, Rocha JBT, Dalla Corte CL (2017) Diphenyl diselenide protects against methylmercury-induced toxicity in *Saccharomyces cerevisiae* via the Yap1 transcription factor. *Chem Res Toxicol* 30:1134–1144. <https://doi.org/10.1021/acs.chemrestox.6b00449>
- Magos L (1976) The effects of dimercaptosuccinic acid on the excretion and distribution of mercury in rats and mice treated with mercuric chloride and methylmercury chloride. *Br J Pharmacol* 56:479–484
- Morris GM, Huey R, Lindstrom W, Sanner MF, Belew RK, Goodsell DS, Olson AJ (2009) AutoDock4 and AutoDockTools4: automated docking with selective receptor flexibility. *J Comput Chem* 30:2785–2791. <https://doi.org/10.1002/jcc.21256>
- Mrdaković M, Ilijin L, Vlahović M, Filipović A, Grčić A, Todorović D, Perić-Mataruga V (2019) Effects of dietary fluoranthene on nymphs of *Blattica dubia* S. (Blattodea: Blaberidae). *Environ Sci Pollut Res* 26:6216–6222. <https://doi.org/10.1007/s11356-019-04133-1>
- Mueller GA, Soheila JM, Lars CP (2014) The molecular basis of peanut allergy. *Curr Allergy Asthma Rep* 14:429. <https://doi.org/10.1007/s11882-014-0429-5>
- Naganuma A, Imura N (1984) Species difference in biliary excretion of methylmercury. *Biochem Pharmacol* 33:679–682. [https://doi.org/10.1016/0006-2952\(84\)90325-3](https://doi.org/10.1016/0006-2952(84)90325-3)
- Newland MC (2010) Fish nutrients and methylmercury: a view from the laboratory. In: Wang C, Slikker W Jr (eds) *Developmental neurotoxicology research: principles, models, techniques, strategies and mechanisms*. Wiley, Hoboken, New Jersey, pp 279–318. <https://doi.org/10.1002/9780470917060.ch15>
- Nogara PA, Oliveira CS, Schmitz GL, Piquini PC, Farina M, Aschner M, Rocha JBT (2019a) Methylmercury's chemistry: from the environment to the mammalian brain. *Biochim Biophys Acta Gen Subj* 1863:129284. <https://doi.org/10.1016/j.bbagen.2019.01.006>
- Nogara PA, Farina M, Aschner M, Rocha JBT (2019b) Mercury in our food. *Chem Res Toxicol* 32:1459–1461. <https://doi.org/10.1021/acs.chemrestox.9b00126>
- Oliveira CS, Piccoli BC, Aschner M, Rocha JBT (2017a) Chemical speciation of selenium and mercury as determinant of their

- neurotoxicity. In: Aschner M, Costa L (eds) Neurotoxicity of metals. Advances in Neurobiology. Springer, New York, New York, pp 53–83. https://doi.org/10.1007/978-3-319-60189-2_4
- Oliveira C, Joshee L, George H, Nijhara S, Bridges C (2017b) Oral exposure of pregnant rats to toxic doses of methylmercury alters fetal accumulation. *Reprod Toxicol* 69:265–275. <https://doi.org/10.1016/j.reprotox.2017.03.008>
- Oliveira CS, Nogara PA, Ardisson-Araújo DMP, Aschner M, Rocha JBT, Dórea JG (2018) Neurodevelopmental effects of mercury. In: Aschner M, Costa L (eds) Linking environmental exposure to neurodevelopmental disorders. Advances in Neurotoxicology, vol 2. Elsevier. <https://doi.org/10.1016/bs.ant.2018.03.005>
- Oliveira CS, Nogara PA, Garlet QI, Rieder GS, JBT R (2019) Biological thiols and their interaction with mercury. In: CC MA (ed) Thiols: Structure, properties and reactions, 1st edn. Nova Science Publishers, Hauppauge, pp 1–60.
- Pérez-Severiano F, Santamaría A, Pedraza-Chaverri J, Medina-Campos ON, Ríos C, Segovia J (2004) Increased formation of reactive oxygen species, but no changes in glutathione peroxidase activity, in striata of mice transgenic for the Huntington's disease mutation. *Neurochem Res* 29:729–733. <https://doi.org/10.1023/B:NERE.0000018843.83770.4b>
- Peterson RT, Nass R, Boyd WA, Freedman JH, Dong K, Narahashi T (2008) Use of non-mammalian alternative models for neurotoxicological study. *Neurotoxicology* 29:545–554. <https://doi.org/10.1016/j.neuro.2008.04.006>
- Rand MD, Prince LM, Vorojekina D (2019) Drosophotoxology: elucidating kinetic and dynamic pathways of methylmercury toxicity in a *Drosophila* model. *Front Genet* 10:666. <https://doi.org/10.3389/fgene.2019.00666>
- Rice DC (1996) Evidence for delayed neurotoxicity produced by methylmercury. *Neurotoxicology* 17:583–596
- Rodrigues NR, Nunes ME, Silva DG, Zemolin AP, Meinerz DF, Cruz LC, Pereira AB, Rocha JB, Posser T, Franco JL (2013) Is the lobster cockroach *Nauphoeta cinerea* a valuable model for evaluating mercury induced oxidative stress? *Chemosphere* 92:1177–1182. <https://doi.org/10.1016/j.chemosphere.2013.01.084>
- Rodrigues APC, Carvalheira RG, Gomes V, Arias ARL, Almosny NRP, Castilhos ZC, Bidone ED (2018) Acetylcholinesterase activity in fish exposed to mercury in Guanabara bay, RJ, Brazil. *Environ Pollut Prot* 3(4):91–99. <https://doi.org/10.22606/epp.2018.34001>
- Ronco C, Foucault R, Gillon E, Bohn P, Nachon F, Jean L, Renard PY (2011) New huprine derivatives functionalized at position 9 as highly potent acetylcholinesterase inhibitors. *ChemMedChem* 6:876–888. <https://doi.org/10.1002/cmdc.201000523>
- Rudd JWM, Bodaly RA, Fisher NS, Kelly CA, Kopec D, Whipple C (2018) Fifty years after its discharge, methylation of legacy mercury trapped in the Penobscot estuary sustains high mercury in biota. *Sci Total Environ* 642:1340–1352. <https://doi.org/10.1016/j.scitotenv.2018.06.060>
- Salami AT, Odukanmi OA, Olagoke CO, Iyiola TO, Olaleye SB (2016) Role of nitric oxide and endogenous antioxidants in thyroxine facilitated healing of ischemia-reperfusion induced gastric ulcers. *J Pharm Res* 12:189–206
- Shambaugh GF (1969) Toxicity and effects on motor coordination of some neurotropic drugs on the cockroach *Nauphoeta cinerea*. *Ann Entomol Soc Am* 62:370–375. <https://doi.org/10.1093/aesa/62.2.370>
- Sheehan D, Meade G, Foley VM, Dowd CA (2001) Structure, function and evolution of glutathione transferases: implications for classification of non-mammalian members of an ancient enzyme superfamily. *Biochem J* 360:1–16. <https://doi.org/10.1042/0264-6021:3600001>
- Silva FD, Nogara PA, Braga MM, Piccoli BC, Rocha JBT (2018) Molecular docking analysis of acetylcholinesterase corroborates the protective effect of pralidoxime against chlorpyrifos-induced behavioral and neurochemical impairments in *Nauphoeta cinerea*. *Comput Toxicol* 8:25–33. <https://doi.org/10.1016/j.comtox.2018.07.003>
- Stein AF, Gregus Z, Klaassen CD (1988) Species variation in biliary excretion of glutathione-related thiols and methylmercury. *Toxicol Appl Pharmacol* 93:351–359. [https://doi.org/10.1016/0041-008X\(88\)90037-3](https://doi.org/10.1016/0041-008X(88)90037-3)
- Stewart JJP (2007) Optimization of parameters for semiempirical methods v: modification of NDDO approximations and application to 70 elements. *J Mol Model* 13:1173–1213. <https://doi.org/10.1007/s00894-007-0233-4>
- Streets DG, Horowitz HM, Jacob DJ, Lu Z, Levin L, Ter Schure AFH, Sunderland EM (2017) Total mercury released to the environment by human activities. *Environ Sci Technol* 51:5969–5977. <https://doi.org/10.1021/acs.est.7b00451>
- Trott O, Olson AJ (2009) AutoDock Vina: improving the speed and accuracy of docking with a new scoring function, efficient optimization, and multithreading. *J Comput Chem* 31:455–461. <https://doi.org/10.1002/jcc.21334>
- Vorojekina D, Broberg K, Love TM, Davidson PW, Wijngaarden EV, Rand MD (2017) Glutathione S-transferase activity moderates methylmercury toxicity during development in *Drosophila*. *Toxicol Sci* 157:211–221. <https://doi.org/10.1093/toxsci/kfx033>
- Waczuk EP, Wagner R, Bruna K, Rocha JBT, Ardisson-Araújo DMP, Barbosa NV (2019) Assessing the toxicant effect of spontaneously volatilized 4-vinylcyclohexane exposure in nymphs of the lobster cockroach *Nauphoeta cinerea*. *Environ Toxicol Pharmacol* 72:103264. <https://doi.org/10.1016/j.etap.2019.103264>
- Weiss B, Clarkson TW, Simon W (2002) Silent latency periods in methylmercury poisoning and in neurodegenerative disease. *Environ Health Perspect* 110:851–854. <https://doi.org/10.1289/ehp.02110s5851>
- Wiederstein M, Sippl MJ (2007) ProSA-web: interactive web service for the recognition of errors in three-dimensional structures of proteins. *Nucleic Acids Res* 35:407–410. <https://doi.org/10.1093/nar/gkm290>
- Zhang Y, Jacob DJ, Horowitz HM, Chen L, Amos HM, Krabbenhoft DP, Slemr F, St Louis VL, Sunderland EM (2016) Mercury transformation and speciation in flue gases from anthropogenic emission sources: a critical review. *Atmos Chem Phys* 16:2417–2433. <https://doi.org/10.5194/acp-16-2417-2016>

Publisher's note Springer Nature remains neutral with regard to jurisdictional claims in published maps and institutional affiliations.

3 ARTIGO 2 – Transcriptional analyses of acute *per os* exposure and co-exposure of 4-vinylcyclohexene and methylmercury-contaminated diet in adults of *Drosophila melanogaster*

Environmental Pollution 263 (2020) 114632



Contents lists available at ScienceDirect

Environmental Pollution

journal homepage: www.elsevier.com/locate/envpol



Transcriptional analyses of acute *per os* exposure and co-exposure of 4-vinylcyclohexene and methylmercury-contaminated diet in adults of *Drosophila melanogaster*[☆]



Bruna Candia Piccoli ^a, Ana Lúcia Anversa Segatto ^a, Élgion L.S. Loreto ^a, José Cláudio Fonseca Moreira ^b, Daniel M.P. Ardisson-Araújo ^{a, **}, João B.T. Rocha ^{a, *}

^a Programa de Pós-graduação em Ciências Biológicas: Bioquímica Toxicológica, Department of Biochemistry and Molecular Biology, Federal University of Santa Maria, Santa Maria, RS, 97105-900, Brazil

^b Programa de Pós-graduação em Ciências Biológicas: Bioquímica ICBS/UFRGS, Department of Biochemistry, Federal University of Rio Grande do Sul, Porto Alegre, RS, 90035-003, Brazil

ARTICLE INFO

Article history:

Received 13 November 2019
Received in revised form
15 April 2020
Accepted 16 April 2020
Available online 21 April 2020

Keywords:

Drosophila melanogaster
Selenoprotein
Thiol-containing protein
Next-generation sequencing

ABSTRACT

Continuous exposure to low levels of toxic substances can be associated with delayed physical disturbances, which can be preceded by changes in enzyme activities and gene expression. Thus, understanding changes in the transcriptional profile could help in recognition of early molecular events involved in the toxicity mechanism of toxicants. Vinylcyclohexene (VCH) and methylmercury (MeHg⁺) are xenobiotics, which do not present a completely elucidated mechanism of toxicity. Metabolites of both compounds have some overlapping chemical properties that involve moderate to high affinity for thiol and selenol groups. In this work, we characterized by deep-sequencing transcriptomic approach the effects of VCH and MeHg⁺ on the mRNA transcriptional profile of adults fruit flies (*Drosophila melanogaster*) after individual and concomitant exposure to VCH and MeHg⁺. The flies were separated into four groups: control, VCH, MeHg⁺, and VCH + MeHg⁺. After individual exposure, VCH deregulated 38 genes (of which the majority was up-regulated), whereas MeHg⁺ altered 26 genes (i.e., 14 down-regulated). VCH and MeHg⁺ co-exposure changed 72 genes with a high number of genes down-regulated. Together, the results suggest that although the compounds could have some similar protein targets (e.g., sulfhydryl-containing proteins), the transcriptional profile after individual exposures and co-exposure were completely different.

© 2020 Elsevier Ltd. All rights reserved.

1. Introduction

Several organisms, including humans, other animals, plants, and microorganisms, are constantly exposed to a wide range of xenobiotics as most of the human activities have increased the release of toxicants that affect the environment (Grandjean and Landrigan, 2006; Tousova et al., 2017). Continuous exposure to small levels of toxicants can be associated with delayed toxicity (i.e., explicit physical impairments) that will appear only after a silent period. However, gene transcription and/or protein synthesis or activity

might be modified at earlier stages of exposure (Scumaci et al., 2018; Wilson et al., 2013). The complex molecular responses to intoxication can lead to a series of deleterious phenotypes and loss of the organism's fitness (Banks and Lein, 2012; Carter et al., 2019). The detection of changes in gene transcription may contribute to the identification of molecular initiating events and the sequence of events that culminate in cellular dysfunctions (Hartung et al., 2017), as well as in the identification of biomarkers of toxicity.

Vinylcyclohexene (VCH) is an epoxy resin diluent used in the production of plastic, rubber, and pesticides (Huff, 2001) and commonly present in the wastewater of hydroxylated liquid polybutadiene production (Gonçalves et al., 2016). The routes of VCH exposure might be respiratory, digestive, and dermal (NTP, 1989). VCH-derived epoxy metabolites produced in the targeted organism is the toxic acting agent. These metabolites are formed by cytochrome P450, expressed in liver and ovaries (Cannady et al., 2003;

[☆] This paper has been recommended for acceptance by CHSAM-Harmon.

* Corresponding author.

** Corresponding author.

E-mail addresses: daniel_ardisson@yahoo.com.br (D.M.P. Ardisson-Araújo), jbtrocha@yahoo.com.br (J.B.T. Rocha).

Doerr-Stevens et al., 1999), which oxidizes the double bonds of VCH into epoxides generating two types of metabolites: monoepoxide (4-vinylcyclohexene 1,2 epoxide or 4-vinylcyclohexene 7,8 epoxide) and diepoxide (4-vinylcyclohexene diepoxide) (Keating et al., 2008). The epoxide group is an electrophilic center having moderate reactivity with nucleophilic centers in the organisms, including thiol (-SH) and, possibly selenol (-SeH) groups (Abolaji et al., 2015; Barret et al., 1982; He et al., 2015; Oliveira et al., 2017).

Mercury is an environmental contaminant released by natural and anthropogenic activities (Oliveira et al., 2017). Once the inorganic forms Hg^0 , Hg^+ , and Hg^{2+} reach the aquatic environment, the sediment bacteria can methylate them to form methylmercury ($MeHg^+$) (Ranchou-Peyruse et al., 2018; Xing et al., 2018). $MeHg^+$ is biomagnified in the aquatic trophic chain, and piscivorous fish can accumulate Hg in the range of <0.5 up to 5.0 mg $MeHg^+$ /Kg muscle weight (Oliveira et al., 2017). $MeHg^+$ can also be accumulated in aquatic and terrestrial plants (Boening, 2000; Cui et al., 2017). In this way, ingestion is the most important exposure route for $MeHg^+$ (Martínez-Salcido et al., 2018; Pazi et al., 2017). $MeHg^+$ is a soft electrophile with a strong affinity for -SH and -SeH, which are the functional groups of amino acids cysteine and selenocysteine, respectively. Of particular importance, the loss of function of thiol- and selenol-containing proteins by electrophile $MeHg^+$ is central in $MeHg^+$ toxicity (Farina et al., 2011; Oliveira et al., 2017). When cysteine is bound to $MeHg^+$, it mimics the amino acid methionine, which facilitates blood-brain barrier crossing and causes damage to the central nervous system (Bridges and Zalups, 2016).

In fruit flies, $MeHg^+$ and VCH exposure have been reported to cause oxidative stress in adults (Abolaji et al., 2014, 2015; Chauhan and Chauhan, 2016; Leão et al., 2018), as well as, $MeHg^+$ was associated with impairments in neurodevelopment (Rand et al., 2019), locomotion (Algarve et al., 2018) and reproduction (Chauhan et al., 2017; Leão et al., 2018). Using classical biochemical approaches, our research group showed that VCH and $MeHg^+$ co-exposure caused an increase in the production of reactive species and glutathione S-transferase activity (Piccoli et al., 2019). However, little is known about the effects of these toxicants on gene expression at the cell transcription level. We also inquired whether individual VCH and $MeHg^+$ exposure trigger similar transcriptional responses as co-exposure. Therefore, we hypothesized that as VCH and $MeHg^+$ are electrophiles, the compounds would interact with distinct (Zhang et al., 2016) and overlapping nucleophilic centers (Barret et al., 1982; He et al., 2015), which includes thiol and selenol-containing groups (e.g. proteins, aminoacyl-tRNAs or free amino acids). Then they could hypothetically have additive or synergistic effects in a wide manner that would interfere at the transcriptional profile of adult fruit flies exposed and co-exposed to VCH and $MeHg^+$. For this purpose, we carried out a deep-sequencing analysis of mRNA transcripts of fruit flies adults after *per os* acute exposure or co-exposure to non-lethal doses of VCH and $MeHg^+$. We found that individual exposure to VCH caused up-regulation of various genes while individual exposure to $MeHg^+$ up- and down-regulated a similar number of genes. Surprisingly, VCH + $MeHg^+$ co-exposure down-regulated several genes. Although the compounds can have partially overlapping targets, the genetic response was different.

2. Material and methods

2.1. Chemicals

Chemicals had analytical grade. 4-vinylcyclohexene (99%) and methylmercury chloride (CH_3HgCl) were purchased from Sigma Aldrich (St. Louis, MO, USA).

2.2. Insect colony

The fruit fly *D. melanogaster* strain Oregon R colony was maintained in the Laboratory of Toxicological Biochemistry, Federal University de Santa Maria (UFSM), Brazil. The flies were reared on agar meal (1% agar, 1% cornmeal, 1% sucrose, 1% powdered milk, 2% yeast extract, and 0.08% nipagin in ddH₂O) at 23 ± 1 °C and 60% of relative humidity with 12 h l/d cycle according to previously published protocols (Schou et al., 2017).

2.3. Individual exposure to VCH and $MeHg^+$ and co-exposure

Seven hundred twenty juvenile flies (male and female) with 3-days after eclosion were divided into four groups and treated for three days in agar meal. To obtain the desired concentrations of the compounds, we dilute the VCH and dissolve the $MeHg^+$ in ethanol and add to the agar at final concentrations of 0.1% ethanol. We set the control (ethanol 0.1%), VCH (1 mM), $MeHg^+$ (0.2 mM), and VCH + $MeHg^+$ (1 mM and 0.2 mM) treated groups. The exposure experiments were performed in triplicates.

2.4. RNA extraction

Forty flies per sample were anesthetized on ice and immediately placed in Trizol® (Thermo Fisher Scientific, Waltham, Massachusetts, EUA). The total RNA was extracted according to the manufacturer's protocol. Total RNA was quantified in both Nanodrop2000TM (Thermo Fisher Scientific) and Qubit 4TM fluorimeter (Thermo Fisher Scientific) using the Qubit™ RNA HS Assay kit (Thermo Fisher Scientific). The mRNA was isolated using the Dynabeads™ mRNA Purification Kit (Thermo Fisher Scientific) from 10 µg of crude purified RNA.

2.5. Library sequencing, assembly using reference genome and differential expression analysis

The library preparation was performed using Ion Total RNA-Seq Kit v2 (Thermo Fisher Scientific) for each purified RNA. The sequencing was performed on IonGeneStudio S5 equipment (Thermo Fisher Scientific) using the Ion 540 TM Kit-OT2. Single-reads were trimmed using the TrimGalore program (Wu et al., 2011). The quality of the readings was visualized and checked before and after the trimming using FastQC (Andrews, 2010). The transcripts assembly and differential expression analysis were performed according to Trapnell et al. (2012). The TopHat program (Trapnell et al., 2009) was used to map the reads of each group replicates (control, VCH, $MeHg^+$, and VCH + $MeHg^+$) in the *D. melanogaster* reference genome (Genbank accession number: SRX3797402). Differential expressed genes (DEGs) were defined as significant when presented a $p < 0.05$ and fold change (FC) > 0.5 on the Student t-test. Moreover, DEGs among the treatments were plotted in a Venn diagram (<http://bioinformatics.psb.ugent.be/webtools/Venn/>).

2.6. Chromosome expression

The percent coverage of the *D. melanogaster* chromosomes was performed in the Geneious 9.0.5 (Kearse et al., 2012). We mapped the trimmed reads from each replicate on each of the four chromosomes, with a pairwise identity of 99% and allowing a gap size of 1000 to deal with spliced exon limits. To normalize the comparison, the total number of nucleotides mapped in the entire chromosome for each replicate was divided by the chromosome size and by the total number of nucleotides sequenced in the sample. The data were expressed as Reads Per Kilobase Million (RPKM).

2.7. Gene enrichment analysis

The enrichment of DEGs in gene ontology (GO) was performed on the Panther Classification System (Mi et al., 2013). The Mann-Whitney *U* Test (Wilcoxon Rank-Sum Test) was used to determine the *p*-value and results of these analyses were corrected for multi-testing following Bonferroni.

2.8. Relative expression of selenol- and thiol-containing proteins

To define which proteins have selenocysteine and cysteine residues, the amino acids that contain the selenol and thiol groups, we used the fruit fly proteome (UP000000803) from the UniProt platform. We added the proteome in the Geneious 9.0.5 (Kearse et al., 2012) and searched for the amino acids selenocysteine (U) and cysteine (C), and the most common motifs among oxidoreductase enzymes (CC, CXC, CXXC). To do the relative expression analysis, we downloaded the mRNAs of the interest genes and compared the nucleotide sequence with the amino acid sequence of the proteins. The CDS sequence was used as a reference for mapping the trimmed reads of each replicate of the groups. The number of mapped nucleotides was divided by the number of CDS nucleotides and by the total number of nucleotides sequenced in the sample. We analyzed the relative expression of the genes encoding selenoproteins and antioxidant system thiol-containing proteins of *D. melanogaster*, according to Orr et al. (2013). The data were expressed as Reads Per Kilobase Million (RPKM).

2.9. Statistical analyses

All results were expressed as the mean \pm standard error of the mean (SEM). Student's *t*-test analyzed data on differentially expressed genes. Two-way ANOVA (treatment \times chromosome) analyzed data from global mRNA expression. Two-way ANOVA (2 with/without VCH \times 2 with/without MeHg⁺) analyzed data derived from the relative gene expression of selenoprotein and thiol-containing proteins. Main effect and lower-order interactions were discussed only when higher-order interactions were statistically not significant. The results were considered significant when $p \leq 0.05$.

3. Results

3.1. Transcriptome characteristics

RNA-seq determined the transcriptional profile of whole body adult fruit flies (male and female) after acute feeding exposure and co-exposure to VCH and MeHg⁺. The intoxicant concentration, *i.e.* 1 mM VCH and/or 200 μ M MeHg⁺ did not influence the flies survival rates, (Piccoli et al., 2019). After three days of feeding exposure, the whole body total RNA was extracted and prepared for mRNA deep-sequencing using the IonTorrent methodology. 46,325,074 raw reads were sequenced, and after trimming, 39,152,950 (Table S1) were used for further analyses.

3.2. Global mRNA transcription analysis

To evaluate the global mRNA transcription changes caused by the individual exposure and co-exposure to VCH and MeHg⁺, we performed the analysis of the chromosome or chromosome arms coverage percentages (Fig. 1). *D. melanogaster* presents four chromosomes, including chromosome 2 (two arms 2L/2R, accession numbers NT_033779 and NT_033778, respectively), 3 (two arms 3L/3R, accession numbers NT_037436 and NT_033777, respectively), 4 (NC_004353), and X/Y (NC_004354 and NC_024512,

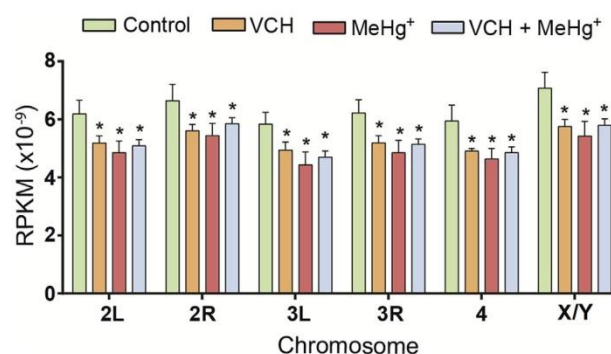


Fig. 1. Global mRNA expression of *D. melanogaster* chromosomes [2 (two arms 2L/2R), 3 (two arms 3L/3R), 4, and X] after acute feeding exposure and co-exposure to VCH and MeHg⁺ for three days. Data expressed as the mean \pm SEM. Results analyzed by Two-way ANOVA (treatment and chromosome as factors). * indicate a significant difference from control ($p < 0.05$). Statistical analysis indicated the main effect of treatment because VCH and MeHg⁺ exposures decreased the global mRNA expression. The analysis also indicated the main effect of chromosome due to 2 (arm 2R) and X/Y have a greater expression than the others.

respectively). Two-way ANOVA (treatment and chromosome as independent factors) revealed a significant main effect of treatments [$F(3,48) = 16.18$; $p < 0.0001$] due to individual VCH and MeHg⁺ exposure and the co-exposure presented a lower global mRNA chromosome transcription than the control group. Statistical analysis also indicated a main effect of chromosome [$F(5,48) = 5.642$; $p = 0.0004$] by arm 2R and X/Y presented a higher expression than arm 2L, arm 3L, arm 3R, and 4.

3.3. Differentially expressed genes with fold change > 0.5 and > 1.5

To evaluate the deregulations caused by VCH and MeHg⁺ in exposed flies, differential expression analysis was performed (Table S2). We represent the DEGs in a Venn Diagram and show in blue the total number of up-regulated genes and in red the down-regulated genes with a FC > 0.5 (Fig. 2A). The individual exposure to VCH deregulated 38 genes with most (31 genes) being up-regulated. On the other hand, the individual exposure to MeHg⁺ deregulated 26 genes with most (14 genes) being down-regulated. Only the *Fst* gene was altered by both individual exposures in an up-regulation manner. Surprisingly, the presence of VCH in a co-exposure manner caused higher gene down-regulation, modifying several other genes (*i.e.*, 47 different genes) not altered in the two individual treatments. Only four altered genes were shared by both co-exposure and VCH individual exposure treatment: *Lsp2* was down-regulated and *Cyp1*, *Cp16*, *Cp18* were up-regulated. Comparing co-exposure and MeHg⁺ individual exposure treatments, five altered genes were shared, including *RpL17*, *RpL35A*, *Tap δ* , *Hoip* being down-regulated, and *CG13947* up-regulated.

We identified indeed only the most altered genes (*i.e.*, FC > 1.5 and $p < 0.05$ on the Student's *t*-test) observed during feeding exposure and co-exposure to the intoxicants. We also represent the > 1.5-DEGs in a Venn Diagram, where we colored in blue > 1.5-fold up-regulated and in red > 1.5-fold down-regulated genes (Fig. 2B). Individual exposure to VCH and MeHg⁺ were able to deregulate nine genes each, with most up-regulated (*i.e.*, a total of six genes for MeHg⁺ and eight genes for VCH). The unique gene transcriptionally altered by the individual treatments codes for a stressor peptide, the *Fst*. Different from that observed for individual VCH and MeHg⁺ effects, the co-exposure down-regulated nine genes and overexpressed six genes. *Hoip* was an example of the down-regulated gene that was also altered by individual exposure to MeHg⁺.

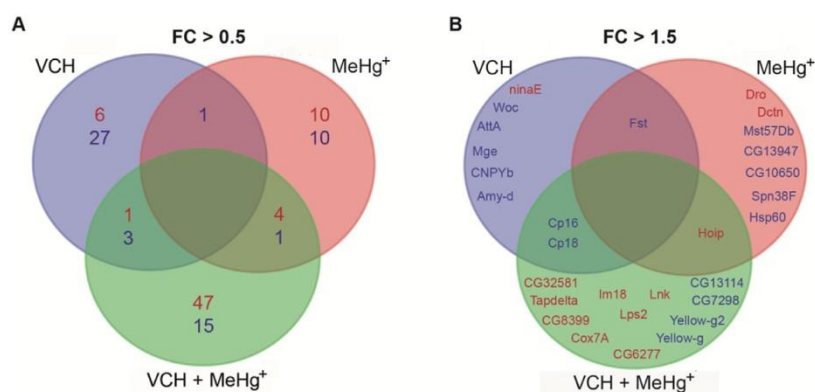


Fig. 2. Venn diagram of significantly up- (blue) and down- (red) regulated genes in *D. melanogaster* after acute feeding exposure and co-exposure to VCH and MeHg⁺ for three days compared with the control group. Genes with fold change (FC) > 0.5 (A) and the most altered genes that presented FC > 1.5 (B) and $p < 0.05$ on the Student's *t*-test. (For interpretation of the references to color in this figure legend, the reader is referred to the Web version of this article.)

Among the overexpressed genes, two chorionic proteins (*Cp16* and *Cp18*) were altered after co-exposure as well as individual exposure to VCH.

3.4. Gene enrichment analyses

GO enrichment analysis was carried out to identify biological processes affected by the toxicants. GOs were assigned in all three domains: biological process, cellular component, and molecular function with 25 GO terms enriched by DEGs (Fig. 3). Overall, the predominant GO terms of the 'biological process' were 'cellular and metabolic processes' with 'cell part and organelle' as the main enriched terms for all treatments. For 'molecular function', assignments were related mostly to 'binding and catalytic activity'. Although the GO-enrichment patterns were similar, individual VCH treatment-deregulated genes were mostly up-regulated (Fig. 3A), whereas MeHg⁺ and VCH + MeHg⁺ co-exposure (Fig. 3B and C) induced down-regulation.

3.5. Potential targets of VCH and MeHg⁺: relative expression of selenol- and thiol-containing proteins

The main targets of VCH and MeHg⁺ are likely selenol and thiol groups of proteins or other non-protein molecules like aminoacyl-tRNAs and free amino acids. We have found in the *D. melanogaster* proteome five selenoproteins (three largely confirmed and two putative proteins), each containing at least one putative seleno-cysteine residue: *Bthd*, *Gld*, *Kel*, *SelG*, and *SelD*. This result was found according to searches at the UNIPROT database. For thiol-containing proteins, we found 290,886 cysteine residues in the entire proteome of the fruit fly. The Cys-containing motif residues most encountered was CXXC (14,764), followed by CXC (12,092), and CC (6,636). Those are motifs related to oxidoreductases (reviewed by Oliveira et al., 2018) with a total of 9,354 different proteins. All those would be potential targets of VCH and MeHg⁺ with several proteins related to the antioxidant cell system. Therefore, we focused on the relative transcription of some specific putative targets of VCH and MeHg⁺, including genes that code for selenoproteins and antioxidant system-related oxidoreductases. For the selenoprotein transcripts, only *Gld* during exposure to VCH was down-regulated when compared to the control (Fig. 4). Two-way ANOVA revealed a significant second-order interaction (VCH x MeHg⁺) in *Gld* [$F(1,8) = 6.68$; $p = 0.03$]. Surprisingly, MeHg⁺

suppressed the effects of VCH, during co-exposure treatment.

Most of the proteins that were described as the main players in the antioxidant cell system functioning of *D. melanogaster* are thiol-containing enzymes, such as peroxiredoxins, thioredoxins, thioredoxin reductases, glutathione S-transferases, glutaredoxins, and sulfiredoxin. After relative expression gene analysis, we found that peroxiredoxins, thioredoxin reductases, and sulfiredoxin were shown not to be altered by the individual treatments (Figs. S1–S3). Oppositely, the thioredoxin transcripts of *Dhd* and *Trx-T* were affected by the VCH and MeHg⁺ exposures, respectively (Fig. 5). *Dhd* transcripts were up-regulated by VCH exposure and the co-exposure suppressed this effect (two-way ANOVA revealed a significant second-order interaction (VCH x MeHg⁺) [$F(3,56) = 3.787$; $p = 0.0152$]). Moreover, in a similar fashion as that observed for the selenoprotein *Gld* transcripts, the co-exposure treatment suppressed the deregulation. Two-way ANOVA indicated a main effect of MeHg⁺ in *TrxT* due transcripts up-regulation by this toxicant [$F(1,8) = 7.37$; $p = 0.026$].

The relative transcriptions of glutathione s-transferases (*Gst*) are shown in Fig. 6. In insects, GSTs are divided into six classes, which are named by delta, epsilon, omega, sigma, theta, and zeta. Thirty-one genes from the different classes were evaluated, including 10 delta, 13 epsilon, 3 Ω , one sigma, two theta, and two zeta *Gst*. Two-way ANOVA indicated a main effect of MeHg⁺ in *GstD1* [$F(1,8) = 6.32$; $p = 0.036$], *GstD5* [$F(1,8) = 13.95$; $p = 0.005$], *GstD8* [$F(1,8) = 12.87$; $p = 0.007$], *GstE8* [$F(1,8) = 5.62$; $p = 0.04$], *GstS1* [$F(1,8) = 16.68$; $p = 0.003$], and *GstT4* [$F(1,8) = 4.97$; $p = 0.05$]. In all of these genes, MeHg⁺ induced up-regulation and the co-exposure did not alter the effect of MeHg⁺.

Seven genes encoding glutaredoxins have also been assessed (Fig. 7). Two-way ANOVA revealed a main effect of MeHg⁺ in the glutaredoxin domain-containing cysteine-rich protein (CG12206) [$F(1,8) = 5.03$; $p = 0.05$] and *Grx1t* [$F(1,8) = 9.39$; $p = 0.015$] genes. MeHg⁺ induced overexpression of these genes, which was not reverted by the co-exposure with VCH.

4. Discussion

In this study, we analyzed the transcriptional profile of adult fruit flies *per os* exposed and co-exposed to non-lethal doses of VCH and MeHg⁺. The intoxicants were included into the artificial diet, and the flies were fed for three days. After deep-sequencing transcriptomic analyses, we found remarkable differences in gene

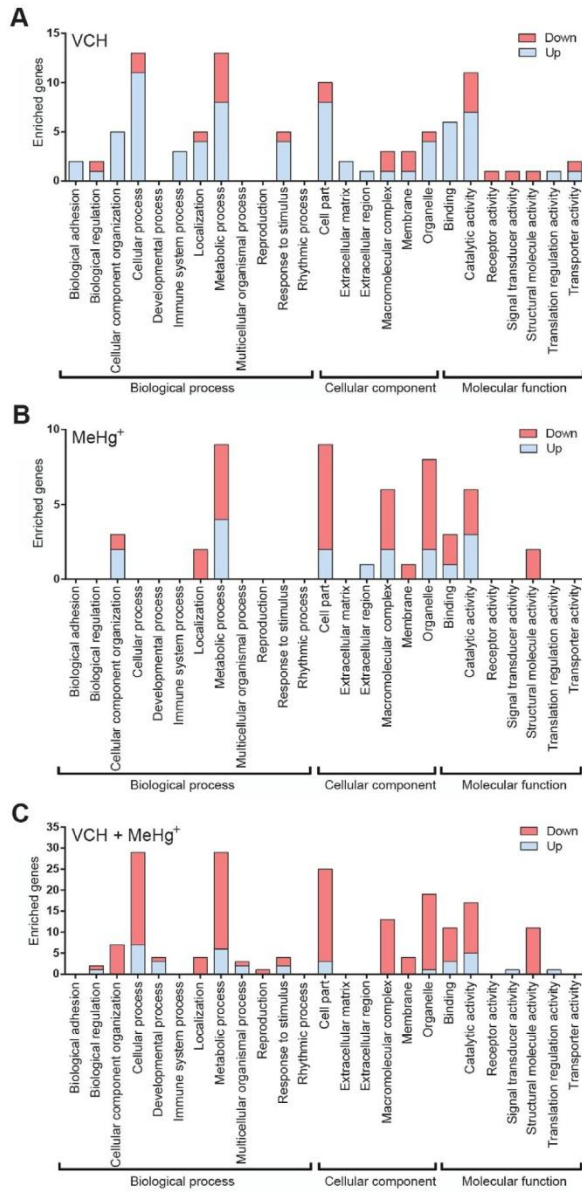


Fig. 3. Number of significantly deregulated genes in gene ontology in *D. melanogaster* after acute feeding exposure to VCH (A) and MeHg⁺ (B), and VCH + MeHg⁺ co-exposure (C) for three days. Gene ontology is divided into three domains: biological process, cellular component, and molecular function, which shown on the x-axis. Y-Axis presents the number of genes enriched in the terms (in red the down-regulated genes and blue the up-regulated). (For interpretation of the references to color in this figure legend, the reader is referred to the Web version of this article.)

transcription responses for individuals after the exposure to each treatment. Individual exposure to MeHg⁺ up- (12 genes) and down- (14 genes) regulated a smaller number of genes when compared to VCH, which caused deregulation of 38 genes with most being up-regulated (31 genes). On the other hand, an opposite effect was observed for the co-exposure treatment: much more genes were deregulated (71 genes in total) with most of each (52 genes) being down-regulated. Thus, the response to co-exposure to

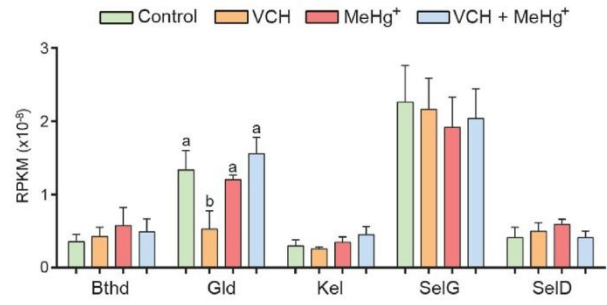


Fig. 4. Relative expression of selenoprotein-encoding genes (selenoprotein birthday (*Bthd*), glucose dehydrogenase (*Gld*), ring canal kelch protein (*Kel*), glycine-rich selenoprotein (*SelG*), and selenide, water diiknase (*SelD*)) of *D. melanogaster* after acute feeding exposure and co-exposure to VCH and MeHg⁺ for three days. Data expressed as the mean ± SEM. Results analyzed by Two-way ANOVA (VCH and MeHg⁺ as factors). Different letters indicate a significant difference ($p < 0.05$). Statistical analysis revealed VCH x MeHg⁺ interaction in *Gld* by decreasing the relative expression induced by VCH, which was suppressed by MeHg⁺ co-exposure.

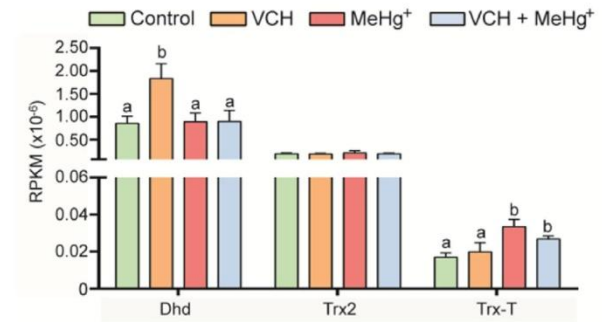


Fig. 5. Relative expression of thioredoxin genes of *D. melanogaster* after acute feeding exposure and co-exposure to VCH and MeHg⁺ for three days. Data expressed as the mean ± SEM. Results analyzed by Two-way ANOVA (VCH, and MeHg⁺ as factors). Different letters indicate a significant difference ($p < 0.05$). Statistical analysis indicated VCH x MeHg⁺ interaction in *Dhd* attributed to up-regulation by VCH, which was not maintained by the simultaneous exposure to MeHg⁺. Statistical analysis also revealed the main effect of MeHg⁺ in *Trx-T*. MeHg⁺ overexpressed *Trx-T*, and this effect was not altered by VCH co-exposure.

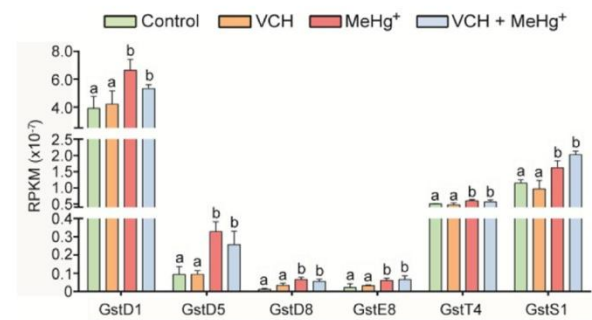


Fig. 6. Relative expression of glutathione S-transferase genes of *D. melanogaster* after acute feeding exposure and co-exposure to VCH and MeHg⁺ for three days. Glutathione S-transferase delta (D1, D5, and D8), epsilon (E8), theta (T4), and sigma (S1) genes. Data expressed as the mean ± SEM. Results analyzed by Two-way ANOVA (VCH, and MeHg⁺ as factors). Different letters indicate a significant difference ($p < 0.05$). Statistical analysis indicated the main effect of MeHg⁺ in six *Gst*-coding genes. MeHg⁺ up-regulated these genes, and the effect was not altered by VCH co-exposure.

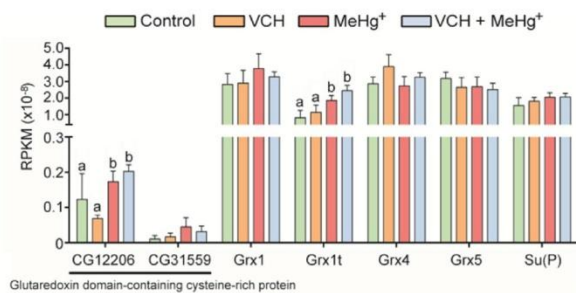


Fig. 7. Relative expression of glutaredoxin genes of *D. melanogaster* after acute feeding exposure and co-exposure to VCH and MeHg⁺ for three days. Data expressed as the mean \pm SEM. Results analyzed by Two-way ANOVA (VCH, and MeHg⁺ as factors). Different letters indicate a significant difference ($p < 0.05$). Statistical analysis indicated the main effect of MeHg⁺ in CG12206 and *Grx1t* due to overexpression caused by MeHg⁺ that was not maintained by VCH co-exposure.

intoxicants may have a different profile and even opposite to individual exposure. Interestingly, all treatments presented a global mRNA chromosome transcription lower than the unexposed insects. In fact, the tendency for VCH to reverse MeHg⁺-induced toxicity during co-exposure has to be further analyzed. In addition, the design of our global transcript analyses is not sufficient to make certain conclusions on this relationship. The regional transcription yield varied according to specific gene expression following a specific response to each of the treatments.

A previous study evaluated adult fruit flies exposed in a similar protocol as that carried out in the present work. The study focused on biomarkers of electrophilic toxicity of MeHg⁺ and VCH, including reactive species production and total GST activity. VCH and MeHg⁺ co-exposure caused an increase in reactive species production and a decrease in the survival rate of flies, reinforcing the toxic effects of the two electrophile xenobiotics (Piccoli et al., 2019). Surprisingly, exposure to MeHg⁺ caused an increase in GST activity in a similar fashion as that observed for simultaneous exposure to VCH (Piccoli et al., 2019), which is consistent with the findings here that generally show transcriptional up-regulation of GST genes.

The most highly down-regulated gene by the individual exposure to VCH was found to be *ninaE*. This gene codes for the protein rhodopsin (Rh1), a G-protein-coupled receptor that function as light sensor in the phototransduction machinery (Mitra et al., 2011; Xiong and Bellen, 2013). Low levels of rhodopsin might be related to retinal degeneration (Elsaesser et al., 2010) and may operate in circadian light responses (Pickard and Sollars, 2012; Schmidt et al., 2011; Xiong and Bellen, 2013). Circadian clock influences the transcription of several genes that encode proteins related to mRNA translation (Jouffe et al., 2013). Therefore, the cell response to VCH intoxication seems to play a role in protein biogenesis, which is reinforced by the enrichment terms (Fig. 3).

In the case of individual exposure to MeHg⁺, we found *Dro* as the greatest down-regulated gene. The product of *Dro* is an antimicrobial peptide usually activated after Gram-negative bacteria infection through stimuli of Relish, a transcription factor that participates on the NF- κ B signaling network of *D. melanogaster* (Leclerc and Reichhart, 2004; Myllymäki et al., 2014). We hypothesized that MeHg⁺, as an oral intoxicant, seemed to act as an immunosuppressor that allows for opportunistic commensals to become potential pathogens. For instance, immunotoxicity of MeHg⁺ has already been reported in mice and humans (Blakley et al., 1980; Nyland et al., 2011; Oulhote et al., 2017). In the same way, VCH + MeHg⁺ co-exposure down-regulated immune induced peptide (*Im18*) (gene with lowest FC), which is also related with

immune response (Arefin et al., 2014; Durdevic et al., 2013).

The co-exposure treatment to VCH + MeHg⁺ induced more significant overexpression in the genes that code for the proteins *Yellow-g2* and *Yellow-g*. *Yellow-g2* and *Yellow-g* are members of the Yellow protein family and may play a role in the vitelline membrane or eggshell formation in *Drosophila* (Claycomb et al., 2004). Similar to *Yellow-g2* and *Yellow-g*, two chorion-associated proteins (*Cp16* and *Cp18*) were differentially up-regulated after individual VCH exposure and VCH + MeHg⁺ co-exposure (Fig. 2). They are required for the formation of eggshell in developing oocytes during stages 11–14 of choriogenesis, the last oogenesis period along with other chorion proteins (for instance, *Cp19* and *Cp15*) (Papantonis et al., 2015; Velentzas et al., 2016). The eggshell protects the developing embryo from environmental insults (Niepielko et al., 2013), which could explain the over transcription of *Cp16* and *Cp18* after co-exposure to VCH + MeHg⁺. The increase in the translation of more chorionic proteins might generate greater protection to the eggshell. A similar gene activation response was found after exposure to sigma and Nora virus (Carpenter et al., 2009; Cordes et al., 2013). The roles in adult fruit flies are not entirely described and further analyses are needed.

Venn diagram analysis indicated *Hoip* was a common DEG after individual MeHg⁺ exposure and VCH + MeHg⁺ co-exposure. The protein product of *Hoip* binds to RNA in the striated muscle and regulates the elongation of myotubes and the expression of sarcomeric proteins in adult flies (Johnson et al., 2013; Williams et al., 2015). The individual exposure to MeHg⁺ and the co-exposure with VCH induced a decrease in the *Hoip* expression. We hypothesized that the down-regulation of *Hoip* may potentially lead to damage in fly myogenesis. In fact, the toxicity of MeHg⁺ has already been related to myogenesis in *D. melanogaster* as indicated by changes in the expression of *E(spl)m6* (Prince and Rand, 2018), *kirre(duf)*, *sns*, *if*, *kon* and *rols* genes (Montgomery et al., 2014). On the other hand, individual VCH and MeHg⁺ exposure up-regulated *Fst*. This gene is mainly involved in the tolerance of the fly to cold (Colinet et al., 2010) as signaling protein during acute stress and apoptosis (Bing et al., 2012). Increased expression of *Fst* has already been related to dietary changes (Carsten et al., 2005), bacterial and fungal infection (Buchon et al., 2009; Chamilos et al., 2008), and exposure to methotrexate (a synthetic folate analog that inhibits folate synthesis) (Affleck et al., 2006) and cyclophosphamide (Stoffel et al., 2020). All of these are stressful situations for the flies which can up-regulate genes by a mechanism not yet understood.

Focusing on MeHg⁺ and VCH targets, we identify genes encoding selenoproteins. The number of selenoproteins is restricted in *D. melanogaster*, when compared to other animals, such as human (25 selenoproteins), mice (24 selenoproteins), and fish (37 selenoproteins). *D. melanogaster* codes in its genome only for five genes: *Bthd*, *Gld*, *Kel*, *SelG*, and *SelD*. The transcription of the selenoprotein-coding genes is regulated by the availability of the element selenium (Se). If Se is available, Sec is synthesized on its tRNA^{Ser}^{Sec} and then incorporated into the so called selenoprotein (Hatfield et al., 2006; Oliveira et al., 2017). In this study, VCH induced a decrease in *Gld* transcription. The presence of electrophiles as VCH may interact with a selenol group, making it unavailable and preventing the transcription of this selenoprotein. Surprisingly, the soft electrophile MeHg⁺ did not affect the expression of this gene. When flies were exposed to both compounds, MeHg⁺ suppressed the isolated effect of VCH. In adult flies, this gene participates in both female and male fertility and immunity (Keplinger et al., 2001). Moreover, regarding thiol-containing molecules, we identified more than 9000 proteins that could be targeted by the intoxicants VCH and MeHg⁺. For instance, focusing on those that play central roles in the antioxidant system, including thioredoxins, glutaredoxins, and GSTs; we found that all

of those genes were altered especially by MeHg⁺ at transcriptional level. Of particular importance, GSH up-regulation has already been linked to MeHg⁺ tolerance due to MeHg-GSH conjugate formation (Rand et al., 2019).

In our study, we considered deep-sequencing analysis of adult fruit fly whole body not taking into account neither insect sex nor dissected tissue. In fact, this a limiting choice that has been overcome in future works. This is a first step to draw a wide landscape of transcriptional response during exposure and co-exposure to electrophile xenobiotics in the contaminated environment. Overall, future studies are needed using dissected tissues like fat body, brain, muscle, and guts together with specific sex separation to better understand the toxic effects of VCH and MeHg⁺ on flies.

5. Conclusion

In summary, our study showed that individual exposures to VCH and MeHg⁺ altered the gene expression in a very different way than when they were co-exposed even though the two compounds can have partially overlapping electrophilic-interacting targets. Individual exposure to VCH caused up-regulation of various genes while individual exposure to MeHg⁺ up- and down-deregulated a similar number of genes. Surprisingly, VCH + MeHg⁺ co-exposure down-regulated several genes. Some thiol- and one selenol-containing protein were altered by the toxicant treatments. However, these proteins may not be the main target of VCH and MeHg⁺. Therefore, a study focusing on individual exposure to some toxicants may not reflect exactly what is taking place in the co-exposure condition.

Funding

This work was supported by Brazilians' development agencies: CNPq, FAPERGS/CNPq, 12/2014-PRONEX: n° 16/2551-0000, CAPES/PROEX (88882.182155/2018-01; 23038.004173/2019-93; n° 0493/2019), INCT-EN: For Cerebral Diseases, Excitotoxicity and Neuroprotection, and FAPERGS/CAPES 04/2018 DOCFIX: 33581.466.15808.03042018.

Declaration of competing interest

None.

CRediT authorship contribution statement

Bruna Candia Piccoli: Conceptualization, Methodology, Formal analysis, Investigation, Data curation, Writing - original draft, Visualization. **Ana Lúcia Anversa Segatto:** Conceptualization, Methodology, Data curation, Writing - review & editing, Supervision. **Élgion L.S. Loreto:** Methodology, Data curation, Funding acquisition. **José Cláudio Fonseca Moreira:** Methodology, Data curation, Funding acquisition. **Daniel M.P. Ardisson-Araújo:** Conceptualization, Investigation, Resources, Data curation, Writing - review & editing, Visualization, Supervision. **João B.T. Rocha:** Conceptualization, Investigation, Resources, Writing - review & editing, Supervision, Project administration, Funding acquisition.

Appendix A. Supplementary data

Supplementary data to this article can be found online at <https://doi.org/10.1016/j.envpol.2020.114632>.

References

- Abolaji, A.O., Kamdem, J.P., Lugokenski, T.H., Nascimento, T.K., Waczuk, E.P., Farombi, E.O., Loreto, E.L., Rocha, J.B.T., 2014. Involvement of oxidative stress in 4-vinylcyclohexene-induced toxicity in *Drosophila melanogaster*. *Free Radical Biol. Med.* 71, 99–108. <https://doi.org/10.1016/j.freeradbiomed.2014.03.014>.
- Abolaji, A.O., Kamdem, J.P., Lugokenski, T.H., Farombi, E.O., Souza, D.O., Loreto, E.L.S., Rocha, J.B.T., 2015. Ovotoxicants 4-vinylcyclohexene 1,2-monoepoxide and 4-vinylcyclohexene diepoxide disrupt redox status and modify different electrophile sensitive target enzymes and genes in *Drosophila melanogaster*. *Redox Biol.* 5, 328–339. <https://doi.org/10.1016/j.redox.2015.06.001>.
- Affleck, J.G., Neumann, K., Wong, L., Walker, V.K., 2006. The effects of methotrexate on *Drosophila* development, female fecundity, and gene expression. *Toxicol. Sci.* 89, 495–503. <https://doi.org/10.1093/toxsci/kfj036>.
- Algarve, T.D., Assmann, C.E., Aigaki, T., Cruz, I.B.M., 2018. Parental and preimaginal exposure to methylmercury disrupts locomotor activity and circadian rhythm of adult *Drosophila melanogaster*. *Drug Chem. Toxicol.* 22, 1–11. <https://doi.org/10.1080/01480545.2018.1485689>.
- Andrews, S., 2010. FastQC: a quality control tool for high throughput sequence data. Available online at: <http://www.bioinformatics.babraham.ac.uk/projects/fastqc>.
- Arefin, B., Kucerova, L., Dobes, P., Markus, R., Strnad, H., Wang, Z., Hyrsil, P., Zurovec, M., Theopold, U., 2014. Genome-wide transcriptional analysis of *Drosophila* larvae infected by entomopathogenic nematodes shows involvement of complement, recognition and extracellular matrix proteins. *J. Innate Immun.* 6, 192–204. <https://doi.org/10.1159/000353734>.
- Banks, C.N., Lein, P.J., 2012. A review of experimental evidence linking neurotoxic organophosphorus compounds and inflammation. *Neurotoxicology* 33, 575–584. <https://doi.org/10.1016/j.neuro.2012.02.002>.
- Barret, A.J., Kembhavi, A.A., Brown, M.A., Kirschke, H., Knight, C.G., Tamai, M., Hanada, K., 1982. L-trans-Epoxy succinyl-leucylamido(4-guanidino)butane (E-64) and its analogues as inhibitors of cysteine proteinases including cathepsins B, H and L. *Biochem. J.* 201, 189–198. <https://doi.org/10.1042/bj2010189>.
- Bing, X., Zhang, J., Sinclair, B.J., 2012. A comparison of Frost expression among species and life stages of *Drosophila*. *Insect Mol. Biol.* 21, 31–39. <https://doi.org/10.1111/j.1365-2583.2011.01108.x>.
- Blakley, B.R., Sisodia, C.S., Mukkur, T.K., 1980. The effect of methylmercury, tetraethyl lead, and sodium arsenite on the humoral immune response in mice. *Toxicol. Appl. Pharmacol.* 52, 245–254. [https://doi.org/10.1016/0041-008x\(80\)90111-8](https://doi.org/10.1016/0041-008x(80)90111-8).
- Boening, D.W., 2000. Ecological effects, transport, and fate of mercury: a general review. *Chemosphere* 40, 1335–1351. [https://doi.org/10.1016/s0045-6535\(99\)00283-0](https://doi.org/10.1016/s0045-6535(99)00283-0).
- Bridges, C.C., Zalups, R.K., 2016. Mechanisms involved in the transport of mercuric ions in target tissues. *Arch. Toxicol.* 91, 63–81. <https://doi.org/10.1007/s00204-016-1803-y>.
- Buchon, N., Broderick, N.A., Poidevin, M., Pradervand, S., Lemaitre, B., 2009. *Drosophila* intestinal response to bacterial infection: activation of host defense and stem cell proliferation. *Cell Host Microbe* 5, 200–211. <https://doi.org/10.1016/j.chom.2009.01.003>.
- Cannady, E.A., Dyer, C.A., Christian, P.J., Sipes, I.G., Hoyer, P.B., 2003. Expression and activity of cytochromes P450 2E1, 2A, and 2B in the mouse ovary: the effect of 4-vinylcyclohexene and its diepoxide metabolite. *Toxicol. Sci.* 73, 423–430. <https://doi.org/10.1093/toxsci/kfg077>.
- Carpenter, J., Hutter, S., Baines, J.F., Roller, J., Saminandin-Peter, S.S., Parsch, J., Jiggins, F.M., 2009. The transcriptional response of *Drosophila melanogaster* to infection with the Sigma virus (Rhabdoviridae). *PLoS One* 4, e6838. <https://doi.org/10.1371/journal.pone.0006838>.
- Carsten, L.D., Watts, T., Markow, T.A., 2005. Gene expression patterns accompanying a dietary shift in *Drosophila melanogaster*. *Mol. Ecol.* 14, 3203–3208. <https://doi.org/10.1111/j.1365-294x.2005.02654.x>.
- Carter, L.J., Chefetz, B., Abdeen, Z., Boxall, A.B.A., 2019. Emerging investigator series: towards a framework for establishing the impacts of pharmaceuticals in wastewater irrigation systems on agro-ecosystems and human health. *Environ. Sci. Process. Impacts* 21, 605–622. <https://doi.org/10.1039/c9em00020h>.
- Chamilos, G., Lewis, R.E., Hu, J., Xiao, L., Zal, T., Gilliet, M., Halder, G., Kontoyiannis, D.P., 2008. *Drosophila melanogaster* as a model host to dissect the immunopathogenesis of zygomycosis. *Proc. Natl. Acad. Sci. U.S.A.* 105, 9367–9372. <https://doi.org/10.1073/pnas.0709578105>.
- Chauhan, V., Chauhan, A., 2016. Effects of methylmercury and alcohol exposure in *Drosophila melanogaster*: potential risks in neurodevelopmental disorders. *Int. J. Dev. Neurosci.* 51, 36–41. <https://doi.org/10.1016/j.ijdevneu.2016.04.010>.
- Chauhan, V., Srikumar, S., Aamer, S., Pandareesh, M.D., Chauhan, A., 2017. Methylmercury exposure induces sexual dysfunction in male and female *Drosophila melanogaster*. *Int. J. Environ. Res. Publ. Health* 14, 1–11. <https://doi.org/10.3390/ijerph14101108>.
- Claycomb, J.M., Benasutti, M., Bosco, G., Fenger, D.D., Orr-Weaver, T.L., 2004. Gene amplification as a developmental strategy: isolation of two developmental amplicons in *Drosophila*. *Dev. Cell* 6, 145–155. [https://doi.org/10.1016/S1534-5807\(03\)00398-8](https://doi.org/10.1016/S1534-5807(03)00398-8).
- Colinet, H., Lee, S.F., Hoffmann, A., 2010. Functional characterization of the Frost gene in *Drosophila melanogaster*: importance for recovery from chill coma. *PLoS One* 5, e10925. <https://doi.org/10.1371/journal.pone.01010925>.
- Cordes, E.J., Licking-Murray, K.D., Carlson, K.A., 2013. Differential gene expression related to Nora virus infection of *Drosophila melanogaster*. *Virus Res.* 175,

- 95–100. <https://doi.org/10.1016/j.virusres.2013.03.021>.
- Cui, W., Liu, G., Bezerra, M., Lagos, D.A., Li, Y., Cai, Y., 2017. Occurrence of methylmercury in rice-based infant cereals and estimation of daily dietary intake of methylmercury for infants. *J. Agric. Food Chem.* 65, 9569–9578. <https://doi.org/10.1021/acs.jafc.7b03236>.
- Doerr-Stevens, J.K., Liu, J., Stevens, G.J., Kraner, J.C., Fontaine, S.M., Halpert, J.R., Sipes, I.G., 1999. Induction of cytochrome P-450 enzymes after repeated exposure to 4-vinylcyclohexene in B6C3F1 mice. *Drug Metab. Dispos.* 27, 281–287.
- Durdevic, Z., Hanna, K., Gold, B., Pollex, T., Cherry, S., Lyko, F., Schaefer, M., 2013. Efficient RNA virus control in *Drosophila* requires the RNA methyltransferase Dnm2. *EMBO Rep.* 14, 269–275. <https://doi.org/10.1038/embor.2013.3>.
- Elsaesser, R., Kalra, D., Li, R., Montell, C., 2010. Light-induced translocation of *Drosophila* visual Arrestin2 depends on Rac2. *Proc. Natl. Acad. Sci. U.S.A.* 107, 4740–4745. <https://doi.org/10.1073/pnas.0906386107>.
- Farina, M., Aschner, M., Rocha, J.B.T., 2011. Oxidative stress in MeHg-induced neurotoxicity. *Toxicol. Appl. Pharmacol.* 256, 405–417. <https://doi.org/10.1016/j.taap.2011.05.001>.
- Gonçalves, L.V.F., Azevedo, E.B., Aquino-Neto, F.R., Billa, D.M., Sant'Anna Jr., G.L., Dezotti, M., 2016. Treatment of an industrial stream containing vinylcyclohexene by the H₂O₂/UV process. *Environ. Sci. Pollut. Res.* 23, 19626–19633. <https://doi.org/10.1007/s11356-016-7120-4>.
- Grandjean, P., Landrigan, P.J., 2006. Developmental neurotoxicity of industrial chemicals. *Lancet* 368, 2167–2178. [https://doi.org/10.1016/S0140-6736\(06\)69665-7](https://doi.org/10.1016/S0140-6736(06)69665-7).
- Hartung, T., FitzGerald, R.E., Jennings, P., Mirams, G.R., Peitsch, M.C., Rostami-Hodjegan, A., Shah, I., Wilks, M.F., Sturja, S.J., 2017. Systems toxicology: real world applications and opportunities. *Chem. Res. Toxicol.* 30, 870–882. <https://doi.org/10.1021/acs.chemrestox.7b00003>.
- Hatfield, D.L., Carlson, B.A., Xu, X.M., Mix, H., Gladyshev, V.N., 2006. Selenocysteine incorporation machinery and the role of selenoproteins in development and health progress nucleic acid. *Prog. Nucleic Acid Res. Mol. Biol.* 81, 97–142. [https://doi.org/10.1016/S0079-6603\(06\)81003-2](https://doi.org/10.1016/S0079-6603(06)81003-2).
- He, Q., Titov, D.V., Li, J., Tan, M., Ye, Z., Zhao, Y., Romo, D., Liu, J.O., 2015. Covalent modification of a cysteine residue in the XPB subunit of the general transcription factor TFIID through single epoxide cleavage of the transcription inhibitor triptolide. *Angew. Chem. Int. Ed.* 54, 1859–1863. <https://doi.org/10.1002/anie.201408817>.
- Huff, J., 2001. Carcinogenicity bioassays of bisphenol A, 4-vinylcyclohexene diepoxide, and 4-vinylcyclohexene. *Toxicol. Sci.* 64, 282–283. <https://doi.org/10.1093/toxsci/64.2.282>.
- Johnson, A.N., Mokalled, M.H., Valera, J.M., Poss, K.D., Olson, E.N., 2013. Post-transcriptional regulation of myotube elongation and myogenesis by Hoi Polloi. *Development* 140, 3645–3656. <https://doi.org/10.1242/dev.095596>.
- Jouffe, C., Cretenet, G., Symul, L., Martin, E., Atger, F., Naef, F., Gachon, F., 2013. The circadian clock coordinates ribosome biogenesis. *PLoS Biol.* 11, 1–17. <https://doi.org/10.1371/journal.pbio.1001455>.
- Kearse, M., Moir, R., Wilson, A., Stones-Havas, S., Cheung, M., Sturrock, S., Thierer, T., 2012. Geneious Basic: an integrated and extendable desktop software platform for the organization and analysis of sequence data. *Bioinformatics* 28, 1647–1649. <https://doi.org/10.1093/bioinformatics/bts199>.
- Keating, A.F., Rajapaksa, K.S., Sipes, G., Hoyer, P.B., 2008. Effect of CYP2E1 gene deletion in mice on expression of microsomal epoxide hydrolase in response to VCD exposure. *Toxicol. Sci.* 105, 351–359. <https://doi.org/10.1093/toxsci/kfn136>.
- Keplinger, B.L., Guo, X., Quine, J., Feng, Y., Cavener, D.R., 2001. Complex organization of promoter and enhancer elements regulate the tissue- and developmental stage-specific expression of the *Drosophila melanogaster* *Gld* gene. *Genetics* 157, 699–716.
- Leão, M.B., Rosa, P.C.C., Wagner, C., Lugokenski, T.H., Dalla Corte, C.L., 2018. Methylmercury and diphenyl diselenide interactions in *Drosophila melanogaster*: effects on development, behavior, and Hg levels. *Environ. Sci. Pollut. Res.* 25, 21568–21576. <https://doi.org/10.1007/s11356-018-2293-7>.
- Leclerc, V., Reichhart, J., 2004. The immune response of *Drosophila melanogaster*. *Immunol. Rev.* 198, 59–71. <https://doi.org/10.1111/j.0105-2896.2004.0130.x>.
- Martínez-Salcedo, A.L., Ruelas-Inzunza, J., Gil-Manrique, B., Nateras-Ramírez, O., Amezcua, F., 2018. Mercury levels in fish for human consumption from the southeast Gulf of California: tissue distribution and health risk assessment. *Arch. Environ. Contam. Toxicol.* 74, 273–283. <https://doi.org/10.1007/s00244-017-0495-5>.
- Mi, H., Muruganujan, A., Thomas, P.D., 2013. PANTHER in 2013: modeling the evolution of gene function, and other gene attributes, in the context of phylogenetic trees. *Nucleic Acids Res.* 41, 377–386. <https://doi.org/10.1093/nar/gks1118>.
- Mitra, A., Chinchore, Y., Kinser, R., Dolph, P.J., 2011. Characterization of two dominant alleles of the major rhodopsin encoding gene *ninaE* in *Drosophila*. *Mol. Vis.* 17, 3224–3233.
- Montgomery, S.L., Vorojeikina, D., Huang, W., Mackay, T.F.C., Anholt, R.R.H., Rand, M.D., 2014. Genome-wide association analysis of tolerance to methylmercury toxicity in *Drosophila* implicates myogenic and neuromuscular developmental pathways. *PLoS One* 9, e110375. <https://doi.org/10.1371/journal.pone.0110375>.
- Myllymäki, H., Valanne, S., Rämetsä, M., 2014. The *Drosophila* imd signaling pathway. *J. Immunol.* 192, 3455–3462. <https://doi.org/10.4049/jimmunol.1303309>.
- Niepielko, M.G., Marmion, R.A., Kim, K., Luor, D., Ray, C., Yakoby, N., 2013. Chorion patterning: a window into gene regulation and *Drosophila* species' relatedness. *Mol. Biol. Evol.* 31, 154–164. <https://doi.org/10.1093/molbev/mst186>.
- NTP (National Toxicology Program), 1989. Toxicology and carcinogenesis studies of 4-vinyl-1-cyclohexene diepoxide (CAS No. 106-87-6) in F344/N rats and B6C3F1 mice (dermal studies). *Natl. Toxicol. Progr. Tech. Rep.* 362, 1–249.
- Nyland, J.F., Fillion, M., Barbosa Jr., F., Shirley, D.L., Chine, C., Lemire, M., Mergler, D., Silbergeld, E.K., 2011. Biomarkers of methylmercury exposure immunotoxicity among fish consumers in Amazonian Brazil. *Environ. Health Perspect.* 119, 1733–1738. <https://doi.org/10.1289/ehp.1103741>.
- Oliveira, C.S., Piccoli, B.C., Ashner, M., Rocha, J.B.T., 2017. Chemical speciation of selenium and mercury as determinant of their neurotoxicity. *Adv. Neurobiol.* 18, 53–83. https://doi.org/10.1007/978-3-319-60189-2_4.
- Oliveira, C.S., Nogaara, P.A., Ardisson-Araújo, D.M.P., Aschner, M., Rocha, J.B.T., Dórea, J.G., 2018. Neurodevelopmental Effects of Mercury. <https://doi.org/10.1016/bs.ant.2018.03.005>.
- Orr, W.C., Radyuk, S.N., Sohal, R.S., 2013. Involvement of redox state in the aging of *Drosophila melanogaster*. *Antioxidants Redox Signal.* 19, 788–803. <https://doi.org/10.1089/ars.2012.5002>.
- Oulhote, Y., Shamim, Z., Kielsen, K., Weihe, P., Grandjean, P., Ryder, L.P., Heilmann, C., 2017. Children's white blood cell counts in relation to developmental exposures to methylmercury and persistent organic pollutants. *Reprod. Toxicol.* 68, 207–214. <https://doi.org/10.1016/j.reprotox.2016.08.001>.
- Papantonis, A., Swevers, L., Latrou, K., 2015. Chorion genes: a landscape of their evolution, structure, and regulation. *Annu. Rev. Entomol.* 60, 177–194. <https://doi.org/10.1146/annurev-ento-010814-020810>.
- Pazi, I., Gonul, L.T., Kucuksezgin, F., Avaz, G., Tolun, L., Unluoglu, A., Karaasian, Y., Gucver, S.M., Orhon, A.K., Siltu, E., Olmez, G., 2017. Potential risk assessment of metals in edible fish species for human consumption from the Eastern Aegean Sea. *Mar. Pollut. Bull.* 15, 409–413. <https://doi.org/10.1016/j.marpolbul.2017.05.004>.
- Piccoli, B.C., Segatto, A.L.A., Oliveira, C.S., Silva, F.D., Aschner, M., Rocha, J.B.T., 2019. Simultaneous exposure to vinylcyclohexene and methylmercury in *Drosophila melanogaster*: biochemical and molecular analysis. *BMC Pharmacol. Toxicol.* 20, 83. <https://doi.org/10.1186/s40360-019-0356-0>.
- Pickard, G.E., Sollars, P.J., 2012. Intrinsically photosensitive retinal ganglion cells. *Rev. Physiol. Biochem. Pharmacol.* 162, 59–90. https://doi.org/10.1007/112_2011_4.
- Prince, L.M., Rand, M.D., 2018. Methylmercury exposure causes a persistent inhibition of myogenin expression and C2C12 myoblast differentiation. Notch Target Gene E(spl)^{md} is a Mediator of Methylmercury-Induced Myotoxicity in *Drosophila*. *Front. Genet.* 8, 233. <https://doi.org/10.3389/fgene.2017.00233>.
- Ranchou-Peyruse, M., Goni-Urriza, M., Guignard, M., Goas, M., Ranchou-Peyruse, A., Guyoneaud, R., 2018. Pseudodesulfobrevibrio hydrargyri sp. nov., a mercury-methylating bacterium isolated from a brackish sediment. *Int. J. Syst. Evol. Microbiol.* 68, 1461–1466. <https://doi.org/10.1099/ijsem.0.002173>.
- Rand, M.D., Vorojeikina, D., Peppriell, A., Gunderson, J., Prince, L.M., 2019. Drosophila phototoxicology: elucidating kinetic and dynamic pathways of methylmercury toxicity in a *Drosophila* model. *Front. Genet.* 10, 666. <https://doi.org/10.3389/fgene.2019.00666>.
- Schmidt, T.M., Chen, S., Hattar, S., 2011. Intrinsically photosensitive retinal ganglion cells: many subtypes, diverse functions. *Trends Neurosci.* 36, 572–580. <https://doi.org/10.1016/j.tins.2011.07.001>.
- Schou, M.F., Kristensen, T.N., Pedersen, A., Karlsson, G., Loeschke, V., Malmendal, A., 2017. Metabolic and functional characterization of effects of developmental temperature in *Drosophila melanogaster*. *Am. J. Physiol. Regul. Integr. Comp. Physiol.* 312, 211–222. <https://doi.org/10.1152/ajpregu.00268.2016>.
- Scumaci, D., Oliva, A., Concolino, A., Curcio, A., Fiumara, C.V., Tammè, L., Campuzano, O., Pascali, V.L., Coll, M., Iglesias, A., Berne, P., Casu, G., Olivo, E., Ausania, F., Ricci, P., Indolfi, C., Brugada, J., Brugada, R., Cuda, G., 2018. Integration of "Omics" strategies for biomarkers discovery and for the elucidation of molecular mechanisms underlying Brugada Syndrome. *Proteomics Clin. Appl.* 12, e1800065. <https://doi.org/10.1002/prca.201800065>.
- Stoffel, T.J.R., Segatto, A.L., Silva, M.M., Prestes, A., Barbosa, N.B.V., Rocha, J.B.T., Loreto, E.L.S., 2020. Cyclophosphamide in *Drosophila* promotes genes and transposable elements differential expression and mitochondrial dysfunction. *Comp. Biochem. Physiol. C* 230, 108718. <https://doi.org/10.1016/j.cbpc.2020.108718>.
- Trapnell, C., Pachter, L., Salzberg, S.L., 2009. TopHat: discovering splice junctions with RNA-Seq. *Bioinformatics* 25, 1105–1111. <https://doi.org/10.1093/bioinformatics/btp120>.
- Tousova, Z., Oswald, P., Slobodnik, J., Blaha, L., Muz, M., Hu, M., Brack, W., Krauss, M., Di Paolo, C., Tarcai, Z., Seiler, T.B., Hollert, H., Koprivica, S., Ahel, M., Schollée, J.E., Hollender, J., Suter, M.J.F., Hidas, A.O., Schirmer, K., Sonavane, M., Ait-aissa, S., Creusot, N., Brion, F., Froment, J., Almeida, A.C., Thomas, K., 2017. European demonstration program on the effect-based and chemical identification and monitoring of organic pollutants in European surface waters. *Sci. Total Environ.* 601–602, 1849–1868. <https://doi.org/10.1016/j.scitotenv.2017.06.032>.
- Trapnell, C., Roberts, A., Goff, L., Pertea, G., Kim, D., Kelley, D.R., Pimentel, H., Salzberg, S.L., Rinn, J.L., Pachter, L., 2012. Differential gene and transcript expression analysis of RNA-seq experiments with TopHat and Cufflinks. *Nat. Protoc.* 7, 562–578. <https://doi.org/10.1038/nprot.2012.016>.
- Velentzas, A.D., Velentzas, P.D., Sagioglou, N.E., Konstantakou, E.G., Anagnostopoulos, A.K., Tsioka, M.M., Mpakou, V.E., Kollia, Z., Consoulas, C., Margaritis, L.H., Papassideri, I.S., Tsangaris, G.T., Sarantopoulou, E., Cefalas, A.C., Stravopodis, D.J., 2016. Targeted downregulation of s36 protein unearths its cardinal role in chorion biogenesis and architecture during *Drosophila*

- melanogaster* oogenesis. *Sci. Rep.* 6, 35511. <https://doi.org/10.1038/srep35511>.
- Williams, J., Boin, N.J., Valera, J.M., Johnson, A.N., 2015. Noncanonical roles for tropomyosin during myogenesis. *Development* 142, 3440–3452. <https://doi.org/10.1242/dev.117051>.
- Wilson, V.S., Keshava, N., Hester, S., Segal, D., Chiu, W., Thompson, C.M., Euling, S.Y., 2013. Utilizing toxicogenomic data to understand chemical mechanism of action in risk assessment. *Toxicol. Appl. Pharmacol.* 271, 299–308. <https://doi.org/10.1016/j.taap.2011.01.017>.
- Wu, Z., Wang, X., Zhang, X., 2011. Using non-uniform read distribution models to improve isoform expression inference in RNA-seq. *Bioinformatics* 27, 502–508. <https://doi.org/10.1093/bioinformatics/btq696>.
- Xing, Z., Zhao, T., Bai, W., Yang, X., Liu, S., Zhang, L., 2018. Temporal and spatial variation in the mechanisms used by microorganisms to form methylmercury in the water column of Changshou Lake. *Ecotoxicol. Environ. Saf.* 160, 32–41. <https://doi.org/10.1016/j.ecoenv.2018.05.018>.
- Xiong, B., Bellen, H.J., 2013. Rhodopsin homeostasis and retinal degeneration: lessons from the fly. *Trends Neurosci.* 36, 652–660. <https://doi.org/10.1016/j.tins.2013.08.003>.
- Zhang, J., Wang, C., Ji, L., Liu, W., 2016. Modeling of toxicity-relevant electrophilic reactivity for guanine with epoxides: estimating hard and soft acids and bases (HSAB) parameter as a predictor. *Chem. Res. Toxicol.* 29, 841–850. <https://doi.org/10.1021/acs.chemrestox.6b00018>.

4 DISCUSSÃO

Esta tese mostrou estudos sobre a toxicidade aguda, intermediária e crônica após a exposição *per os* a xenobióticos em insetos modelos na busca pela compreensão de seus mecanismos de toxicidade. Dentre as vias de tratamento a compostos tóxicos, este trabalho buscou assemelhar-se ao tipo de exposição humana ao MeHg⁺ e ao VCH para que os resultados apresentados pudessem refletir possíveis alterações nos seres humanos e outros vertebrados devido à conservação evolutiva entre as espécies. Da mesma forma, diferentes níveis e períodos de exposição foram abordados. Consideramos também que as interações de mais de uma substância tóxica nos organismos vivos são de grande importância, pois podem gerar efeitos aditivos, sinérgicos ou antagônicos, principalmente, se possuem propriedades eletrônicas semelhantes.

Como dito anteriormente, utilizou-se a via oral para o tratamento dos insetos para mimetizar o modo de exposição humana a estes xenobióticos (BHATTACHARYA; KEATING, 2012; NOGARA et al., 2019a; 2019b). A principal forma de exposição humana ao MeHg⁺ é através da ingestão de peixes contaminados. A maioria do MeHg⁺ encontrado no músculo dos peixes está complexada a proteínas que contém –SH ou –SeH (NOGARA et al., 2019a; 2019b). No feitiço da dieta para o tratamento das baratas e moscas, era esperado que a maioria do MeHg⁺ se ligasse com proteínas que contém –SH presente nos componentes da dieta (PICCOLI et al., 2019). Já o VCH, forma não metabolizada, apresenta baixa reatividade frente aos componentes da dieta, sendo possível prever que ficaria na forma livre. Desta forma, os insetos se expunham ao VCH através da ingestão e da inalação, devido à volatilidade deste composto. Também especulamos que o VCH não poderia interagir com o MeHg⁺ durante o período de tratamento, pois o MeHg⁺ estaria ligado as proteínas já que tem maior afinidade por –SH (PICCOLI et al., 2019). Após a ingestão e absorção, o VCH é oxidado por enzimas da família do citocromo P450 (fase I de desintoxicação) formando metabólitos epóxidos (KEATING et al., 2008). O MeHg⁺ não sofre alterações pelas enzimas da fase I de desintoxicação se mantendo ligado à moléculas que contém –SH ou –SeH presentes no organismo (NOGARA et al., 2019a). Devido a eletrofilicidade do MeHg⁺ e dos metabólitos epóxidos do VCH, assim como a ausência de MeHg⁺ livre, especulamos que não há possibilidade de interação entre estes xenobióticos no organismo.

Para o melhor entendimento da afinidade do MeHg⁺ e dos grupamentos epóxidos pelo –SH e –SeH é importante descrever a teoria de *Hard Soft Acid Base* (HSAB) de Pearson. Segundo esta teoria, espécies duras apresentam baixa polarizabilidade, tamanho pequeno, alta

densidade de carga negativa no local doador (bases) e alto estado de oxidação (ácidos). Em contraste, as espécies moles são caracterizadas por alta polarizabilidade orbital, tamanho grande, baixa densidade de carga negativa no local doador (bases), estado de baixa oxidação (ácidos) (NOGARA et al., 2019a). Neste sentido, o MeHg^+ é considerado um ácido/eletrofílico mole, enquanto que os grupamentos epóxido são considerados ácidos/eletrofílicos duros. Isto influencia diretamente a afinidade destas substâncias por grupamentos básicos/nucleofílicos moles de interesse neste estudo ($-\text{SH}$ e $-\text{SeH}$). De modo geral, o MeHg^+ possui maior afinidade por $-\text{SeH}$ e $-\text{SH}$ (devido a moleza de ambas as espécies eletrofílicas e nucleofílicas) do que os grupamentos epóxido (eletrofílico duro). Embora ambos os grupamentos ($-\text{SH}$ e $-\text{SeH}$) sejam considerados básicos/nucleofílicos moles, o $-\text{SeH}$ é mais mole do que o $-\text{SH}$. Por isso, o MeHg^+ possui maior afinidade por selenol do que tiol (espécies moles tem maior afinidade entre si) e os grupamentos epóxido possuem o padrão oposto, maior afinidade por tiol do que selenol.

A toxicidade do MeHg^+ ganhou evidência após os surtos de envenenamento no Japão e no Iraque onde a população foi exposta a altos níveis deste xenobiótico (BAKIR et al., 1973; EKINO et al., 2007). Entretanto, ainda hoje a população é exposta ao MeHg^+ devido à contaminação do ambiente e consequente biomagnificação na cadeia alimentar (DÓREA; MARQUES, 2016). No ambiente aquático, quanto mais no topo da cadeia alimentar o peixe estiver, mais MeHg^+ é acumulado e estima-se que peixes piscívoros possam atingir $< 0,5$ a 5 mg de MeHg^+ /kg de músculo (BASTOS et al., 2015; OLIVEIRA et al., 2017). Estes níveis mais altos de MeHg^+ são encontrados nos peixes de áreas de mineração de ouro como na bacia amazônica, no Brasil (BASTOS et al., 2015).

O MeHg^+ só é encontrado livre na presença de altas concentrações de HCl , como no estômago dos vertebrados. Nas outras regiões do trato gastrointestinal, dentro das células e nos fluidos corporais, o MeHg^+ está complexado com moléculas de baixa massa molecular como a cisteína e GSH , ou alta massa molecular como as proteínas que contêm tiol e as selenoproteínas (NOGARA et al., 2019a). As enzimas que pertencem ao sistema antioxidante dos organismos vivos possuem cisteína ou selenocisteína no sítio ativo (as quais possuem $-\text{SH}$ e $-\text{SeH}$, respectivamente) para reações de oxirredução. Uma vez que o MeHg^+ se liga a estas proteínas, estas perdem sua função, pois a ligação Hg-Y ($Y = \text{S}$ ou Se) é covalente (OLIVEIRA et al., 2017). Desta forma, o estresse oxidativo pela depleção de enzimas antioxidantes é um dos mecanismos de toxicidade do MeHg^+ . Estresse oxidativo induzido por MeHg^+ já foi relatado em *D. melanogaster* (CHAUHAN; CHAUHAN, 2016; PICCOLI et al., 2019) e em *N. cinerea* (AFOLABI et al., 2018). Este trabalho corrobora com estes achados,

pois também encontramos aumento de EROs após exposição *per os* aguda e crônica ao MeHg^+ (artigo 1).

Uma das estratégias do organismo para eliminar o MeHg^+ é conjugando-o com a GSH, reação catalisada pela enzima GST, a fim de que o complexo GS-HgMe seja incorporado na bile e eliminado pelas fezes (BRIDGES; ZALUPS, 2017; NOGARA et al., 2019a). A GST faz parte da fase de desintoxicação II dos organismos a qual conjuga a GSH com compostos eletrofílicos (SHEEHAN et al., 2001), mas também atua como peroxidase sobre peróxidos derivados de lipídeos ou H_2O_2 (TU; AKGÜL, 2005). Na verdade, a GST compreende uma série de proteínas citosólicas que são codificadas por uma superfamília de genes. A *D. melanogaster* possui seis classes *Gst* (delta, épsilon, ômega, sigma, teta e zeta) que totalizam mais de 30 genes (TU; AKGÜL, 2005) e ainda não se tem dados sobre as classes de *Gst* da *N. cinerea*. É importante ressaltar que esta enzima pode ser considerada um biomarcador de contaminação ambiental (CARVALHO-NETA; ABREU-SILVA, 2013). Neste trabalho observamos que a exposição aguda ao MeHg^+ induziu aumento na expressão de seis genes que codificam *Gst* da *D. melanogaster* (artigo 2) o que está de acordo com estudo prévio onde a atividade desta enzima aumentou (PICCOLI et al., 2019). O aumento na atividade enzimática da GST também ocorreu após a exposição aguda, intermediária e crônica ao MeHg^+ na *N. cinerea* (artigo 1). A interrupção da exposição ao MeHg^+ fez com que a atividade da GST retornasse aos níveis basais (artigo 1). Devido à escassez de dados sobre a GST na *N. cinerea*, realizamos uma simulação molecular para propor à conjugação do MeHgCl e Cys-HgMe com a GSH pela GST utilizando a sequência da *Blatella germanica*, barata que apresenta alta porcentagem de identidade com a *N. cinerea*. Os testes *in silico* indicaram que as espécies de MeHg^+ se ligam ao sítio ativo da enzima e também interagem com o átomo de enxofre da GSH podendo formar o complexo GS-HgMe (artigo 1). A GST também é responsável pela conjugação dos metabólitos epóxidos do VCH com a GSH para que este xenobiótico seja inativado e eliminado do organismo (RAJAPAKSA, 2007). Entretanto as alterações na GST encontradas neste trabalho foram relacionadas apenas ao MeHg^+ (artigo 2).

Estudos prévios em diferentes modelos experimentais (moscas, baratas e ratos) demonstraram que o MeHg^+ é capaz de inibir a AChE (ADEDARA et al. 2016, WOOTTEN et al., 1985, HAN et al., 2017). Corroborando com estes resultados, a exposição *per os* aguda e crônica ao MeHg^+ também inibiu esta enzima (artigo 1). A AChE é expressa em vários tipos de células do organismo, com destaque para o SNC, onde há também a maior concentração de acetilcolina presente nos neurônios colinérgicos (WEVERS, 2011). Esta enzima é responsável

pela degradação da acetilcolina em acetato e colina o que ocasiona a interrupção da transmissão sináptica. O sítio ativo da AChE é composto por três aminoácidos serina, histidina e glutamina, chamados de tríade catalítica (SILMAN; SUSSMAN, 2008). Existem outros sítios de ligação onde às moléculas podem interagir como: Omega Loop (OL), buraco de oxianion (Oxyanion Hole - OH), subsítio aniônico (Anionic Subsite - AS), sítio de ligação acil (acyl binding pocket - ABP) e o sítio aniônico periférico (peripheral anionic - PAS) (SOREQ; SEIDMAN, 2001; SILVA et al., 2018). A inibição da AChE faz com que a acetilcolina permaneça na fenda sináptica continuamente estimulando os receptores nicotínicos e muscarínicos. Os sintomas típicos de envenenamento agudo com agentes inibidores irreversíveis da AChE (organofosforados e carbamatos, por exemplo) são agitação, fraqueza, fasciculações musculares, hipersalivação e sudorese, sendo que em casos mais graves pode ocasionar insuficiência respiratória, inconsciência, convulsões, e morte (POHANKA, 2012; ČOLOVIĆ et al., 2013). O clorpirifós, organofosforado utilizado como inseticida, se liga ao -OH da serina da tríade catalítica (SILVA et al., 2018), sendo este o principal sítio de ligação de compostos inibidores da AChE. Neste trabalho utilizamos testes *in silico* para determinar o local de ligação do MeHgCl e seus metabólitos (Cys-HgMe and GSH-HgMe) na AChE da barata já que não há -SH no sítio catalítico desta enzima. Os sítios ABP e o PAS foram os lugares onde o MeHgCl e seus metabólitos se ligaram, sendo importante ressaltar que uma possível interação com um resíduo de cisteína foi verificada indicando a formação de um aduto e consequente desnaturação da proteína (artigo 1). Portanto, este seria o mecanismo de inibição enzimática causado pelo MeHg⁺.

Testes comportamentais prévios indicam que o MeHg⁺ também induz alterações em padrões comportamentais (ADEDARA et al., 201; AFOLABI et al., 2018). Um teste amplamente utilizado na pesquisa que avalia, principalmente, a memória é o teste de reconhecimento de objeto. Neste teste um objeto familiar e um novo são pareados, e o reconhecimento do objeto é inferido pela observação/exploração preferencial pelo novo alvo. A não exploração do objeto desconhecido normalmente é associada a déficit de memória do animal, entretanto, esta associação deve ser cautelosa (LEGER et al., 2013). Neste estudo utilizamos o teste de reconhecimento de objeto para avaliar a memória da *N. cinerea* após a exposição *per os* ao MeHg⁺ (artigo 1). Observou-se que as baratas expostas a maior concentração de MeHg⁺ (100 µg MeHg⁺/g de dieta) por 90 dias e por 30 dias seguidos de um período de desintoxicação (60 dias) exploraram menos ambos os objetos familiar e não familiar. Já as baratas tratadas com MeHg⁺ (100 µg MeHg⁺/g de dieta) por 30 dias exploraram menos o objeto não-familiar e permaneceram mais tempo imóveis. Estes resultados são

complexos e podem multicausais, principalmente, tratando-se de insetos onde o padrão comportamental ainda esta sendo estudado. Hipotetizamos que estes resultados podem ser atribuídos ao déficit de memória, entretanto também acreditamos que pode ser comportamento ansioso e/ou tipo-depressivo devido a não exploração dos objetos ou ainda a um déficit locomotor. É importante destacar que mesmo após um período de desintoxicação de 60 dias, as baratas apresentaram novas alterações comportamentais o que foi caracterizado como toxicidade tardia, sendo a primeira vez que é relatada em insetos.

Comportamentos como depressão e ansiedade ocorrem tanto em modelos experimentais (SILVA et al., 2018; SIQUEIRA et al., 2019) quanto em humanos (MALEKIRAD et al., 2013; HARRISON; MACKENZIE ROSS, 2016; SUAREZ-LOPEZ et al., 2019). Nos animais, a ansiedade caracteriza-se pela antecipação de uma ameaça futura, sendo associada ao medo e tem como finalidade a preservação da vida (LANG; DAVIS; OHMAN, 2000). O padrão de comportamento ansioso é variado e pode ser organizado em duas classes: (1) imobilidade defensiva caracterizado pelo congelamento, bradicardia e hiperatensão ou (2) ação defensiva como luta ou fuga (LANG; DAVIS; OHMAN, 2000). A imobilidade também pode representar um comportamento tipo-depressivo causada pelo desespero do animal que cessa formas ativas de lidar com situações de estresse (CRYAN; SLATTERY, 2007; PETIT-DEMOULIERE; CHENU; BOURIN, 2005). Estes padrões de fuga e imobilidade pela *N. cinerea* foram observados durante o teste de reconhecimento de objeto (artigo 1).

Além disso, a imobilidade também pode estar relacionada com distúrbios neuromusculares. De fato, a toxicidade do MeHg^+ já foi associada a miogênese (MONTGOMERY et al., 2014; PRINCE; RAND, 2018a; 2018b). Perda de coordenação, marcha prejudicada e atraso na função motora, como sentar e caminhar foram déficits motores observados nos envenenamentos acidentais por MeHg^+ no Japão e no Iraque e em estudos epidemiológicos mais recentes (ROEGGE; SCHANTZ, 2006). Muitos pesquisadores atribuíram os déficits motores associados à exposição ao MeHg^+ ao dano no SNC (ETO, 1997; PEDERSEN et al., 1999; KAKITA et al., 2003). Entretanto outras consequências como perda de massa muscular (YOO et al., 2016) e fraqueza não eram totalmente compreendidos (USUKI et al., 1998) e sugeriam algum alvo nos músculos (PRINCE; RAND, 2018a). Estudos em *D. melanogaster* identificaram alguns alvos potenciais do MeHg^+ no músculo como os genes potenciador do gene mDelta do complexo Split (*E(spl)mδ*) (ENGEL; RAND, 2014; PRINCE; RAND, 2018b), *dumbfounded* (*kirre(duf)*), *sticks and stones* (*sns*), *integrin alpha-PS2* (*if*), *kon* e *rolling pebbles* (*rols*) (MONTGOMERY et al., 2014) e miogenina

(*MyoG*) em camundongo (PRINCE; RAND, 2018a). Neste estudo, moscas expostas ao MeHg^+ e ao VCH + MeHg^+ apresentaram uma diminuição da expressão do *Hoip*, o qual pode ser outro alvo do MeHg^+ (artigo 2). A proteína codificada por este gene regula o alongamento dos miotubos e a expressão de proteínas sarcoméricas em moscas adultas (JOHNSON et al., 2013; WILLIAMS et al., 2015). Tanto a imobilidade da *N. cinerea* após exposição ao MeHg^+ , assim como a morte durante a ecdise, podem estar associadas a miotoxidade do MeHg^+ (artigo 1). As mortes durante a ecdise indicam uma possível disfunção neuromotora que prejudicou a saída da *N. cinerea* do exoesqueleto. Surpreendentemente, foram registradas mortes durante a ecdise pelas baratas expostas ao MeHg^+ (100 $\mu\text{g MeHg}^+/\text{g}$ de dieta) durante 90 dias e também nas baratas tratadas com MeHg^+ (100 $\mu\text{g MeHg}^+/\text{g}$ de dieta) durante 30 dias e que foram submetidas a um período de desintoxicação (60 dias). A morte durante a ecdise e as alterações comportamentais, que ocorreram nas baratas mesmo após a interrupção da exposição ao MeHg^+ , nos levou a acreditar na toxicidade tardia deste xenobiótico em insetos.

Sabe-se que a exposição a pequenas doses de xenobióticos retardam a ocorrência de sinais e sintomas de intoxicação, mas causam alterações na expressão gênica e/ou na função de proteínas. O MeHg^+ pode alterar a expressão gênica por modificar a estrutura das histonas, metilar o DNA e alterar a expressão de miRNA (GOODRICH et al., 2013; CULBRETH; ASCHNER, 2019). Algumas modificações relacionadas à hipo ou hipermetilação do DNA causadas pelo MeHg^+ são encontradas nos gametas e prole de indivíduos expostos a este xenobiótico (CULBRETH; ASCHNER, 2019). É importante ressaltar que o MeHg^+ e o VCH também induzem estresse oxidativo (FARINA, ASCHNER, ROCHA, 2011; RIZZO et al., 2012; FARINA et al., 2013) e as espécies reativas geradas podem interagir com o DNA (COOKE et al., 2003) ou com as histonas alterando a expressão gênica (NIU et al., 2015). Sobre a possível interação direta do VCH e seus metabólitos com o DNA e suas proteínas adjacentes, estudos indicam que o VCD é capaz de degradar o DNA dos folículos primários e primordiais e induzir apoptose nestas células (SPRINGER et al., 1996), mas ainda é desconhecida uma possível modulação na expressão gênica causada pelo VCH e seus metabólitos.

Um estudo prévio do nosso grupo de pesquisa avaliando a exposição *per os* ao VCH e MeHg^+ demonstrou que a coexposição aguda (três dias) a estes compostos induz maior mortalidade e aumento das espécies reativas de oxigênio (ERO). Entretanto, as alterações enzimáticas encontradas (GST e AChE) foram relacionadas apenas ao MeHg^+ (PICCOLI et al., 2019). Devido a eletrofilicidade tanto dos metabólitos epóxidos do VCH como do MeHg^+ , hipotetizamos que a exposição ao VCH e ao MeHg^+ alterariam genes pertencentes a vias

diferentes e semelhantes e que a coexposição a estes xenobióticos acentuaria os efeitos isolados, de forma aditiva ou sinérgica, de modo a interferir no perfil transcricional. Utilizamos a mosca *D. melanogaster* para avaliar o perfil transcricional após exposição *per os* aguda ao VCH e MeHg⁺ devido à facilidade da realização de estudos toxicogenômicos neste modelo experimental (artigo 2).

A exposição ao VCH alterou 38 genes, sendo que a maioria (31 genes) foi super-expressa. Por outro lado, a exposição MeHg⁺ desregulou 26 genes, sendo que a maior parte teve sua expressão diminuída (14 genes). Já na coexposição ao VCH + MeHg⁺ mais genes foram desregulados (71 genes no total), com o predomínio de genes sub-expressos (52 genes). A resposta das moscas a exposição a cada xenobiótico foi diferente, até mesmo oposta, e na coexposição VCH + MeHg⁺ parece que os efeitos do MeHg⁺ sobressairam. Entretanto, quando a expressão de forma global a exposição ao VCH, MeHg⁺ e VCH + MeHg⁺ induziram uma diminuição na transcrição.

O conjunto de selenoproteínas ou selenoma é muito pequeno em *D. melanogaster*, correspondendo apenas a BTHD, GLD, KEL, SELG e SELD, segundo seu proteoma. A selenocisteína é o 21º aminoácido proteinogênico, codificado pelo códon UGA (mesmo códon de terminação) e sua síntese ocorre em seu tRNA^{[Ser]Sec} necessitando de Se disponível. Inicia com a aminoacilação da serina (Ser) no tRNA^{[Ser]Sec}, reação catalisada pela seril-tRNA sintetase (SerS) na presença de ATP. Subsequentemente, o grupo –OH da Ser é fosforilado pela fosfoseril-tRNA cinase (PSTK) formando fosfoseril (PO₄³Ser). Concomitantemente, a selenofosfato sintetase 2 (SPS2 ou SELD) sintetiza o monoselenofosfato tendo como substrato seleneto e ATP. A incorporação do um átomo de Se na Ser é catalisada pela enzima fosfoseril-tRNA selênio transferase (SEPsecS) e tem como resultando a síntese do resíduo de Sec ligado covalentemente ao tRNA^{[Ser]Sec} e um pirofosfato. Para a decodificação do códon UGA como uma Sec é necessário uma maquinaria composta, principalmente, pela sequência de inserção de selenocisteína (SECIS) (elemento *cis*), proteína de ligação a SECIS (SBP2) e fator de alongamento específico de Sec (eEFSec) (elementos *trans*). Esta maquinaria é necessária para a inserção da Sec na proteína impedindo que a tradução seja interrompida (HATFIELD et al. 2006; OLIVEIRA et al. 2017). Em vários organismos, inclusive na *D. melanogaster*, a SELD também é uma seleproteína (HIROSAWA-TAKAMORI; JÄCKLE; VORBRÜGGEN, 2000).

Neste estudo, o VCH induziu uma diminuição na expressão da *Gld* e o MeHg⁺ não a alterou (artigo 2). Quando as moscas foram expostas a ambos os compostos, o MeHg⁺ suprimiu o efeito isolado do VCH. Nas moscas adultas, este gene é expresso no complexo

anteno-maxilar, e em alguns órgãos reprodutivos somáticos (machos: ducto e bulbo ejaculatório; fêmeas: oviduto, receptáculo seminal e espermateca). A *Gld* participa da fertilidade das fêmeas e da imunidade de fêmeas e machos (KEPLINGER et al., 2001) os quais, provavelmente, sofreram algum declínio pela exposição ao VCH. Nós especulamos que metabólitos eletrofílicos do VCH podem interagir com o seleneto, tornando-o indisponível e impedindo a transcrição dessa selenoproteína. As outras selenoproteínas não foram alteradas pela exposição ao VCH e/ou MeHg^+ .

Para determinar o grupo de proteínas que contém $-\text{SH}$ livre, identificamos os principais motivos presentes nas enzimas oxidoredutases (CC, CXC, CXXC) (OLIVEIRA et al., 2018) (artigo 2). O número de Cys não representa o número de $-\text{SH}$ livre que pode interagir com moléculas eletrofílicas, pois muitas Cys fazem parte de ligações dissulfeto inter e/ou intramoleculares para estabilizar a estrutura terciária das proteínas. Para corroborar com achados anteriores onde tanto o MeHg^+ (artigo 1), quanto o VCH (WACZUK et al., 2019) e a coexposição a ambos xenobióticos (PICCOLI et al., 2019) aumentam as EROs e devido a impossibilidade de avaliarmos todas as oxidoredutases (9,354 proteínas) focamos nas enzimas presentes no sistema antioxidante da *D. melanogaster* (ORR; RADYUK; SOHAL 2013). Esse sistema é composto por GSH e Trx e enzimas, como peroxirroxinas, tioredoxinas, tioredoxinas redutases, glutarredoxina e glutathione S-transferases e sulfirredoxina. Nessa perspectiva, a Trx é uma família de pequenas proteínas que possuem em sua estrutura grupos $-\text{SH}$, que podem doar equivalentes redutores a várias moléculas, gerando a Trx oxidada [Trx(S-S)Trx]. A reativação da Trx oxidada é catalisada pela enzima TrxR em uma reação dependente de NADPH (NORBERG; ARNÉR, 2001; SVENSSON; LARSSON, 2007). Neste estudo, os genes *Dhd* e *Trx-T* foram positivamente regulados após a exposição ao VCH e ao MeHg^+ , respectivamente. Esses genes são sexo-específicos, no qual o *Dhd* é expresso nos ovários e a *Trx-T* nos testículos (SVENSSON; LARSSON, 2007). Além disso, a expressão da *Grx1t* (glutarredoxina 1, específica de testículo) também é limitada aos testículos (MERCER; BURKE, 2016) sendo sido aumentada pela exposição ao MeHg^+ . As glutarredoxinas catalisam a desglutathionilação de proteínas, utilizando resíduos de cisteína em seus sítios ativos (ORR et al., 2013). Esses resultados corroboram com a análise de expressão diferencial onde vários genes relacionados ao sistema reprodutor/reprodução foram alterados.

5 CONCLUSÃO

Em resumo, nosso estudo mostrou que, exposição *per os* ao MeHg⁺ causa alterações comportamentais e bioquímicas nas baratas, e algumas destas alterações persistiram após a interrupção da exposição a este xenobiótico. Devido resultados similares já terem sido reportados em humanos, consideramos a *N. cinerea* um organismo propício para estudos translacionais. Além disso, o mecanismo de toxicidade semelhante do MeHg⁺ e dos metabólitos do VCH não geraram efeito aditivo, pelo contrário, em alguns parâmetros analisados observou-se um provável efeito antagônico. Ressaltamos os efeitos desses compostos no sistema reprodutor das moscas, um fato que precisa ser melhor investigado. A prospecção do selenoma e o tioloma de *D. melanogaster* indicaram alterações nas vias da tioredoxina, glutaredoxina, GST e glicose desidrogenase. Finalmente, os resultados mostram a complexidade da interação entre xenobióticos e a necessidade de estudos retratando os efeitos da exposição a mais de uma substância tóxica.

6 PERSPECTIVAS

- Validar o *SelG*, *Bthd*, *Sps2*, *Gld* e *Kel* como selenoproteínas na mosca *D. melanogaster*;
- Fazer a prospecção das selenoproteínas da barata *N. cinerea* através de seu transcriptoma;
- Verificar quais fatores alteram a expressão das selenoproteínas da *D. melanogaster*.

REFERÊNCIAS BIBLIOGRÁFICAS

- ABOLAJI, A. O. et al. **Involvement of oxidative stress in 4-vinylcyclohexene-induced toxicity in *Drosophila melanogaster***. *Free Radical Biology and Medicine*, v. 71, p. 99-108, 2014.
- ABOLAJI, A. O. et al. **Ovotoxicants 4-vinylcyclohexene 1,2-monoepoxide and 4-vinylcyclohexene diepoxide disrupt redox status and modify different electrophile sensitive target enzymes and genes in *Drosophila melanogaster***. *Redox Biology*, v. 5, p. 328–339, 2015.
- ADAMS, M. D. et al. **The genome sequence of *Drosophila melanogaster***. *Science*, v. 287, p. 2185–2195, 2000.

ADEDARA, I. A. et al. **Biochemical and behavioral deficits in the lobster cockroach *Nauphoeta cinerea* model of methylmercury exposure.** *Toxicological Research*, v. 4, p. 442–451, 2015.

ADEDARA, I. A. et al. **Neuroprotection of luteolin against methylmercury-induced toxicity in lobster cockroach *Nauphoeta cinerea*.** *Environmental Toxicology and Pharmacology*, v. 42, p. 243–251, 2016.

AFOLABI, B. A. et al. **Dietary co- exposure to methylmercury and monosodium glutamate disrupts cellular and behavioral responses in the lobster cockroach, *Nauphoeta cinerea* model.** *Environmental Toxicology and Pharmacology*, v. 64, p. 70–77, 2018.

AHMED, M. et al. **Inhibitor of two different cholinesterases by tacrine.** *Chemico-Biological Interactions*, v. 162, p. 165-171, 2006.

ASCHNER, M. **Brain, kidney and liver ^{203}Hg -methyl mercury uptake in the rat: relationship to the neutral amino acid carrier.** *Basic Clinic Pharmacology and Toxicology*, v. 65, p. 17–20, 1989.

ASHBURNER, M. et al. **Gene Ontology: tool for the unification of biology.** *Nature Genetics*, v. 25, n. 1, p. 25–29, 2000.

ASSIS, A, et al. **What is the transcriptome and how it is evaluated?** *Transcriptomics in Health and Disease*. 1 ed. Cham: Springer International Publishing, p. 3–48, 2014.

BAKIR, F. et al. **Methylmercury poisoning in Iraq.** *Science*, v. 181, p. 230–241, 1973.

BALACHANDRAN, N. et al. **In vitro anticancer activity of methyl caffeate isolated from *Solanum torvum* Swartz. Fruit.** *Chemico-Biological Interactions*, v. 242, p. 81–90, 2015.

BALI, Y. A. et al. **Learning and memory impairments associated to acetylcholinesterase inhibition and oxidative stress following glyphosate based-herbicide exposure in mice.** *Toxicology*, v. 415, p. 18-25, 2019.

BASTOS, W. R. et al. **Mercury in fish of the Madeira river (temporal and spatial assessment), Brazilian Amazon.** *Environmental Research*, v. 140, p. 191– 197, 2015.

BERGER J. **Preclinical testing on insects predicts human haematotoxic potentials.** *Lab Animal*, v. 43, p. 328–332, 2009.

BISEN-HERSHA, E. B. et al. **Behavioral effects of developmental methylmercury drinking water exposure in rodents.** *Journal of Trace Elements in Medicine and Biology*, v. 28, p. 117–124, 2014.

BHATTACHARYA, P.; KEATING, A. F. **Impact of environmental exposures on ovarian function and role of xenobiotic metabolism during ovotoxicity.** *Toxicology and Applied Pharmacology*, v. 261 p. 227–235, 2012.

BOENING, D. W. **Ecological effects, transport, and fate of mercury: a general review.** Chemosphere, v. 40, 2000.

BRADLEY, M. A; BARST, B. D.; BASU, N. **A review of mercury bioavailability in humans and fish.** International Journal of Environmental Research and Public Health, v. 14, p. 169-189, 2017.

BRANDÃO, F. et al. **Unravelling the mechanisms of mercury hepatotoxicity in wild fish (*Liza aurata*) through a triad approach: bioaccumulation, metabolomic profiles and oxidative stress.** Metallomics, v. 7, p. 1352-1363, 2015.

BRIDGES, C. C.; ZALUPS, R. K. **Transport of inorganic mercury and methylmercury in target tissues and organs.** Journal of Toxicology and Environmental Health: Part B, Critical Reviews, v.13, n. 5, p. 385-410, 2010.

BRIDGES, C. C.; ZALUPS, R. K. **Mechanisms involved in the transport of mercuric ions in target tissues.** Archives of Toxicology, v. 91, p. 63-81, 2016.

BRIDGES, C. C.; ZALUPS, R. K. **Mechanisms involved in the transport of mercuric ions in target tissues.** Archives of Toxicology, v. 91, n 1, p. 63-81, 2017.

BRINKE, A.; BUCHINGER, S. **Toxicogenomics in environmental science.** Advances in Biochemical Engineering/Biotechnology, p. 159–186, 2016. DOI: 10.1007/10_2016_15

CHAMBERS et al. **Transcriptomics and single-cell RNA-sequencing.** Respirology, 2018. DOI: 10.1111/resp.13412

CANNADY, E. A. et al. **Expression and activity of microsomal epoxide hydrolase in follicles isolated from mouse ovaries.** Toxicological Sciences, v. 68, n. 1, p. 24–31, 2002.

CARBON, S. et al. **Expansion of the Gene Ontology knowledgebase and resources: The Gene Ontology Consortium.** Nucleic Acids Research, v. 45, p. 331-338, 2017.

CARR, M. C. **The emergence of the metabolic syndrome with menopause.** Journal of Clinical Endocrinology Metabolism, v. 88, p. 2404–2411, 2003.

CARVALHO, L. V. B. et al. **Oxidative stress levels induced by mercury exposure in amazon juvenile populations in Brazil.** International journal of environmental research and public health, v. 16, n. 15, p. 2682, 2019.

CARVALHO-NETA, R. N. F., ABREU-SILVA, A. L. **Glutathione S-transferase as biomarker in *Sciades herzbergii* (Siluriformes: Ariidae) for environmental monitoring: the case study of São Marcos Bay, Maranhão, Brazil.** Latin American Journal of Aquatic Research, v. 41, p. 217–225, 2013.

CASTELLANO, S. et al. **In silico identification of novel selenoproteins in the *Drosophila melanogaster* genome.** Scientific Reports, v. 2, n. 8, p. 697-702, 2011.

CHAUHAN, V.; CHAUHAN, A. **Effects of methylmercury and alcohol exposure in *Drosophila melanogaster*: potential risks in neurodevelopmental disorders.** International Journal of Developmental Neuroscience, v. 51, p. 36–41, 2016.

CHELUVAPPA, R.; SCOWEN, P.; ERI, R. **Ethics of animal research in human disease remediation, its institutional teaching; and alternatives to animal experimentation.** Pharmacology Research and Perspective, v. 5, p. 1–14, 2017.

CHIEN, S. et al. **Homophila: human disease gene cognates in *Drosophila*.** Nucleic Acids Research, v. 30, n. 1, p. 149-51, 2002.

CHINTAPALLI, V. R.; WANG, J.; DOW, J. A. **Using FlyAtlas to identify better *Drosophila melanogaster* models of human disease.** Nature Genetics, v. 39, n. 6, p. 715-720, 2007.

CLARK, J. M. **The 3Rs in research: a contemporary approach to replacement, reduction and refinement.** British Journal of Nutrition 120:1–7, 2018.

CLARKSON, T. W.; MAGOS, L.; MYERS, G. J. **The toxicology of mercury– Current exposures and clinical manifestations.** The New England Journal of Medicine. Rochester, v. 349, p. 1731-1737, 2003.

ČOLOVIĆ, M. B. et al. **Acetylcholinesterase Inhibitors: Pharmacology and Toxicology.** Current Neuropharmacology, v. 11, p. 312-335, 2013.

COMPEAU, G. C.; BARTHA, R. **Sulfate-reducing bacteria: principal methylators of mercury in anoxic estuarine sediment.** Applied and Environmental Microbiology, v. 50, p. 498-502, 1985.

COOKE, M. S. et al. **Oxidative DNA damage: mechanisms, mutation, and disease.** FASEB Journal, v. 17, n. 10, p. 1195-1214, 2003.

CROES, K. et al. **Health effects in the Flemish population in relation to low levels of mercury exposure: from organ to transcriptome level.** International Journal of Hygiene and Environmental Health, v. 217, n. 2-3, p. 239-47, 2014.

CROOM, E. **Metabolism of Xenobiotics of Human Environments.** Toxicology and Human Environments, p. 31–88, 2012.

CRYAN, J. F.; SLATTERY, D. A. **Animal models of mood disorders: Recent developments.** Current Opinion in Psychiatry, v. 20, n. 1, p. 1–7, 2007.

CUI, W. et al. **Occurrence of methylmercury in rice-based infant cereals and estimation of daily dietary intake of methylmercury for infants.** Journal of Agricultural and Food Chemistry, v. 65, 2017.

CULBRETH, M.; ASCHNER, M. **Methylmercury Epigenetics.** Toxics, v. 7, p. 56-66, 2019.

DANI, S. U.; WALTER, G. F. **Chronic arsenic intoxication diagnostic score (CA_sIDS).** Journal of Applied Toxicology, v. 38, n. 1, p. 122-144, 2018.

DANTAS, N. et al. **Aminoguanidine hydrazones (AGH's) as modulators of norfloxacin resistance in *Staphylococcus aureus* that overexpress NorA efflux pump.** *Chemico-Biological Interactions*, v. 280, p. 8–14, 2018.

DÓREA, J. G.; MARQUES, R. C. **Mercury levels and human health in the Amazon Basin.** *Annals of Human Biology*, v. 43, p. 349–359, 2016.

EKINO, S. et al. **Minamata disease revisited: An update on the acute and chronic manifestations of methyl mercury poisoning.** *Journal of the Neurological Sciences*, v. 262, p. 131-144, 2007.

ELPIDINA, E. N. et al. **Compartmentalization of proteinases and amylases in *Nauphoeta cinerea* midgut.** *Archives of Insect Biochemistry and Physiology*, v. 48, n. 4, p. 206–216, 2001

ENGEL, G. L.; RAND, M. D. **The Notch target *E(spl)mδ* is a muscle-specific gene involved in methylmercury toxicity in motor neuron development.** *Neurotoxicology and Teratology*, v. 43, p. 11-8, 2014.

ETO, K. **Pathology of Minamata disease.** *Toxicologic Pathology*, v. 25, n. 6, p. 614-623, 1997.

EVANGELISTA, R. L. et al. **Ensemble-based docking: From hit discovery to metabolism and toxicity predictions.** *Bioorganic and Medicinal Chemistry*, v. 24, p. 4928–4935, 2016.

EWING, B. et al. Base-calling of automated sequencer traces using phred. I. Accuracy assessment. *Genome Research*, v. 8, n. 3, p. 175–185, 1998.

FARINA, M.; ASCHNER, M.; ROCHA, J. B. T. **Oxidative stress in MeHg-induced neurotoxicity.** *Toxicology and Applied Pharmacology*, v. 256, p. 405–417, 2011.

FARINA, M. et al. **Metals, oxidative stress and neurodegeneration: a focus on iron, manganese and mercury.** *Neurochemistry international*, v. 62, n. 5, p. 575-594, 2013.

FERNANDES, G. W. et al. **Deep into the mud: ecological and socio-economic impacts of the dam breach in Mariana, Brazil.** *Natureza & Conservação*, v. 14, p. 35-45, 2016.

FERNÁNDEZ-MORENO, M. A. et al. ***Drosophila melanogaster* as a model system to study mitochondrial biology.** *Methods in molecular biology*, v. 372, p. 33-49, 2007.

FERREIRA, L. M.; HOCHMANN, B.; BARBOSA, M. V. J. **Modelos experimentais em pesquisa.** *Acta Cirurgica Brasileira*, v. 20, 2005.

FERREIRA, L. G. et al. **Molecular docking and structure-based drug design strategies.** *Molecules*, v. 20, n. 7, p. 13384-13421, 2015.

FERREIRA, F. F. et al. **Impacts of the Samarco Tailing Dam Collapse on Metals and Arsenic Concentration in Freshwater Fish Muscle from Doce River, Southeastern Brazil.** *Integrated Environmental Assessment and Management*, v. 16, n. 5, p. 622-630, 2019.

FRIEDMAN, R.; BOYE, K.; FLATMARK, K. **Molecular modelling and simulations in cancer research.** *Biochimica et Biophysica Acta - Reviews on Cancer*, v. 1836, n. 1, p. 1–14, 2013.

GOODRICH, J. M. et al. **Mercury biomarkers and DNA methylation among Michigan dental professionals.** *Environmental and molecular mutagenesis*, v. 54, n. 3, p. 195-203, 2013.

GRANDJEAN, P.; LANDRIGAN, P. J. **Developmental neurotoxicity of industrial chemicals.** *The Lancet*, v. 368, p. 2167-2178, 2006.

HAN, J. et al. **Hydrogen sulfide may attenuate methylmercury-induced neurotoxicity via mitochondrial preservation.** *Chemico-Biological Interactions*, v. 1, p. 66-73, 2017.

HARADA, M. **Minamata disease: methylmercury poisoning in Japan causes by environmental pollution.** *Critical Reviews in Toxicology*, v. 25, p. 1–24, 1995.

HARRISON, V.; MACKENZIE ROSS, S. **Anxiety and depression following cumulative lowlevel exposure to organophosphate pesticides.** *Environmental Research*, v. 151, p. 528–536, 2016.

HARTUNG, T. et al. **Systems toxicology: Real world applications and opportunities.** *Chemical Research in Toxicology*, v. 30, p. 870–882, 2017.

HATFIELD, D. L. et al. **Selenocysteine incorporation machinery and the role of selenoproteins in development and health progress nucleic acid.** *Progress in Nucleic Acid Research and Molecular Biology*, 81:97–142, 2006.

HAUSEN, J. et al. **Fishing for contaminants: identification of three mechanism specific transcriptome signatures using Danio rerio embryos.** *Environmental Science and Pollution Research*, v. 25, n. 5, p. 4023-4036, 2017.

HINTELMANN, H. **Organomercurials.** Their formation and pathways in the environment. *Metal Ions in Life Sciences*, v. 7, p. 365–401, 2010.

HIROSAWA-TAKAMORI M, JÄCKLE H, VORBRÜGGEN G. **The class 2 selenophosphate synthetase gene of Drosophila contains a functional mammalian-type SECIS.** *EMBO Reports*, v. 1, n. 5, p. 441-446, 2000.

HO, N. Y. et al. **Gene responses in the central nervous system of zebrafish embryos exposed to the neurotoxicant methyl mercury.** *Environmental Science and Technology*, v. 47, n. 7, p. 3316-3325, 2013.

JENKO, K.; KAROUNA-RENIER, N. K.; HOFFMAN, D. J. **Gene expression, glutathione status, and indicators of hepatic oxidative stress in laughing gull (*Larus atricilla*) hatchlings exposed to methylmercury.** *Environmental Toxicology and Chemistry*, v. 31, n. 11, p. 2588-2596, 2012.

JOHNSON, A. N. et al. **Post-transcriptional regulation of myotube elongation and myogenesis by Hoi Polloi.** *Development*, v. 140, p. 3645-3656, 2013.

KAKITA, A. et al. **Disruption of postnatal progenitor migration and consequent abnormal pattern of glial distribution in the cerebrum following administration of methylmercury.** *Journal of Neuropathology & Experimental Neurology*, v. 62, n. 8, p. 835-847, 2003.

KAPPELER, C. J.; HOYER, P. B. **4-vinylcyclohexene diepoxide: a model chemical for ovotoxicity.** *Systematic Biology Reproductive Medicine*, v. 58 p. 57-62, 2012.

KEATING, A. F. et al. **Effect of CYP2E1 gene deletion in mice on expression of microsomal epoxide hydrolase in response to VCD exposure.** *Toxicology Sciences*, v. 105, p. 351–359, 2008.

KEPLINGER, B. L. et al. **organization of promoter and enhancer elements regulate the tissue- and developmental stage-specific expression of the *Drosophila melanogaster* Gld gene.** *Genetics*, v. 157, p. 699–716, 2001.

LANG, C. et al. **Replacement, reduction, refinement - animal welfare progress in european pharmacopoeia monographs: activities of the European pharmacopoeia commission from 2007 to 2017.** *Pharmeuropa, Pharmeuropa Bio and Scientific Notes*, p. 12–36, 2018

LEGER, M. et al. **Object recognition test in mice.** *Nature Protocols*, v. 8, n. 12, p. 2531–2537, 2013.

LIU, Y.; ZHOU, J.; WHITE, K. P. **RNA-seq differential expression studies: more sequence or more replication?** *Bioinformatics*, v. 30, p. 301–304, 2014.

LIU, S. et al. **Design, synthesis, molecular docking studies and anti-HBV activity of phenylpropanoid derivatives.** *Chemico-Biological Interactions*, v. 251, p. 1-9, 2016.

LIU, Q. et al., **Maternal methylmercury from a wild-caught walleye diet induces developmental abnormalities in zebrafish.** *Reproductive Toxicology*, v. 65, p. 272-282, 2016.

LOVATO, F. L.; ROCHA, J. B. T.; DALLA CORTE, C. L. **Diphenyl diselenide protects against methylmercury-induced toxicity in *Saccharomyces cerevisiae* via the Yap1 transcription factor.** *Chemical Research in Toxicology*, v. 30, p. 1134–1144, 2017.

LU, X. et al. **Nanomolar copper enhances mercury methylation by *Desulfovibrio desulfuricans* ND132.** *Environmental Science and Technology Letters*, v. 5, p. 372-376, 2018.

MAHAPATRA, C. T. et al. **Identification of methylmercury tolerance gene candidates in *Drosophila*.** *Toxicological Science*, v. 116, n. 1, p. 225-38, 2010.

MALEKIRAD, A. A. et al. **Neurocognitive, mental health, and glucose disorders in farmers exposed to organophosphorus pesticides.** Archives of Industrial Hygiene and Toxicology, v. 64, p. 1–8, 2013.

MANCHESTER FLY FACILITY (2015). **droso4schools: Online resources for school lessons using the fruit fly *Drosophila*** — <https://droso4schools.wordpress.com/>

MARTIN-ROMERO, F. J. et al. **Selenium metabolism in *Drosophila*: selenoproteins, selenoprotein mRNA expression, fertility, and mortality.**

MARTIN, J. A.; WANG, Z. **Next-generation transcriptome assembly.** Nature Reviews Genetics, v. 12, n. 10, p. 671–682, 2011.

MARTÍNEZ-SALCIDO, A. I. et al. **Mercury levels in fish for human consumption from the southeast Gulf of California: Tissue distribution and health risk assessment.** Archives of Environmental Contamination Toxicology, v. 74, p. 273–283, 2018.

MAYER, L. P. et al. **Long-term effects of ovarian follicular depletion in rats by 4-vinylcyclohexene diepoxide.** Reproductive Toxicology, v. 16, p. 775–781, 2002.

MERCER, S. W.; BURKE, R. **Evidence for a role for the putative *Drosophila* hGRX1 orthologue in copper homeostasis.** Biometals, v. 29, n. 4, p. 705–713, 2016.

MILATOVIĆ, D.; DETTBARN, W. D. **Modification of acetylcholinesterase during adaptation to chronic, subacute paraoxon application in rat.** Toxicology Applied Pharmacology, v. 136, p. 20–28, 1996.

MOHAMMADPOUR, R. et al. **Subchronic and chronic toxicity evaluation of inorganic nanoparticles for delivery applications.** Advanced Drug Delivery Reviews, v. 144, p. 112–132, 2019.

MONTGOMERY, S. L. et al. **Genome-wide association analysis of tolerance to methyl-mercury toxicity in *Drosophila* implicates myogenic and neuromuscular developmental pathways.** PloS One, v. 9, e110375, 2014.

MOORE, A. J.; GOWATY, P. A.; MOORE, P. J. **Females avoid manipulative males and live longer.** Journal of Evolutionary Biology, v. 16, n. 3, p. 523–530, 2003.

MRDAKOVIĆ, M. et al. **Effects of dietary fluoranthene on nymphs of *Blattica dubia* S. (Blattodea: Blaberidae).** Environmental Science and Pollution Research, v. 26, p. 6216–6222, 2019.

MUNTEAN, M. et al. **Trend analysis from 1970 to 2008 and model evaluation of EDGARv4 global gridded anthropogenic mercury emissions.** Science of the Total Environment, v. 494–495, p. 337–50, 2014.

NARASIMHA, S. et al. ***Drosophila melanogaster* cloak their eggs with pheromones, which prevents cannibalism.** PLoS Biology, v. 17, n. 1, p. e2006012, 2019.

NIU, Y. et al. **Oxidative stress alters global histone modification and DNA methylation.** *Free Radical Biology and Medicine*, v. 82, p. 22-28, 2015.

NOGARA, P. A. et al. **Methylmercury's chemistry: from the environment to the mammalian brain.** *Biochimica et Biophysica Acta – General Subjects*, v. 1863, 2019a.

NOGARA, P. A. et al. **Mercury in our food.** *Chemical Research in Toxicology*, v. 32, p. 1459-1461, 2019b.

NORDBERG, J.; ARNÉR, E. S. **Reactive oxygen species, antioxidants, and the mammalian thioredoxin system.** *Free Radical Biology and Medicine*, v. 31, n. 11, p. 1287-1312, 2001.

OLIVEIRA, C. S. et al. **Chemical speciation of selenium and mercury as determinant of their neurotoxicity.** *Advances in neurobiology*, v. 18, p. 53-83, 2017.

OLIVEIRA, C. S. et al. **Neurodevelopmental effects of mercury.** In: Aschner, M., Costa, L. (Eds) *Linking environmental exposure to neurodevelopmental disorders. Advances in Neurotoxicology*, v. 2. 2018.

OLIVEIRA, C. S. et al. **Transcriptomic and Proteomic Tools in the Study of Hg Toxicity: What Is Missing?** *Frontiers Genetics*, v. 11, p. 425, 2020.

ORR, W. C.; RADYUK, S. N.; SOHAL, R. S. **Involvement of redox state in the aging of *Drosophila melanogaster*.** *Antioxidant and Redox Signaling*, v. 19, p. 788–803, 2013.

PADHI, B. K. et al. **Gene expression profiling in rat cerebellum following in utero and lactational exposure to mixtures of methylmercury, polychlorinated biphenyls and organochlorine pesticides.** *Toxicology Letters*, v. 176, n. 2, p. 93-103, 2008.

PEDERSEN, M. B. et al. **Mercury accumulations in brains from populations exposed to high and low dietary levels of methyl mercury.** Concentration, chemical form and distribution of mercury in brain samples from autopsies. *International Journal of Circumpolar Health*, v. 58, n. 2, p. 96-107, 1999.

PETERSON, R. T. et al. **Use of non-mammalian alternative models for neurotoxicological study.** *NeuroToxicology*, v. 29, p. 545–554, 2008.

PETIT-DEMOULIERE, B.; CHENU, F.; BOURIN, M. **Forced swimming test in mice: a review of antidepressant activity.** *Psychopharmacology*, v. 177, n. 3, p. 245–255, 2005.

PICCOLI, B. C. et al. **Simultaneous exposure to vinylcyclohexene and methylmercury in *Drosophila melanogaster*: biochemical and molecular analysis.** *BMC Pharmacology and Toxicology*, v. 20, p. 83, 2019.

POHANKA, M. **Acetylcholinesterase inhibitors: a patent review.** *Expert Opinion on Therapeutic Patents*, v. 22, p. 871-886, 2012.

PRINCE, L. M.; RAND, M. D. **Methylmercury exposure causes a persistent inhibition of myogenin expression and C2C12 myoblast differentiation.** *Toxicology*, v. 393, p. 113-122, 2018a.

PRINCE, L. M.; RAND, M. D. **Notch Target Gene E(spl)mδ Is a Mediator of Methylmercury-Induced Myotoxicity in Drosophila.** *Frontiers in Genetics*, v. 8, p. 233, 2018b.

RADONJIC, M. et al. **Delay and impairment in brain development and function in rat offspring after maternal exposure to methylmercury.** *Toxicological Science*, v. 133, n. 1, p. 112-24, 2013.

RAJAPAKSA, K. S. **The role of ovarian metabolism in 4-vinylcyclohexene metabolites and 7, 12-dimethylbenz[a]anthracene-induced ovotoxicity in mice.** Department of Physiology, University of Arizona. Dissertation, 2007.

RAMOS, A. M. et al. **Monitoring the water quality of the paraopeba river and surroundings after the breakage of the waste dam in Brumadinho, Minas Gerais, Brazil.** *Research, Society and Development*, v. 9, n. 9, p. 1-26, 2020.

RANCHOU-PEYRUSE, M. et al. **Pseudodesulfovibrio hydrargyri sp. nov., a mercury-methylating bacterium isolated from a brackish sediment.** *International Journal of Systematic and Evolutionary Microbiology*, v. 68, p. 1461-1466, 2018.

RAND, M. D.; PRINCE, L. M.; VOROJEIKINA, D. **Drosophotoxicology: elucidating kinetic and dynamic pathways of methylmercury toxicity in a Drosophila model.** *Frontiers in Genetics*, v. 10, p. 666, 2019.

REITER L. T. et al. **A systematic analysis of human disease-associated gene sequences in Drosophila melanogaster.** *Genome Research*, v. 11, p. 1114–1125, 2001.

RICE, D. C. **Evidence for delayed neurotoxicity produced by methylmercury.** *Neurotoxicology*, 17, p. 583–596, 1996.

RIZZO, A. et al. **Roles of reactive oxygen species in female reproduction.** *Reproduction in Domestic Animals*, v. 47, n. 2, p. 344–352, 2012.

ROBERTSON, G. et al. **De novo assembly and analysis of RNA-seq data.** *Nature Methods*, v. 7, n. 11, p. 909-912, 2010.

ROBINSON, D. N.; COOLEY, L. **Drosophila kelch is an oligomeric ring canal actin organizer.** *Journal of Cell Biology*, v. 138, n. 4, p. 799–810, 1997.

ROCHA, J. B. T.; PICCOLI, B. C.; OLIVEIRA, C. S. **Biological and chemical interest in selenium: a brief historical account.** *Arkivoc*, 2017. DOI: 10.3998/ark.5550190.p009.784

RODRIGUES, N. R. et al. **Is the lobster cockroach Nauphoeta cinerea a valuable model for evaluating mercury induced oxidative stress?** *Chemosphere*, v. 92, p. 1177–1182, 2013.

ROEGGE, C. S.; SCHANTZ, S. L. **Motor function following developmental exposure to PCBs and/or MeHg.** *Neurotoxicology and Teratology*, v. 28, n. 2, p. 260-277, 2006.

SCHIRMEIER, S.; KLÄMBT, C. **The *Drosophila* blood-brain barrier as interface between neurons and hemolymph.** *Mechanisms of Development*, v. 138, p. 50–55, 2015.

SCHURCH, N. et al. **How many biological replicates are needed in an RNA-seq experiment and which differential expression tool should you use?** *RNA*, v. 22, p. 1-13, 2016.

SCUMACI, D. et al. **Integration of "Omics" strategies for biomarkers discovery and for the elucidation of molecular mechanisms underlying Brugada Syndrome.** *Proteomics – Clinical Applications*, 2018. DOI: 10.1002/prca.201800065.

SEGATTO, A. L. A. et al. **De novo transcriptome assembly of the lobster cockroach *Nauphoeta cinerea* (Blaberidae).** *Genetics and Molecular Biology*, v. 41, n. 3, p. 1678-4685, 2018.

SHAMBAUGH, G. F. **Toxicity and effects on motor coordination of some neurotropic drugs on the cockroach *Nauphoeta cinerea*.** *Annals of the Entomological Society of America*, v. 62, p. 370–375, 1969.

SHEEHAN, D. et al. **Structure, function and evolution of glutathione transferases: implications for classification of non-mammalian members of an ancient enzyme superfamily.** *Biochemical Journal*, v. 360, p. 1–16, 2001.

SHIMADA, M. et al. **Gene expression profiles in the brain of the neonate mouse perinatally exposed to methylmercury and/or polychlorinated biphenyls.** *Archives of Toxicology*, v. 84, p. 271–286, 2010.

SILMAN, I.; SUSSMAN, J. L. **Acetylcholinesterase: how is structure related to function?** *Chemical Biological Interactions*, v.175, p. 3-10, 2008.

SILVA, C. P.; LEMOS, F. J. A.; SILVA, J. R. **CAPÍTULO 5- Digestão em Insetos.** In: *Tópicos Avançados em Entomologia Molecular*. Instituto Nacional de Ciência e Tecnologia em Entomologia Molecular INCT – EM – 2012.

SILVA, F. D. et al. **Molecular docking analysis of acetylcholinesterase corroborates the protective effect of pralidoxime against chlorpyrifos-induced behavioral and neurochemical impairments in *Nauphoeta cinerea*.** *Computational Toxicology*, v. 8, p. 25–33, 2018.

SIQUEIRA, A. A. et al. **Atropine counteracts the depressive-like behaviour elicited by acute exposure to commercial chlorpyrifos in rats.** *Neurotoxicology and Teratology*, v. 71, p. 6–15, 2019.

SOWA, S. M., & KEELEY, L. L. **Free amino acids in the hemolymph of the cockroach, *Blaberus discoidalis*.** *Comparative Biochemistry and Physiology Part A: Physiology*, v. 113, n. 2, p. 131–134, 1996.

SOWERS, M. F. R.; LAPIETRA, M. T. **Menopause: Its epidemiology and potential association with chronic diseases.** *Epidemiologic Reviews*, v. 17, p. 287–302, 1995.

SOREQ, H.; SEIDMAN, S. **Acetylcholinesterase** — new roles for an old actor. *Nature Reviews Neuroscience*, v. 2, n. 4, p. 294–302, 2001.

SPRINGER, L. N. et al. **Involvement of apoptosis in 4-vinylcyclohexene diepoxide-induced ovotoxicity in rats.** *Toxicology and Applied Pharmacology*, v. 139, p. 394–401, 1996.

SPRINGHETTI, A.; CIOCI, M. **Sullo sviluppo larvale della *Nauphoeta cinerea* Oliver (Blattoidea, Epilamprinae).** *Italian Journal of Zoology*, v. 28, n. 2, p. 321–330, 1961.

SUAREZ-LOPEZ, J. R. et al. **Associations of acetylcholinesterase activity with depression and anxiety symptoms among adolescents growing up near pesticide spray sites.** *International Journal of Hygiene and Environmental Health*, v. 222, n. 7, p. 981–990, 2019.

SVENSSON, M. J.; LARSSON, J. **Thioredoxin-2 affects lifespan and oxidative stress in *Drosophila*.** *Hereditas*, v. 144, n. 1, p. 25–32, 2007.

TOUSOVA, Z. et al. **European demonstration program on the effect-based and chemical identification and monitoring of organic pollutants in European surface waters.** *Science of the Total Environment*, v. 601–602, p. 1849–1868, 2017.

TRAN, D. N. et al. **Depletion of follicles accelerated by combined exposure to phthalates and 4-vinylcyclohexenediepoxide, leading to premature ovarian failure in rats.** *Reproductive Toxicology*, 2018. DOI: 10.1016/j.reprotox.2018.06.071

TU, C. P.; AKGÜL, B. ***Drosophila* glutathione S-transferases.** *Methods in Enzymology*, v. 401, p. 204–226, 2005.

UGUR, B.; CHEN, K.; BELLEN, H. J. ***Drosophila* tools and assays for the study of human diseases.** *Disease Models & Mechanisms*, v. 9, n. 3, p. 235–244, 2016.

USUKI, F. et al. **The effect of methylmercury on skeletal muscle in the rat: a histopathological study.** *Toxicology Letters*, v. 94, n. 3, p. 227–32, 1998.

VANDERHYDEN, B. C. **Loss of ovarian function and the risk of ovarian cancer.** *Cellular Tissue Research*, v. 322, p. 117–124, 2005.

VESELINOVIĆ, J. B. et al. **Selected 4-phenyl hydroxycoumarins: in vitro cytotoxicity, teratogenic effect on zebrafish (*Danio rerio*) embryos and molecular docking study.** *Chemico-Biological Interactions*, v. 231, p. 10–17, 2015.

VOROJEIKINA, D. et al. **Glutathione S-transferase activity moderates methylmercury toxicity during development in *Drosophila*.** *Toxicological Sciences*, v. 157, p. 211–221, 2017.

WACZUK, E. P. et al. **Assessing the toxicant effect of spontaneously volatilized 4-vinylcyclohexane exposure in nymphs of the lobster cockroach *Nauphoeta cinerea*.** *Environmental Toxicology and Pharmacology*, v. 72, 2019.

WARING, S. C. et al. **Postmenopausal estrogen replacement therapy and risk of AD: A population-based study.** *Neurology*, v. 52, p. 965–970, 1999.

WEISS, B.; CLARKSON, T. W.; SIMON, W. **Silent latency periods in methylmercury poisoning and in neurodegenerative disease.** *Environmental Health Perspectives*, v. 110, p. 851–854, 2002.

WEVERS, A. **Localisation of pre- and postsynaptic cholinergic markers in the human brain.** *Behavioral Brain Research*, v. 221, p. 341-355, 2011.

WHETTEN R, et al. **Molecular structure and transformation of the glucose dehydrogenase gene in *Drosophila melanogaster*.** *Genetics*, v. 120, p. 475-484, 1988.

WILLIAMS, J. et al. **Noncanonical roles for tropomyosin during myogenesis.** *Development*, v. 142, p. 3440-3452, 2015.

WILSON, V. S. et al. **Utilizing toxicogenomic data to understand chemical mechanism of action in risk assessment.** *Toxicology and Applied Pharmacology*, v. 271, p. 299-308, 2013.

WOOTEN, V. et al. **Behavioral and biochemical alterations following in utero exposure to methylmercury.** *Neurobehavioral Toxicology and Teratology*, v. 7, p. 767-773, 1985.

XING, Z. et al. **Temporal and spatial variation in the mechanisms used by microorganisms to form methylmercury in the water column of Changshou Lake.** *Ecotoxicology and Environmental Safety*, v. 160, p. 32-41, 2018.

YADETIE, F. et al. **Global transcriptome analysis of Atlantic cod (*Gadus morhua*) liver after in vivo methylmercury exposure suggests effects on energy metabolism pathways.** *Aquatic Toxicology*, v. 126, p. 314-25, 2013.

YOO, J. I. et al. **High Levels of Heavy Metals Increase the Prevalence of Sarcopenia in the Elderly Population.** *Journal of Bone Metabolism*, v. 23, n. 2, p. 101-109, 2016.

ZAITSU, K. et al. **Application of metabolomics to toxicology of drugs of abuse: A mini review of metabolomics approach to acute and chronic toxicity studies.** *Drug Metabolism and Pharmacokinetics*, v. 31, n. 1, p. 21-26, 2016.

ZAREBA, G. et al. **Thimerosal distribution and metabolism in neonatal mice: comparison with methyl mercury.** *Journal of Applied Toxicology*, v. 27, p. 511–518, 2002.

APÊNDICE A – MATERIAL SUPLEMENTAR ARTIGO 1

Supporting information

High level of methylmercury exposure causes persisted toxicity in *Nauphoeta cinerea*

Bruna C. Piccoli¹, Jéssica C. Alvim¹; Fernanda D. da Silva¹, Pablo A. Nogara¹, Olawande C. Olagoke¹; Michael Aschner²; Cláudia S. Oliveira^{1,3,4}, João B. T. Rocha^{1,*}

¹Departamento de Bioquímica e Biologia Molecular, Centro de Ciências Naturais e Exatas, Universidade Federal de Santa Maria, RS, Brazil; ² Department of Molecular Pharmacology, Albert Einstein College of Medicine, Bronx, NY, United States; ³Instituto de Pesquisa Pelé Pequeno Príncipe, Curitiba, PR, Brazil; ⁴Faculdades Pequeno Príncipe, Curitiba, PR, Brazil.

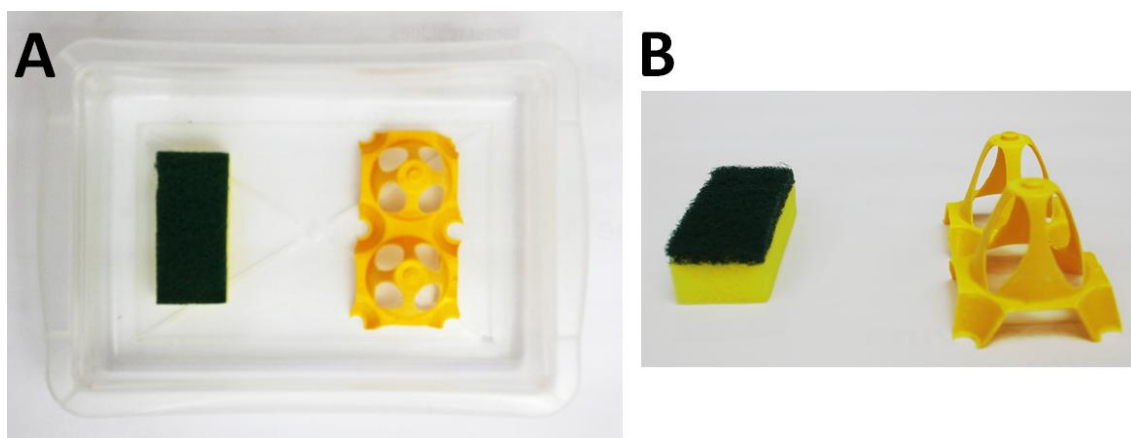


Fig. S1 Apparatus used for object recognition test (A) non-familiar object on the left and familiar on the right side of the box (B)

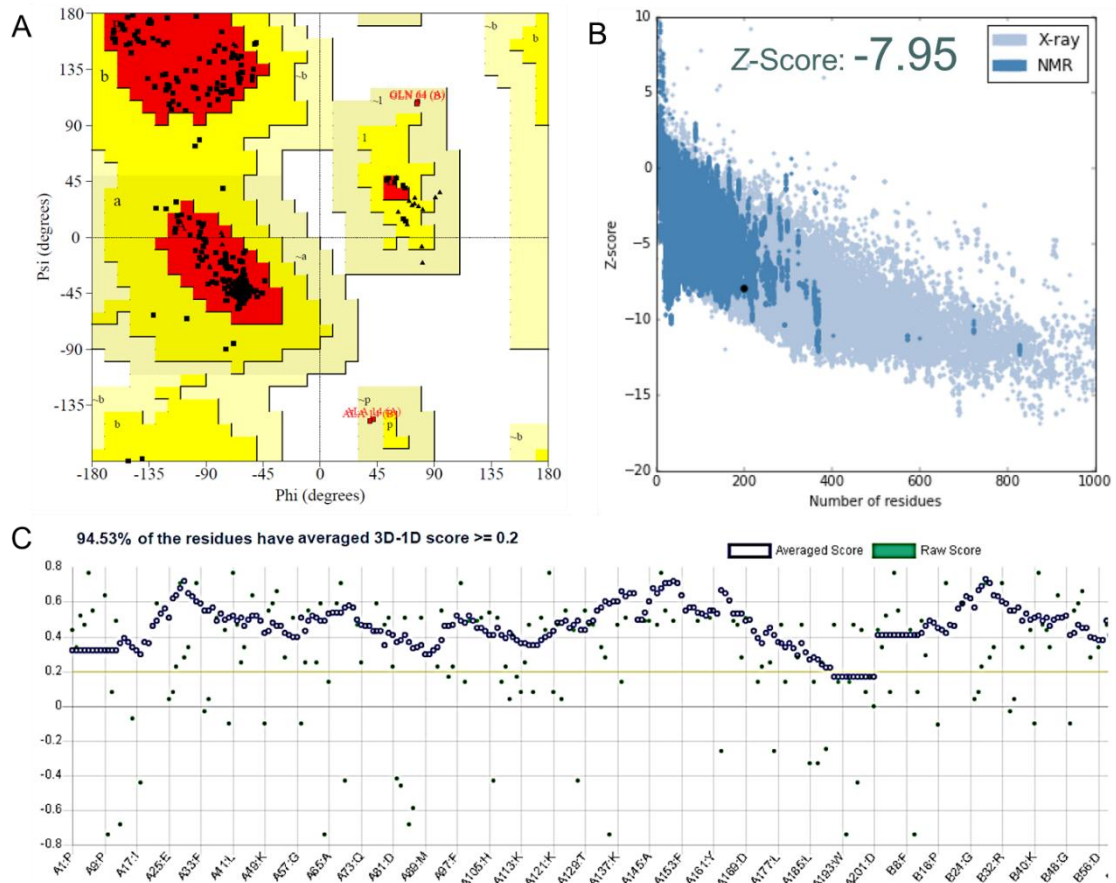


Fig. S2 Validation of cockroach GST model structure. (A) Ramachandran Plot demonstrated that 94.1% of the residues are in the most favored regions (red), 4.8% are in the additional allowed regions (yellow) and 1.1% are in the generously allowed regions (light yellow) (Laskowski et al. 1993). (B) ProSA shown that the GST Z-score value (\bullet) are in the range of native protein conformations (Wiederstein and Sippl 2007). (C) Verify 3D indicates that 94.53% of the residues have averaged 3D-1D score ≥ 0.2 (Eisenberg et al. 1997).

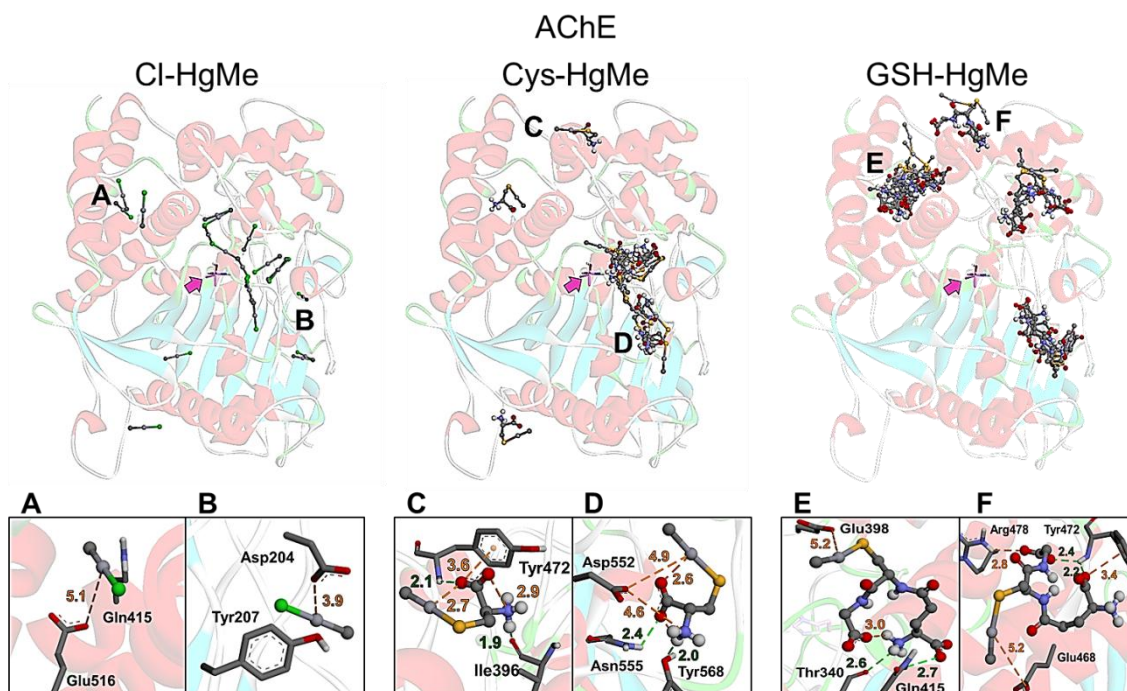


Fig. S3 Blind docking between the cockroach AChE and Cl-MeHg (A, B), Cys-HgMe (C, D), and GSH-HgMe (E, F). The AChE active site is indicated by the pink arrow. Twenty conformers of each molecule were generated during the simulations, presenting spontaneous interactions (Cl-MeHg $\Delta G = -2.2$ to -1.9 kcal/mol; Cys-MeHg $\Delta G = -4.3$ to -3.5 kcal/mol; GSH-MeHg $\Delta G = -5.1$ to -4.8 kcal/mol). Some MeHg interactions were selected and represented in the bottom. The MeHg species are represented in ball and stick, and the main residues involved in the interactions are in stick models. The H-bonds and electrostatic interactions are shown in green and orange dot lines, respectively.

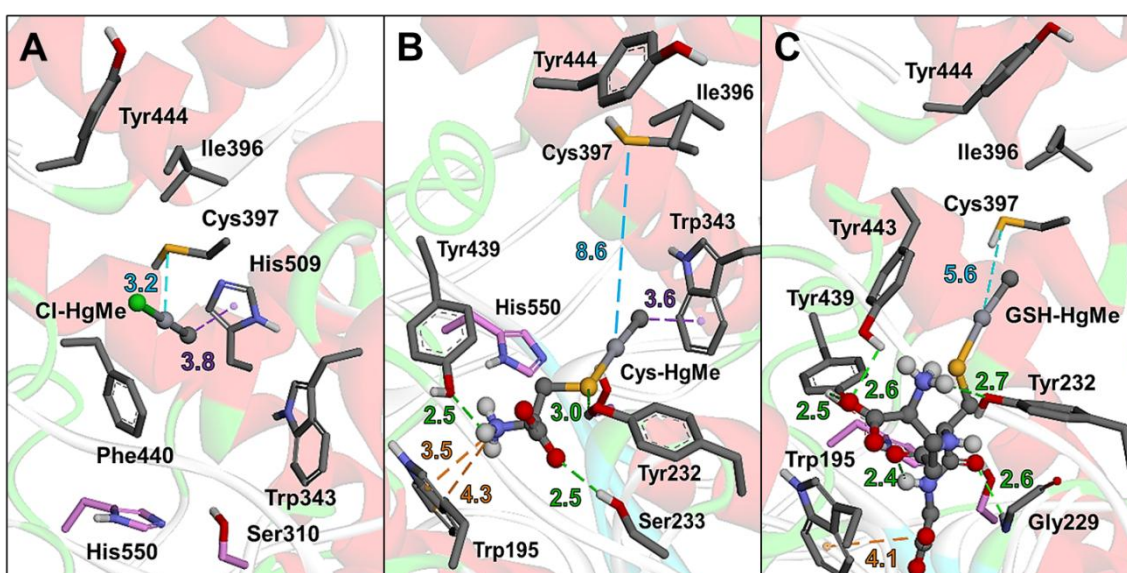


Fig. S4 Flexible docking results for Cl-MeHg (A), Cys-HgMe (B), and GSH-HgMe (C) with AChE. The AChE active site is indicated by the His550 and Ser310 (with the carbon atoms in pink color). The MeHg molecules are represented in ball and stick, and the main residues involved in the interactions are in stick models. In this case, the conformers with the shorter S \cdots Hg distance were selected. The H-bond, electrostatic, hydrophobic, and

mercury interactions are shown in green, orange, pink and blue dot lines, respectively, with the distances in Å. All molecules presented spontaneous interactions with the AChE (Cl-MeHg $\Delta G = -2.0$ kcal/mol; Cys-MeHg $\Delta G = -4.0$ kcal/mol; GSH-MeHg $\Delta G = -7.1$ kcal/mol).

References

- Eisenberg D, Luthy R, Bowie JU (1997) VERIFY 3D: assessment of protein models with three-dimensional profiles. *Methods Enzymol* 277:396–404. [https://doi.org/10.1016/S0076-6879\(97\)77022-8](https://doi.org/10.1016/S0076-6879(97)77022-8)
- Laskowski RA, MacArthur MW, Moss DS, Thornton JM (1993) PROCHECK: a program to check the stereochemical quality of protein structures. *J Appl Cryst* 26:283–291. <https://doi.org/10.1107/S0021889892009944>
- Wiederstein M, Sippl ML (2007) ProSA-web: Interactive web service for the recognition of errors in three-dimensional structures of proteins. *Nucleic Acids Res* 35:407–410. <https://doi.org/10.1093/nar/gkm290>

APÊNDICE B – MATERIAL SUPLEMENTAR ARTIGO 2

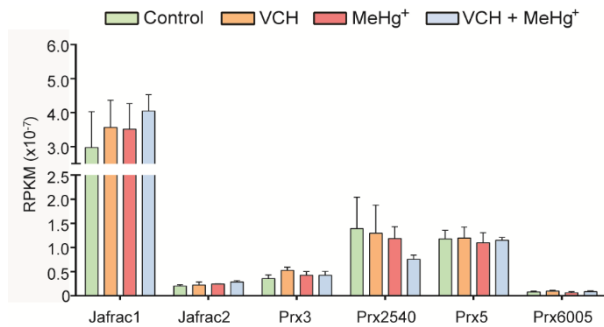


Fig. S1. Relative expression of peroxidorexin genes of *D. melanogaster* after VCH, MeHg⁺, and VCH+MeHg⁺ exposures for three days. Data expressed as the mean \pm SEM. Results analyzed by Two-way ANOVA (VCH, and MeHg⁺ as factors). There were no significant differences between treatments ($p > 0.05$).

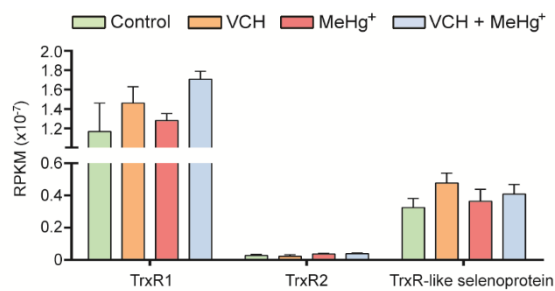


Fig. S2. Relative expression of thioredoxin reductases genes of *D. melanogaster* after VCH, MeHg⁺, and VCH+MeHg⁺ exposures for three days. Data expressed as the mean \pm SEM. Results analyzed by Two-way ANOVA (VCH, and MeHg⁺ as factors). There were no significant differences between treatments ($p > 0.05$).

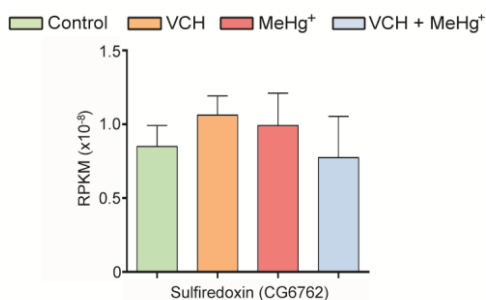


Fig. S3. Relative expression of sulfiredoxin gene of *D. melanogaster* after VCH, MeHg⁺, and VCH+MeHg⁺ exposures for three days. Data expressed as the mean \pm SEM. Results analyzed by Two-way ANOVA (VCH, and MeHg⁺ as factors). There were no significant differences between treatments ($p > 0.05$).

Table S1. Characteristic of trimmed data obtained from *D. melanogaster* RNA-sequencing in a control medium or exposed to VCH, MeHg⁺, and VCH + MeHg⁺ for three days.

| Sample | Total sequences | Nucleotides Sequenced | Mean \pm SD of nucleotides per read |
|---------------------------|-----------------|-----------------------|---------------------------------------|
| Control 1 | 2,447,571 | 194,340,620 | 79.4 \pm 32.2 |
| Control 2 | 1,464,491 | 174,209,371 | 119.0 \pm 54.2 |
| Control 3 | 2,127,723 | 226,076,712 | 106.3 \pm 41.6 |
| VCH 1 | 3,174,698 | 313,204,397 | 98.7 \pm 38.5 |
| VCH 2 | 1,760,085 | 206,833,383 | 117.5 \pm 44.8 |
| VCH 3 | 2,860,990 | 269,388,288 | 94.2 \pm 37.2 |
| MeHg ⁺ 1 | 6,155,792 | 492,193,201 | 80.0 \pm 37.9 |
| MeHg ⁺ 2 | 2,258,927 | 244,744,949 | 108.3 \pm 43.0 |
| MeHg ⁺ 3 | 4,073,003 | 350,962,044 | 86.2 \pm 37.7 |
| VCH + MeHg ⁺ 1 | 3,384,588 | 332,801,762 | 98.3 \pm 38.4 |
| VCH + MeHg ⁺ 2 | 3,110,325 | 281,418,804 | 90.5 \pm 37.7 |
| VCH + MeHg ⁺ 3 | 6,334,757 | 447,563,949 | 70.7 \pm 31.4 |

Table S2. Differentially expressed genes of *D. melanogaster* after VCH, MeHg⁺, and VCH+MeHg⁺ exposures for three days compared with non-exposed flies, as well as VCH and MeHg⁺ individual treatments compared to co-exposure.

| Group | Gene ID | Acronim | Gene name | Locus | Fold Change Log ₂ | P value |
|-------|---------|-----------|---|----------------------|------------------------------------|---------|
| VCH | CG4550 | NinaE | Opsin Rh1 | 3R:15711967-15713928 | -1.567940 | 0.00005 |
| | CG14995 | - | CG14995 | 3L:4076737-4086229 | -1.251680 | 0.00010 |
| | CG12055 | Gapdh1 | Glyceraldehyde-3-phosphate dehydrogenase 1 | 2R:3303710-3318212 | -1.223170 | 0.00005 |
| | CG6806 | Lsp2 | Larval serum protein | 3L:12103339-12105645 | -1.183360 | 0.00005 |
| | CG9042 | Gpdh | Glycerol-3-phosphate dehydrogenase [NAD ⁺] | 2L:5943681-5949092 | -1.151230 | 0.00045 |
| | CG8415 | RpS23 | 40S ribosomal protein S23 | 2R:9730097-9731490 | -0.972710 | 0.00030 |
| | CG1746 | ATPsynC | ATP synthase, subunit C | 3R:27041857-27045357 | -0.903322 | 0.00045 |
| | CG12505 | - | CG12505 | 2R:9872785-9875157 | 0.887012 | 0.00060 |
| | CG1059 | Karybeta3 | Karyopherin beta 3 | 3R:474944-480360 | 0.890293 | 0.00050 |
| | CG33106 | Mask | Ankyrin repeat and KH domain- containing protein mask | 3R:20057445-20075970 | 0.897663 | 0.00035 |
| | CG16858 | Vkg | Viking | 2L:5012143-5027412 | 0.985149 | 0.00025 |
| | CG7052 | Tep2 | Thiolester containing protein 2 | 2L:7693799-7701585 | 0.994643 | 0.00055 |
| | CG9916 | PPIase | Peptidyl-prolyl cis-trans isomerase | X:16151609-16154349 | 0.999734 | 0.00005 |

| /Cyclophilin | | | | | |
|--------------|---------|--|----------------------|----------|---------|
| CG4145 | Col4a1 | Collagen type IV alpha 1 | 2L:5029614-5037114 | 1.008110 | 0.00005 |
| CG2048 | Dco | Discs overgrown protein kinase | 3R:26880904-26886931 | 1.012550 | 0.00015 |
| CG8542 | Hsc70-4 | Heat shock 70 kDa protein cognate 5. | 2R:9767460-9771055 | 1.028000 | 0.00005 |
| CG9674 | - | CG9674 | 3L:16753073-16772987 | 1.052500 | 0.00030 |
| CG1404 | Ran | GTP-binding nuclear protein Ran. | X:10990079-10993807 | 1.095770 | 0.00005 |
| CG7414 | - | Eukaryotic translation initiation factor 2A | 3L:21758659-21762419 | 1.124510 | 0.00005 |
| CG10252 | - | CG10252 | 3R:19520935-19522000 | 1.204190 | 0.00050 |
| CG9796 | GILT1 | GILT-like protein 1 | 3R:9224246-9227580 | 1.248540 | 0.00020 |
| CG18730 | Amy-p | Alpha-amylase A | 2R:12633568-12635166 | 1.251470 | 0.00005 |
| CG4857 | - | CG4857 | X:3963654-3971984 | 1.256110 | 0.00005 |
| CG31509 | TotA | Turandot A | 3R:16696757-16697427 | 1.263090 | 0.00005 |
| CG8553 | SelD | Selenide, water dikinase | 2R:9783632-9785517 | 1.291090 | 0.00030 |
| CG33926 | - | CG33926 | 3L:9417210-9420232 | 1.294450 | 0.00005 |
| CG31508 | TotC | Turandot C | 3R:16698709-16699310 | 1.365770 | 0.00010 |
| CG14027 | TotM | Turandot M | 2L:5329856-5330466 | 1.387180 | 0.00020 |
| CG2727 | Emp | Epithelial membrane protein | 2R:20484203-20492398 | 1.403990 | 0.00060 |
| CG18106 | Dim-2 | Immune-induced peptide 2 precursor | 2R:13901459-13901898 | 1.409950 | 0.00020 |
| CG6533 | Cp16 | Chorion protein S16. | 3L:8705937-8706488 | 1.505400 | 0.00005 |
| CG6517 | Cp18 | Chorion protein S18. | 3L:8700781-8701474 | 1.693860 | 0.00005 |

| | | | | | | |
|-------------------|---------|-----------|------------------------------------|----------------------|-----------|---------|
| | CG5965 | Woc | Without children | 3R:23082314-23089758 | 1.736720 | 0.00005 |
| | CG10146 | AttA | Attacin-A | 2R:10262221-10264938 | 1.835310 | 0.00005 |
| | CG9434 | Fst | Frost | 3R:5463903-5475982 | 1.924590 | 0.00005 |
| | CG14981 | Mge | Maggie | 3L:3888875-3893463 | 2.014830 | 0.00005 |
| | CG17876 | Amy-d | Alpha-amylase B | 2R:12639624-12641245 | 2.096320 | 0.00005 |
| | CG11577 | CNPYb | Canopy b | 3L:19060147-19061485 | 2.418600 | 0.00010 |
| MeHg ⁺ | CG10816 | Dro | Drosocin precursor. | 2R:10260818-10261577 | -1.89970 | 0.00025 |
| | CG8269 | DCTN2-p50 | Dynamitin subunit 2 | 2R:4403652-4405152 | -1.789050 | 0,00005 |
| | CG3949 | Hoip | NHP2-like protein 1 homolog | 2L:9699833-9700465 | -1.686910 | 0.0001 |
| | CG9035 | Tapdelta | Translocon-associated protein | 2R:6886192-6887077 | -1.441140 | 0,00005 |
| | CG8727 | Cyc | Protein cycle | 3L:19747634-19749781 | -1.400290 | 0.0001 |
| | CG1751 | Spase25 | Signal peptidase complex subunit 2 | X:11330469-11331487 | -1.347300 | 0.0001 |
| | CG11642 | - | CG11642 | X:792052-794644 | -1.258300 | 0.0002 |
| | CG2746 | RpL19 | 60S ribosomal protein L19. | 2R:20476044-20477147 | -1.199750 | 0,00005 |
| | CG2879 | - | CG2879 | X:2132113-2133937 | -1.177640 | 0.0003 |
| | CG7070 | PyK | Pyruvate kinase | 3R:18193233-18198464 | -1.124890 | 0.00005 |
| | CG7765 | Khc | Kinesin heavy chain | 2R:11781827-11786841 | -1.118680 | 0.00005 |
| | CG4832 | Cnn | Centrosomin | 2R:8955217-8966392 | -1.079930 | 0.00020 |
| | CG3203 | RpL17 | Ribosomal protein L17 | X:6586772-6589493 | -1.079600 | 0.00005 |
| | CG2099 | RpL35A | Ribosomal protein L35A | 3R:1291288-1292819 | -0.98508 | 0.00005 |
| | CG4836 | - | CG4836 | 3R:15839593-15843976 | 0.991931 | 0.00005 |

| | | | | | | |
|----------------------------|---------|----------|---|----------------------|-----------|---------|
| | CG17097 | - | CG17097 | 2L:10646434-10650044 | 1.01798 | 0.00055 |
| | CG8709 | Lpin | Lipin | 2R:3649254-3657790 | 1.09036 | |
| | CG11796 | Hpd | 4-hydroxyphenylpyruvate dioxygenase | 3L:20370097-20373709 | 1.11056 | 0.00040 |
| | CG13321 | - | CG13321-PA | 2R:8469462-8471082 | 1.17777 | 0.00090 |
| | CG9016 | - | CG9016-PB | 2L:5922903-5923646 | 1.35984 | 0.00005 |
| | CG5016 | Mst57Db | Accessory gland-specific peptide 57Db precursor | 3R:21656443-21656635 | 1.5579 | 0.00005 |
| | CG13947 | | CG13947 | 2L:779186-779652 | 1.57364 | 0.00005 |
| | CG10650 | | CG10650-PA | 2L:18989540-18991859 | 1.62137 | 0.00005 |
| | CG9334 | Spn38F | Serpin 38F | 2L:20824200-20825772 | 1.7144 | 0.00040 |
| | CG9434 | Fst | Frost | 3R:5463903-5475982 | 1.74884 | 0.00075 |
| | CG2830 | Hsp60B | 60 kDa heat shock protein homolog 1, mitochondrial | 2L:728411-730566 | 1.78896 | 0.00040 |
| VCH + MeHg ⁺ | CG33706 | Im18 | Immune-induced peptide 18 precursor | 2R:19108513-19109373 | -2.257790 | 0.00010 |
| | CG9035 | Tapdelta | Translocon-associated protein | 2R:6886192-6887077 | -2.056830 | 0.00090 |
| | CG8399 | | CG8399-PA | 2R:11532601-11543024 | -1.840140 | 0.00005 |
| | CG3949 | Hoip | NHP2-like protein 1 homolog | 2L:9699833-9700465 | -1.834680 | 0.00025 |
| | CG9603 | Cox7A | Probable cytochrome c oxidase polypeptide 7A | 3R:4165658-4166763 | -1.695440 | 0.00005 |

| | | | | | |
|---------|-------------|--|----------------------|-----------|---------|
| CG17367 | Lnk | Lnk | 3R:21714264-21718999 | -1.571310 | 0.00010 |
| CG32581 | - | CG32581 | X:15622829-15633093 | -1.545230 | 0.00015 |
| CG6277 | | CG6277 | 3R:22847790-22848934 | -1.527580 | 0.00005 |
| CG6806 | Lsp2 | Larval serum protein 2 | 3L:12103339-12105645 | -1.520120 | 0.00055 |
| CG31937 | - | CG31937 | 2L:1729945-1731072 | -1.483340 | 0.00010 |
| CG17820 | Fit | Female-specific independent of transformer | 3R:17709639-17710176 | -1.481870 | 0.00010 |
| CG8857 | RpS11 | Ribosomal protein S11 | 2R:7714925-7716735 | -1.426020 | 0.00035 |
| CG9916 | PPIase/Cyp1 | Peptidyl-prolyl cis-trans isomerase | X:16151609-16154349 | -1.371750 | 0.00050 |
| CG7823 | RhoGDI | RhoGDI | 3L:19862647-19866773 | -1.338780 | 0.00060 |
| CG11129 | Yp3 | Vitellogenin-3 | X:13593481-13595113 | -1.323260 | 0.00015 |
| CG11309 | - | CG11309 | 3L:21235498-21238303 | -1.320680 | 0.00010 |
| CG18111 | Obp99a | General odorant-binding protein 99a precursor. | 3R:25497381-25498057 | -1.309350 | 0.00015 |
| CG31740 | - | CG31740 | 2L:18004856-18005631 | -1.273320 | 0.00005 |
| CG1821 | RpL31 | 60S ribosomal protein L31. | 2R:5098995-5099813 | -1.227360 | 0.00035 |
| CG8331 | - | CG8331 | 2R:9686372-9688828 | -1.222500 | 0.00040 |
| CG1970 | ND-49 | NADH dehydrogenase (Ubiquinone) 49 kDa subunit | 4:588537-591044 | -1.194210 | 0.00025 |
| CG3320 | Rab1 | Rab-protein 1 | 3R:17091747-17094831 | -1.161000 | 0.00095 |
| CG4897 | RpL7 | 60S ribosomal protein L7. | 2L:10201100-10202233 | -1.157810 | 0.00040 |

| | | | | | |
|---------|----------|---|----------------------|-----------|---------|
| CG3926 | Spat | Serine-pyruvate aminotransferase | X:6374183-6375962 | -1.131560 | 0.00050 |
| CG16747 | - | | 2R:7682478-7690169 | -1.121030 | 0.00015 |
| CG5525 | CCT4 | T-complex protein 1 subunit delta | 2L:12690324-12692937 | -1.116180 | 0.00075 |
| CG8782 | Oat | Ornithine aminotransferase, mitochondrial | 3L:19612534-19615108 | -1.101070 | 0.00025 |
| CG10691 | l(2)37Cc | Protein l(2)37Cc | 2L:19117968-19119792 | -1.096050 | 0.00085 |
| CG6666 | SdhC | Succinate dehydrogenase, subunit C | 3R:7034855-7035571 | -1.082270 | 0.00075 |
| CG12306 | Polo | Serine/threonine-protein kinase polo | 3L:20243845-20247307 | -1.079200 | 0.00050 |
| CG1263 | RpL8 | 60S ribosomal protein L8. | 3L:2570981-2572529 | -1.074230 | 0.00045 |
| CG18624 | ND-MNLL | NADH dehydrogenase (Ubiquinone) MNLL subunit | X:7738279-7739032 | -1.073210 | 0.00050 |
| CG2099 | RpL35A | Ribosomal protein L35A | 3R:1291288-1292819 | -1.071070 | 0.00075 |
| CG1780 | Idgf4 | Chitinase-like protein Idgf4 | X:9773479-9776200 | -1.060420 | 0.00100 |
| CG6342 | Irp-1B | Iron regulatory protein 1B | 3R:6234336-6238638 | -1.042610 | 0.00085 |
| CG4046 | RpS16 | 40S ribosomal protein S16. | 2R:18113702-18115583 | -1.028500 | 0.00040 |
| CG3203 | RpL17 | Ribosomal protein L17 | X:6586772-6589493 | -1.024280 | 0.00065 |
| CG7726 | RpL11 | 60S ribosomal protein L11. | 2R:14957211-14958382 | -1.021950 | 0.00100 |
| CG11271 | RpS12 | 40S ribosomal protein S12. | 3L:12997314-13010384 | -1.006140 | 0.00010 |
| CG6822 | Ergic53 | Ergic53, isoform A | 3L:8508898-8511965 | -1.003620 | 0.00085 |
| CG30425 | RpL41 | Ribosomal protein L41 | 2R:20401769-20422717 | -1.001690 | 0.00035 |
| CG11276 | RpS4 | 40S ribosomal protein S4. | 3L:13015702-13017859 | -0.984747 | 0.00020 |

| | | | | | |
|---------|----------|---|----------------------|-----------|---------|
| CG14629 | - | CG14629 | X:908357-909449 | -0.976130 | 0.00035 |
| CG4494 | Smt3 | Small ubiquitin-related modifier | 2L:6966775-6967593 | -0.974483 | 0.00005 |
| CG6543 | Echs1 | CG6543 | 2R:9365788-9370255 | -0.967872 | 0.00005 |
| CG10071 | RpL29 | 60S ribosomal protein L29 | 2R:16801351-16803169 | -0.959938 | 0.00015 |
| CG4153 | eIF2beta | Eukaryotic translation initiation factor 2 subunit 2 | 3L:12499037-12500684 | -0.939942 | 0.00095 |
| CG3835 | D2hgdh | D-2-hydroxyglutaric acid dehydrogenase | X:1997643-2001095 | -0.922492 | 0.00005 |
| CG11844 | Vig2 | Vig2, isoform B | 3R:20949094-20951348 | -0.904868 | 0.00005 |
| CG2168 | RpS3A | 40S ribosomal protein S3a | 4:86744-87863 | -0.897093 | 0.00005 |
| CG2207 | - | CG2207 | 2L:21614182-21617521 | -0.894135 | 0.00075 |
| CG4916 | Me31B | Putative ATP-dependent RNA helicase me31b | 2L:10239325-10242175 | -0.856791 | 0.00005 |
| CG5399 | - | CG5399 | 3R:11520991-11522286 | 1.015140 | 0.00005 |
| CG10911 | - | CG10911 | 2R:13567409-13568927 | 1.048920 | 0.00010 |
| CG31029 | - | CG31029 | 3R:25955010-25958117 | 1.112100 | 0.00030 |
| CG9985 | Sktl | Skittles | 2R:16328847-16343646 | 1.119710 | 0.00005 |
| CG4527 | Slik | Sterile20-like kinase | 2R:19899728-19910288 | 1.189110 | 0.00005 |
| CG7203 | - | CG7203 | 2L:7752167-7753160 | 1.195900 | 0.00020 |
| CG14718 | - | CG14718 | 3R:7526335-7528442 | 1.295000 | 0.00005 |
| CG11719 | Mst98Ca | Male-specific RNA 98Ca | 3R:24117054-24118385 | 1.352820 | 0.00005 |

| | | | | | |
|---------|-----------|-------------------------------------|----------------------|----------|---------|
| CG4691 | - | CG4691 | 2L:14756695-14757862 | 1.377660 | 0.00005 |
| CG7756 | Hsc70-2 | Heat shock 70 kDa protein cognate 2 | 3R:8870480-8873106 | 1.377840 | 0.00055 |
| CG6524 | Cp19 | Chorion protein S19. | 3L:8703854-8704465 | 1.417160 | |
| CG13947 | - | CG13947 | 2L:779203-779563 | 1.463090 | 0.00040 |
| CG1361 | Anp | Andropin precursor. | 3R:26035669-26036011 | 1.478510 | 0.00090 |
| CG5717 | Yellow-g | Yellow-g | 3L:2253408-2256223 | 1.585750 | 0.00005 |
| CG6533 | Cp16 | Chorion protein S16. | 3L:8705937-8706488 | 1.588150 | 0.00005 |
| CG6517 | Cp18 | Chorion protein S18. | 3L:8700781-8701474 | 1.643610 | 0.00005 |
| CG7298 | - | CG7298 | 3L:20135905-20137527 | 2.053190 | 0.00005 |
| CG13114 | - | CG13114 | 2L:9545840-9547394 | 2.415920 | 0.00040 |
| CG13804 | Yellow-g2 | yellow-g2 | 3L:2260129-2261336 | 2.614560 | 0.00075 |

Table S3. GO enrichment analysis with differentially expressed genes of *D. melanogaster* after VCH, MeHg⁺, and VCH+MeHg⁺ exposures for three days compared with non-exposed flies.

| Group | Domain | Term | Number of genes | Genes | Protein class |
|-------|--------------------|---------|-----------------|--|---------------|
| VCH | Molecular function | Binding | 6 | Mask (Ankyrin repeat and KH domain-containing protein mask); | - |

| | | | |
|--------------------|----|---|---|
| | | CG7414 (Eukaryotic translation initiation factor 2A); | Nuclease; translation initiation factor |
| | | Karybeta3 (Karyopherin beta 3); | G-protein modulator transfer/carrier protein transporter |
| | | Tep2 (Thioester-containing protein 2); | Complement component cytokine; serine protease inhibitor |
| | | CNPYb (Canopy b) | - |
| | | Hsc70-5 (Heat shock 70 kDa protein cognate 5) | - |
| Catalytic activity | 11 | Lsp2 (Larval serum protein 2); | Oxidase, oxygenase |
| | | GILT1 (GILT-like protein 1); | reductase |
| | | Gpdh (glycerol-3-phosphate dehydrogenase [NAD+]); | dehydrogenase |
| | | Tep2 (Thioester-containing protein 2); | Complement component cytokine; serine protease inhibitor |

| | | | |
|----------------------------|---|---|--|
| | | Ran (GTP-binding nuclear protein Ran) | Small GTPase |
| | | ATPsynC (ATP synthase subunit C) | ATP synthase |
| | | Dco (Discs overgrown protein kinase) | Non-receptor serine/threonine protein kinase |
| | | Gapdh1 (Glyceraldehyde-3-phosphate dehydrogenase 1) | dehydrogenase |
| | | SelD (selenide, water dikinase) | Transferase |
| | | CG9674 | Cysteine protease dehydrogenase reductase |
| | | Hsc70-5 (Heat shock 70 kDa protein cognate 5) | |
| Receptor activity | 1 | NinaE (Opsin Rh1) | G-protein coupled receptor |
| Signal transducer activity | 1 | NinaE (Opsin Rh1) | G-protein coupled receptor |
| Structural | 1 | RpS23 (40S ribosomal protein | Ribosomal protein |

| | | | | |
|--------------------|---------------------------------|---|--|--|
| | molecule activity | | S23) | |
| | Translation regulator activity | 1 | CG7414 (Eukaryotic translation initiation factor 2A) | Nuclease; translation initiation factor |
| | Transporter activity | 2 | Karybeta3 (Karyopherin beta 3) | G-protein modulator transfer/carrier protein transporter |
| | | | ATPsynC (ATP synthase subunit C) | ATP synthase |
| Biological process | Biological adhesion | 2 | Col4a1 (Collagen alpha-1(IV)) | - |
| | | | Vkg (viking) | - |
| | Biological regulation | 2 | NinaE (Opsin Rh1) | G-protein coupled receptor |
| | | | Dco (discs overgrown protein kinase) | Non-receptor serine/threonine protein kinase |
| | Cellular component organization | 5 | Dco (Discs overgrown protein kinase) | Non-receptor serine/threonine protein kinase |

| | | | |
|------------------|----|---|--|
| | | Mask (Ankyrin repeat and KH domain-containing protein mask) | - |
| | | Col4a1 (collagen type IV alpha 1) | - |
| | | Ran (GTP-binding nuclear protein Ran) | Small GTPase |
| | | Vkg (Viking) | - |
| Cellular process | 13 | CG9674 | Cysteine protease dehydrogenase reductase |
| | | Karybeta3 (Karyopherin beta 3) | G-protein modulator transfer/carrier protein transporter |
| | | 40S ribosomal protein S23 | Ribosomal protein |
| | | Dco (Discs overgrown protein kinase) | Non-receptor serine/threonine protein kinase |
| | | Mask (Ankyrin repeat and KH domain-containing protein mask) | - |

| | | | |
|-----------------------|---|--|--|
| | | Col4a1 (collagen type IV alpha 1) | - |
| | | Hsc70-5 (Heat shock 70 kDa protein cognate 5) | - |
| | | CG7414 (Eukaryotic translation initiation factor 2A) | Nuclease; translation initiation factor |
| | | Ran (GTP-binding nuclear protein Ran) | Small GTPase |
| | | SeID (Selenide, water dikinase) | Transferase |
| | | Tep2 (Thioester-containing protein 2) | Complement component cytokine; serine protease inhibitor |
| | | ATPsynC (ATP synthase, subunitC) | ATP synthase |
| | | Vkg (Viking) | - |
| Immune system process | 3 | Col4a1 (collagen type IV alpha 1) | - |
| | | AttA (Attacin-A) | - |

| | | | |
|-------------------|----|---|--|
| | | Vkg (Viking) | - |
| Localization | 5 | Karybeta3 (Karyopherin beta 3) | G-protein modulator transfer/carrier protein transporter |
| | | Dco (Discs overgrown protein kinase) | Non-receptor serine/threonine protein kinase |
| | | Mask (Ankyrin repeat and KH domain-containing protein mask) | - |
| | | Lps2 (Larval serum protein 2) | Oxidase; oxygenase |
| | | Ran (GTP-binding nuclear protein Ran) | Small GTPase |
| Metabolic Process | 13 | Gapdh1 (Glyceraldehyde-3-phosphate dehydrogenase 1) | dehydrogenase |
| | | CG9674 | Cysteine protease dehydrogenase reductase |
| | | RpS23 (40S ribosomal protein S23) | Ribosomal protein |
| | | Dco (Discs overgrown protein | Non-receptor serine/threonine |

| | |
|--|--|
| kinase) | protein kinase |
| Hsc70-5 (Heat shock 70 kDa protein cognate 5) | - |
| CG7414 (Eukaryotic translation initiation factor 2A) | Nuclease; translation initiation factor |
| Gpdh (glycerol-3-phosphate dehydrogenase [NAD+]); | dehydrogenase |
| Lps2 (Larval serum protein 2) | Oxidase; oxygenase |
| Ran (GTP-binding nuclear protein Ran) | Small GTPase |
| GILT1 (GILT-like protein 1) | reductase |
| SelD (Selenide, water dikinase) | Transferase |
| Tep2 (Thioester-containing protein 2) | Complement component cytokine; serine protease inhibitor |
| ATPsynC (ATP synthase subunit C) | ATP synthase |

| | | | | |
|--------------------|----------------------|----|---|--|
| | Response to stimulus | 5 | NinaE (Opsin Rh1) | G-protein coupled receptor |
| | | | Dco (Discs overgrown protein kinase) | Non-receptor serine/threonine protein kinase |
| | | | Hsc70-5 (Heat shock 70 kDa protein cognate 5) | - |
| | | | AttA (Attacin-A) | - |
| | | | Tep2 (Thioester-containing protein 2) | Complement component cytokine; serine protease inhibitor |
| Cellular component | Cell part | 10 | CNPYb (Canopy b) | - |
| | | | CG9674 | Cysteine protease dehydrogenase reductase |
| | | | Karybeta3 (Karyopherin beta 3) | G-protein modulator transfer/carrier protein transporter |
| | | | RpS23 (40S ribosomal protein S23) | Ribosomal protein |

| | | | |
|----------------------|---|--|--|
| | | Dco (Discs overgrown protein kinase) | Non-receptor serine/threonine protein kinase |
| | | Hsc70-5 (Heat shock 70 kDa protein cognate 5) | - |
| | | CG7414 (Eukaryotic translation initiation factor 2A) | Nuclease; translation initiation factor |
| | | Ran (GTP-binding nuclear protein Ran) | Small GTPase |
| | | SelD (Selenide, water dikinase) | Transferase |
| | | ATPsynC (ATP synthase, subunit C) | ATP synthase |
| Extracellular matrix | 2 | Col4a1 (collagen type IV alpha 1) | - |
| | | Vkg (Viking) | - |
| Extracellular region | 1 | AttA (Attacin-A) | - |
| Macromolecular | 3 | RpS23 (40S ribosomal protein) | Ribosomal protein |

| | | | |
|-----------|---|--|---|
| complex | | S23) | |
| | | CG7414 (Eukaryotic translation initiation factor 2A) | Nuclease; translation initiation factor |
| | | ATPsynC (ATP synthase, subunit C) | ATP synthase |
| Membrane | 3 | NinaE (Opsin Rh1) | G-protein coupled receptor |
| | | Karybeta3 (Karyopherin beta 3) | G-protein modulator transfer/carrier protein transporter |
| | | ATPsynC (ATP synthase, subunit C) | ATP synthase |
| Organelle | 5 | Karybeta3 (Karyopherin beta 3) | G-protein modulator transfer/carrier protein transporter |
| | | RpS23 (40S ribosomal protein S23) | Ribosomal protein |
| | | Dco (Discs overgrown protein kinase) | Non-receptor serine/threonine protein kinase |
| | | CG7414 (Eukaryotic translation | Nuclease; translation initiation |

| | | | | | |
|-------------------|--------------------|---------|---|---|-----------------------------------|
| | | | | initiation factor 2A) | factor |
| | | | | Ran (GTP-binding nuclear protein Ran) | Small GTPase |
| MeHg ⁺ | Molecular function | Binding | 3 | Hsp60B (60 kDa heat shock protein homolog 1, mitochondrial) | - |
| | | | | Khc (Kinesin heavy chain) | Microtubule binding motor protein |
| | | | | Hoip (NHP2-like protein 1 homolog) | Ribosomal protein |
| | Catalytic activity | | 6 | Lpin (Lipin) | - |
| | | | | Khc (Kinesin heavy chain) | Microtubule binding motor protein |
| | | | | PyK (Pyruvate kinase) | - |
| | | | | Hpd (4-hydroxyphenylpyruvate dioxygenase) | - |
| | | | | Spase25 (Signal peptidase complex subunit 2) | Enzyme modulator |

| | | | | |
|--------------------|---|---|---|-----------------------------------|
| | | | CG4836 (uncharacterized protein) | Dehydrogenase reductase |
| | Structural molecule activity | 2 | RpL19 (60S ribosomal protein L19) | Ribosomal protein |
| | | | RpL17 (60S ribosomal protein L17) | |
| Biological process | Cellular component organization or biogenesis | 3 | DCTN2-p50 (Dynactin subunit 2) | Microtubule binding motor protein |
| | | | Hsp60B (60 kDa heat shock protein homolog 1, mitochondrial) | - |
| | | | Hoip (NHP2-like protein 1 homolog) | Ribosomal protein |
| | Localization | 2 | Khc (Kinesin heavy chain) | Microtubule binding motor protein |
| | | | Spase25 (Signal peptidase complex subunit 2) | Enzyme modulator |

| | | | | |
|--------------------|-------------------|---|---|-----------------------------------|
| | Metabolic process | 9 | Hsp60B (60 kDa heat shock protein homolog 1, mitochondrial) | - |
| | | | Lpin (Lipin) | - |
| | | | Khc (Kinesin heavy chain) | Microtubule binding motor protein |
| | | | PyK (Pyruvate kinase) | - |
| | | | Hoip (NHP2-like protein 1 homolog) | Ribosomal protein |
| | | | Hpd (4-hydroxyphenylpyruvate dioxygenase) | - |
| | | | RpL17 (60S ribosomal protein L17) | |
| | | | Spase25 (Signal peptidase complex subunit 2) | Enzyme modulator |
| | | | CG4836 | Dehydrogenase reductase |
| Cellular component | Cell part | 9 | DCTN2-p50 (Dynactin subunit 2) | Microtubule binding motor protein |

| | | | |
|----------------------|---|---|-----------------------------------|
| | | Hsp60B (60 kDa heat shock protein homolog 1, mitochondrial) | - |
| | | Khc (Kinesin heavy chain) | Microtubule binding motor protein |
| | | PyK (Pyruvate kinase) | - |
| | | Hoip (NHP2-like protein 1 homolog) | Ribosomal protein |
| | | RpL19 (60S ribosomal protein L19) | Ribosomal protein |
| | | TRAM (Translocating chain-associated membrane protein) | - |
| | | RpL17 (60S ribosomal protein L17) | |
| | | Spase25 (Signal peptidase complex subunit 2) | Enzyme modulator |
| Extracellular region | 1 | Spn38F (Serpine 38F) | Protease inhibitor |
| Macromolecular | 6 | DCTN2-p50 (Dynactin subunit) | Microtubule binding motor |

| complex | | 2) | protein |
|-----------|---|---|-----------------------------------|
| | | Hsp60B (60 kDa heat shock protein homolog 1, mitochondrial) | - |
| | | Hoip (NHP2-like protein 1 homolog) | Ribosomal protein |
| | | RpL19 (60S ribosomal protein L19) | Ribosomal protein |
| | | RpL17 (60S ribosomal protein L17) | |
| | | Spase25 (Signal peptidase complex subunit 2) | Enzyme modulator |
| Membrane | 1 | Spase25 (Signal peptidase complex subunit 2) | Enzyme modulator |
| Organelle | 8 | DCTN2-p50 (Dynactin subunit 2) | Microtubule binding motor protein |
| | | Hsp60B (60 kDa heat shock protein homolog 1, | - |

| | | | | | |
|-------------------------|--------------------|---------|----|--|--|
| | | | | mitochondrial) | |
| | | | | Khc (Kinesin heavy chain) | Microtubule binding motor protein |
| | | | | Hoip (NHP2-like protein 1 homolog) | Ribosomal protein |
| | | | | RpL19 (60S ribosomal protein L19) | Ribosomal protein |
| | | | | TRAM (Translocating chain-associated membrane protein) | - |
| | | | | RpL17 (60S ribosomal protein L17) | |
| | | | | Spase25 (Signal peptidase complex subunit 2) | Enzyme modulator |
| VCH + MeHg ⁺ | Molecular function | Binding | 11 | Hsc70-2 (heat shock 70 kDa protein cognate 2) | - |
| | | | | RhoGDI (RhoGDI) | G-protein modulator signaling molecule |
| | | | | SdhC (Succinate dehydrogenase, subunit C) | - |

| | | | |
|--------------------|----|---|---|
| | | CG14718 | DNA binding protein; mRNA splicing factor; transcription factor |
| | | Vig2 (Vig2, isoform B) | RNA binding protein |
| | | Hoip (NHP2-like protein 1 homolog) | Ribosomal protein |
| | | Oat (Ornithine aminotransferase, mitochondrial) | transaminase |
| | | Slik (Sterile20-like kinase) | - |
| | | CCT4 (T-complex protein 1 subunit delta) | Chaperonin |
| | | CG32581 | Ubiquitin-protein ligase |
| | | Ergic53 (Ergic53, isoform A) | Membrane traffic protein |
| Catalytic activity | 17 | Hsc70-2 (heat shock 70 kDa protein cognate 2) | - |
| | | RhoGDI (RhoGDI) | G-protein modulator signaling |

| | molecule |
|--|-----------------------------------|
| SdhC (Succinate dehydrogenase, subunit C) | - |
| Spat (Serine-pyruvate aminotransferase) | Transaminase |
| Oat (Ornithine aminotransferase, mitochondrial) | transaminase |
| Lsp2 (Larval serum protein 2) | Oxidase; oxygenase |
| Idgf4 (Chitinase-like protein Tdgf4) | - |
| Yellow-g2 (Yellow-g2) | - |
| Slik (Sterile20-like kinase) | - |
| ND-49 (NADH dehydrogenase (Ubiquinone) 49 kDa subunit) | Dehydrogenase; reductase |
| CG6277 | Esterase; lipase; storage protein |
| Rab1 (Rab-protein 1) | - |

| | | | |
|---------------------------------|----|--|---|
| | | Yellow-g (Yellow-g) | - |
| | | Sktl (Skittles) | Kinase |
| | | CG6543 | Acetyltransferase; acetyltransferase; dehydrogenase; epimerase/racemase; hydratase/ ligase |
| | | Yp3 (Vitellogenin-3) | Esterase; lipase; storage protein |
| | | Irp-1B (Iron regulatory protein 1B) | Dehydratase; hydratase |
| Signal transducer activity | 1 | Slik (Sterile20-like kinase) | - |
| Structural molecule activity | 11 | RpS4 (40S ribosomal protein S4) | Ribosomal protein |
| | | RpS3A (40S ribosomal protein S3A) | Cysteine protease; ribosomal protein |
| | | RpS12 (40S ribosomal protein S12) | Ribosomal protein |

| | | | | |
|--------------------|--------------------------------|---|---|-------------------------------|
| | | | RpL11 (60S ribosomal protein L11) | Ribosomal protein |
| | | | RpL31 (60S ribosomal protein L31) | Ribosomal protein |
| | | | RpS16 (40S ribosomal protein S16) | - |
| | | | RpL8 (60S ribosomal protein L8) | Ribosomal protein |
| | | | RpL17 (60S ribosomal protein L17) | - |
| | | | RpL29 (60S ribosomal protein L29) | Ribosomal protein |
| | | | RpS11 (40S ribosomal protein S11) | Ribosomal protein |
| | | | RpL7 (60S ribosomal protein L7) | Ribosomal protein |
| | Translation regulator activity | 1 | eIF2beta (Eukaryotic translation initiation factor 2 subunit 2) | Translation initiation factor |
| Biological process | Biological regulation | 2 | Slik (Sterile20-like kinase) | - |

| | | | |
|---|----|---|--------------------------|
| | | Rab1 (Rab-protein 1) | - |
| Cellular component organization or biogenesis | 7 | RpL11 (60S ribosomal protein L11) | Ribosomal protein |
| | | Hoip (NHP2-like protein 1 homolog) | Ribosomal protein |
| | | RpS16 (40S ribosomal protein S16) | - |
| | | CCT4 (T-complex protein 1 subunit delta) | chaperonin |
| | | Rab1 (Rab-protein 1) | - |
| | | Ergic53 (Ergic53, isoform A) | Membrane traffic protein |
| | | RpL7 (60S ribosomal protein L7) | Ribosomal protein |
| Cellular process | 29 | Hsc70-2 (heat shock 70 kDa protein cognate 2) | - |
| | | RpS4 (40S ribosomal protein S4) | Ribosomal protein |

| | |
|---|---|
| RhoGDI (RhoGDI) | G-protein modulator signaling molecule |
| RpS3A (40S ribosomal protein S3A) | Cysteine protease; ribosomal protein |
| SdhC (Succinate dehydrogenase, subunit C) | - |
| RpL11 (60S ribosomal protein L11) | Ribosomal protein |
| Spat (Serine-pyruvate aminotransferase) | Transaminase |
| CG14718 | DNA binding protein mRNA splicing factor transcription factor |
| RpL31 (60S ribosomal protein L31) | Ribosomal protein |
| Hoip (NHP2-like protein 1 homolog) | Ribosomal protein |
| Oat (Ornithine aminotransferase, mitochondrial) | transaminase |

| | |
|---|--------------------------|
| Smt3 (Small ubiquitin-related modifier) | - |
| Polo (Serine/threonine-protein kinase polo) | - |
| RpS16 (40S ribosomal protein S16) | - |
| Yellow-g2 (Yellow-g2) | - |
| Slik (Sterile20-like kinase) | - |
| RpL8 (60S ribosomal protein L8) | Ribosomal protein |
| RpL17 (60S ribosomal protein L17) | - |
| CCT4 (T-complex protein 1 subunit delta) | chaperonin |
| Rab1 (Rab-protein 1) | - |
| CG32581 | Ubiquitin-protein ligase |
| I(2)37Cc (Protein I(2)37Cc) | - |

| | | | |
|-----------------------|---|---|---|
| | | Yellow-g (Yellow-g) | - |
| | | Ergic53 (Ergic53, isoform A) | Membrane traffic protein |
| | | RpL29 (60S ribosomal protein L29) | Ribosomal protein |
| | | RpL7 (60S ribosomal protein L7) | Ribosomal protein |
| | | Sktl (Skittles) | Kinase |
| | | CG6543 | Acetyltransferase; acetyltransferase; dehydrogenase; epimerase/racemase; hydratase/ ligase |
| | | Lnk (Lnk) | - |
| Developmental process | 4 | Polo (Serine/threonine-protein kinase polo) | - |
| | | Yellow-g2 (Yellow-g2) | - |
| | | Slik (Sterile20-like kinase) | - |

| | | | |
|-------------------|----|---|--------------------------------------|
| | | Yellow-g (Yellow-g) | - |
| Localization | 4 | SdhC (Succinate dehydrogenase, subunit C) | - |
| | | Lsp2 (Larval serum protein 2) | Oxidase; oxygenase |
| | | Rab1 (Rab-protein 1) | - |
| | | Ergic53 (Ergic53, isoform A) | Membrane traffic protein |
| Metabolic process | 29 | Hsc70-2 (heat shock 70 kDa protein cognate 2) | - |
| | | RpS4 (40S ribosomal protein S4) | Ribosomal protein |
| | | RpS3A (40S ribosomal protein S3A) | Cysteine protease; ribosomal protein |
| | | SdhC (Succinate dehydrogenase, subunit C) | - |
| | | Spat (Serine-pyruvate aminotransferase) | Transaminase |
| | | CG14718 | DNA binding protein mRNA |

| | splicing factor transcription factor |
|---|--------------------------------------|
| RpL31 (60S ribosomal protein L31) | Ribosomal protein |
| Hoip (NHP2-like protein 1 homolog) | Ribosomal protein |
| Oat (Ornithine aminotransferase, mitochondrial) | transaminase |
| Lsp2 (Larval serum protein 2) | Oxidase; oxygenase |
| Smt3 (Small ubiquitin-related modifier) | - |
| Idgf4 (Chitinase-like protein Tdgf4) | - |
| RpS16 (40S ribosomal protein S16) | - |
| Yellow-g2 (Yellow-g2) | - |
| Slik (Sterile20-like kinase) | - |

| | |
|---|-----------------------------------|
| ND-49 (NADH dehydrogenase (Ubiquinone) 49 kDa subunit) | Dehydrogenase; reductase |
| RpL8 (60S ribosomal protein L8) | Ribosomal protein |
| RpL17 (60S ribosomal protein L17) | - |
| CCT4 (T-complex protein 1 subunit delta) | chaperonin |
| CG6277 | Esterase; lipase; storage protein |
| Rab1 (Rab-protein 1) | - |
| CG32581 | Ubiquitin-protein ligase |
| I(2)37Cc (Protein I(2)37Cc) | - |
| Yellow-g (Yellow-g) | - |
| RpL29 (60S ribosomal protein L29) | Ribosomal protein |
| RpL7 (60S ribosomal protein L7) | Ribosomal protein |

| | | | |
|--|---|--|---|
| | | CG6543 | Acetyltransferase; acetyltransferase; dehydrogenase; epimerase/racemase; hydratase/ ligase |
| | | Yp3 (Vitellogenin-3) | Esterase; lipase; storage protein |
| | | Irp-1B (Iron regulatory protein 1B) | Dehydratase; hydratase |
| Multicellular organismal process | 3 | Yellow-g2 (Yellow-g2) | - |
| | | Yellow-g (Yellow-g) | - |
| | | Obp99a (General odorant- binding protein 99a) | Signaling molecule |
| Reproduction | 1 | CG6277 | Esterase; lipase; storage protein |
| Response to stimulus | 4 | Hsc70-2 (heat shock 70 kDa protein cognate 2) | - |
| | | Slik (Sterile20-like kinase) | - |

| | | | | |
|--------------------|-----------|----|---|--|
| | | | Rab1 (Rab-protein 1) | - |
| | | | CG32581 | Ubiquitin-protein ligase |
| Cellular component | Cell part | 25 | Hsc70-2 (heat shock 70 kDa protein cognate 2) | - |
| | | | RpS4 (40S ribosomal protein S4) | Ribosomal protein |
| | | | RpS3A (40S ribosomal protein S3A) | Cysteine protease; ribosomal protein |
| | | | SdhC (Succinate dehydrogenase, subunit C) | - |
| | | | RpS12 (40S ribosomal protein S12) | Ribosomal protein |
| | | | RpL11 (60S ribosomal protein L11) | Ribosomal protein |
| | | | Spat (Serine-pyruvate aminotransferase) | Transaminase |
| | | | CG14718 | DNA binding protein; mRNA splicing factor; transcription |

| | |
|---|-------------------|
| | factor |
| RpL31 (60S ribosomal protein L31) | Ribosomal protein |
| Hoip (NHP2-like protein 1 homolog) | Ribosomal protein |
| Oat (Ornithine aminotransferase, mitochondrial) | transaminase |
| Smt3 (Small ubiquitin-related modifier) | - |
| RpS16 (40S ribosomal protein S16) | - |
| Slik (Sterile20-like kinase) | - |
| RpL8 (60S ribosomal protein L8) | Ribosomal protein |
| RpL17 (60S ribosomal protein L17) | - |
| CCT4 (T-complex protein 1 subunit delta) | chaperonin |

| | | | |
|------------------------|----|---|---|
| | | Rab1 (Rab-protein 1) | - |
| | | Ergic53 (Ergic53, isoform A) | Membrane traffic protein |
| | | RpL29 (60S ribosomal protein L29) | Ribosomal protein |
| | | RpS11 (40S ribosomal protein S11) | Ribosomal protein |
| | | RpL7 (60S ribosomal protein L7) | Ribosomal protein |
| | | CG6543 | Acetyltransferase; acetyltransferase; dehydrogenase; epimerase/racemase; hydratase/ligase |
| | | D2hgdh (D-2-hydroxyglutaric acid dehydrogenase) | - |
| | | Obp99a (General odorant-binding protein 99a) | Signaling molecule |
| Macromolecular complex | 13 | RpS4 (40S ribosomal protein S4) | Ribosomal protein |

| | |
|---|-------------------|
| SdhC (Succinate dehydrogenase, subunit C) | - |
| RpS12 (40S ribosomal protein S12) | Ribosomal protein |
| RpL11 (60S ribosomal protein L11) | Ribosomal protein |
| RpL31 (60S ribosomal protein L31) | Ribosomal protein |
| Hoip (NHP2-like protein 1 homolog) | Ribosomal protein |
| RpS16 (40S ribosomal protein S16) | - |
| RpL8 (60S ribosomal protein L8) | Ribosomal protein |
| RpL17 (60S ribosomal protein L17) | - |
| CCT4 (T-complex protein 1 subunit delta) | chaperonin |
| RpL29 (60S ribosomal protein | Ribosomal protein |

| | | | |
|-----------|----|---|--------------------------|
| | | L29) | |
| | | RpS11 (40S ribosomal protein S11) | Ribosomal protein |
| | | RpL7 (60S ribosomal protein L7) | Ribosomal protein |
| Membrane | 4 | SdhC (Succinate dehydrogenase, subunit C) | - |
| | | Rab1 (Rab-protein 1) | - |
| | | Ergic53 (Ergic53, isoform A) | Membrane traffic protein |
| | | D2hgdh (D-2-hydroxyglutaric acid dehydrogenase) | - |
| Organelle | 19 | RpS4 (40S ribosomal protein S4) | Ribosomal protein |
| | | RpS12 (40S ribosomal protein S12) | Ribosomal protein |
| | | RpL11 (60S ribosomal protein L11) | Ribosomal protein |
| | | Spat (Serine-pyruvate aminotransferase) | Transaminase |

| | |
|--|--|
| CG14718 | DNA binding protein mRNA splicing factor transcription factor |
| RpL31 (60S ribosomal protein L31) | Ribosomal protein |
| Hoip (NHP2-like protein 1 homolog) | Ribosomal protein |
| Smt3 (Small ubiquitin-related modifier) | - |
| RpS16 (40S ribosomal protein S16) | - |
| RpL8 (60S ribosomal protein L8) | Ribosomal protein |
| RpL17 (60S ribosomal protein L17) | - |
| CCT4 (T-complex protein 1 subunit delta) | chaperonin |
| Rab1 (Rab-protein 1) | - |
| Ergic53 (Ergic53, isoform A) | Membrane traffic protein |

| | |
|---|---|
| RpL29 (60S ribosomal protein L29) | Ribosomal protein |
| RpS11 (40S ribosomal protein S11) | Ribosomal protein |
| RpL7 (60S ribosomal protein L7) | Ribosomal protein |
| CG6543 | Acetyltransferase; acetyltransferase; dehydrogenase; epimerase/racemase; hydratase/ ligase |
| D2hgdh (D-2-hydroxyglutaric acid dehydrogenase) | - |
